Local Calibration of Mechanistic-Empirical Pavement Design in Tennessee

(Final Report)

Authors:
Baoshan Huang, Ph.D., P.E.,
The Edwin G. Burdette Professor
Department of Civil and Environmental Engineering,
The University of Tennessee

Hongren Gong, Ph.D. candidate
Graduate Research Assistant
Department of Civil and Environmental Engineering,
The University of Tennessee

Xiang Shu, Ph.D.
Research Assistant Professor
Department of Civil and Environmental Engineering,
The University of Tennessee

Sponsored by
The Tennessee Department of Transportation
Research Development and Technology Program
(Project#: RES2013-33)

A report from
Department of Civil and Environmental Engineering,
The University of Tennessee
Knoxville, TN 37996
Ph.: (865) 974-7713
Fax: (865) 974-2669

March, 2016

TABLE OF CONTENTS

LIST OF FIGURES

LIST OF TABLES

EXECUTIVE SUMMARY

The Tennessee Department of Transportation (TDOT) has invested a large number of efforts and resources to make a smooth transition from the AASHTO 1993 pavement design guide to the up-to-date AASHTO Mechanistic-Empirical Pavement Design Guide (MEPDG). To accomplish this goal, several phases of research activities have been conducted. In first phase, a database for soil resilient modulus was established using representative soil samples in Tennessee. In the second phase, a database of concrete coefficient of thermal expansion (CTE) was generated. In another research project, a database was developed for the dynamic modulus of asphalt mixtures. In the current phase, the most important transfer functions in the MEPDG were locally calibrated according to the unique conditions of Tennessee. These models include the alligator cracking (bottom-up cracks), longitudinal cracking or load related wheel-path fatigue cracking, rutting, and smoothness (IRI) models.

The following conclusions were reached from the current research project:

1. The results from the state DOT survey indicated that most of the states in the United States or provinces in Canada have plan to transit from the AASHTO 1993 pavement design guide to the Pavement Mechanistic-Empirical Design Guide in three years. A majority of the states use LTPP database and data stored in pavement management system (PMS) as the main source of data for calibration. Most of the states that provided responses reported the transfer function of alligator cracking is the most difficult to calibrate, followed by longitudinal cracking and transverse function. Sixteen out of 28 responses show they are not fully satisfied with the current version of AASHTOWare pavement design software that entails too many inputs and outputs.

2. The distribution of average annual daily truck traffic (AADTT) on the Interstates was analyzed. The two-way AADTT of most sections fell within in the range of 5000-10000 vehicles/day. The AADTT was analyzed according to the four regions of TDOT. It is observed that Region III has the largest AADTT, whereas the other three regions have similar AADTT distributions.

3. The rutting model was calibrated using data collected from PMS. The data used to calibrate the rutting transfer function were divided into two major classes: the Interstates and the state routes. The rutting transfer function for the state routes was further classified into four classes according to the four regions of TDOT. To refine the calibrated rutting transfer function, random errors in the data were considered. Results show that after calibration, the summed error of estimates reduced (SEE) and biases of the model were eliminated for both Interstates and state routes, demonstrating that the calibrated rutting model significantly improved the accuracy of prediction.

4. The alligator-cracking model was first validated using the data collected from the LTPP online database, the InfoPave. An experiment matrix was used for the verification.

Results show that the default alligator-cracking model underestimated the alligator cracking. Meanwhile, the model gave significant biases and dispersion, indicating that local calibration of the alligator-cracking model was necessary for Tennessee pavements. More data collected from PMS were employed to determine the local calibration coefficients for this model. Since the alligator cracking transfer function has a sigmoidal form, a curve fitting procedure in the MATLAB® was utilized. It is observed that the default alligator transfer function greatly underestimated this distress. With an average of 2%, the predictions from the default model were mostly scattered close to the *x*-axis. After calibration, the slope of the regression line between the measured and predicted alligator cracking changed from 0.003 to 0.836, indicating a significant improvement in prediction accuracy.

5. The longitudinal cracking model was calibrated using the data collected from the Interstates in Tennessee. The distribution of the longitudinal cracking on the Interstates was first analyzed. The results show that the average length of this type of cracking was only 8 ft./mile, far less than the corresponding criterion in the MEPDG (2000 ft./mile). After calibration, the biases were greatly reduced and the slope of the fitting line changed from 18.565 to 1.141. The ratio s_e/s_y, which defines the dispersion of the prediction, reduced from about 11 to less than 1. Therefore, the calibration improved the prediction accuracy and precision.

6. The transverse cracking model was validated using PMS data. Results indicate that the national model underestimated this type of cracking for Tennessee pavements. However, due to the limited data of transverse cracking, it is not feasible to calibrate the transverse cracking until enough data are available (at least 20 sections with noticeable observations).

7. A discussion of the performance threshold values for pavement design was performed using data stored in the PMS of the last 15 years. A model selection analysis was carried out using MATLAB®. Among the normal, gamma, beta, and Weibull distributions, it is found that the Weibull distribution fitted all the data best. Therefore, the Weibull distribution was employed to determine the confidence interval for each type of distress and smoothness indicator (IRI). Results indicate that
    a. The default threshold values in the AASHTO Manual of Practice (MOP) for MEPDG for alligator cracking, longitudinal cracking, and transverse cracking are too stringent, which could possibly result in over design. For the smoothness, indicated by international roughness index (IRI), the default criteria in the MOP are much higher than the average level on both the State Routes and Interstates.
    b. Regarding the IRI on Interstates, 90 percent of observations were less than 114 in./mile, which was far smaller than the recommended value in the MPEDG (170 in./mile). The value on the state routes was 130 in./mile, which was also much lower than the default value recommend in the MOP (200 in./mile).
    c. With respect to the alligator cracking on the Interstates, more than 90% of the observations were less than 31.8 percent, and 50% of the observations even less than 11 percent. These values were quite close to the recommendations in the MEPDG, which is 10% for Interstates, 20% for primary roads, and 35% for

secondary roadways. In contrast to IRI, the alligator cracking seemed to be a more severe problem to pavements in Tennessee. Therefore, more attention should be given how to control this type of distress.

d. For the longitudinal cracking, its maximum on the Interstates was 1108 ft./mile, and 90% of the observations of this distress on Interstates were smaller than 335 ft./mile. For state routes, the corresponding maximum was 2133 ft./mile, and more than 90 percent of the observations were smaller than 355 ft./mile. These values were all far lower than the default criterion for this distress in the MOP. Therefore, if the default trigger value were used, it would produce a design with an unnecessarily thicker pavement.
e. As to the transverse cracking, the observed amount of transverse cracking was less than 170 ft./mile for both Interstates and State Routes, which was far smaller than those recommended by MEPDG (700 ft./mile). In addition, transverse cracking did not seem to be a severe problem on the Tennessee pavements. Therefore, it probably would not affect the final design whether to make adjustment on this criterion or not.

8. The rutting data on both Interstates and state routes were also fitted using the Weibull distribution. For the Interstates, more than 90 percent of the observations were lower than 0.27 inches, which is quite close to the recommended value in the MOP (0.40 inch). Regarding the state routes, the 9th quantile of the observations were lower than 0.28 inches, which is quite close to the recommended one in the MOP. Therefore, it is recommended that pavement design engineers pay more attention to control this type of distress in Tennessee.

CHAPTER 1 INTRODUCTION

1.1 PROBLEM STATEMENT

This research project is the continuation of the previously completed study entitled "Develop Typical Material Input Values for Mechanistic-Empirical Pavement Design in Tennessee" financially sponsored by TDOT. Pavement Design Division of TDOT has been collaborating with the University of Tennessee to develop typical material input values for the AASHTOWare Pavement ME Design (used to be the Mechanistic – Empirical Pavement Design Guide). The research team has established materials input databases for the mixtures TDOT typically uses. Typical TDOT pavement structures have also been evaluated and the main pavement performance (distress) models have been validated. To ensure the smooth transition from the current AASHTO design guide to Pavement ME Design, it is necessary to perform a local calibration of the pavement performance (distress) models in the Pavement ME Design.

In this research project, the research team performed a local calibration of major pavement performance (distress) models in the Pavement ME Design. The rutting and fatigue cracking models (including alligator and longitudinal cracking models) were selected for the calibration. The historical records of pavement performance in the Tennessee Pavement Management System (PMS), the Long-Term Pavement Performance (LTPP) data were utilized for the calibration. Although the National Center for Asphalt Technology (NCAT) has well-controlled test sections, the data from these test sections are currently not available for other institutions. As such, those data have not been included in this study.

The calibration of MEPDG will help Tennessee to take advantage of the advances in pavement design methods. Moreover, the calibration of the transfer functions in the MEPDG also plays a vital role in the future pavement designing work of Tennessee. With all the transfer functions calibrated, the pavement design practice would be able to adapt to the local traffic, materials, and climate conditions. Hence, the accuracy of pavement design is expected to increase noticeably. Consequently, the use of MEPDG with calibrated transfer functions is able to reduce the possibility of generating unreasonable pavement structure design. In other words, it is able to reduce the possibility of generating a thicker pavement structure than it is actually needed, which is not economically viable; or to generate thinner one, which is not structurally acceptable.

1.2 OBJECTIVES

The primary objective of the proposed research is to conduct a local calibration of the pavement performance (distress) models in the AASHTOWare Pavement ME Design software so that improved accuracy can be achieved for the pavement performance models. The calibrated Pavement ME Design models aim to help TDOT transition from the current AASHTO 93 Pavement Design to the Pavement ME Design.

1.3 ORGANIZATION OF THE REPORT

This report consisted of ten chapters. Follows is the organization of the report,

- Chapter 1, Introduction.
- Chapter 2, Literature reviews.
- Chapter 3, Results from the state DOT survey.
- Chapter 4, Data preparation.
- Chapter 5, Local calibration and validation of the rutting transfer function.
- Chapter 6, Local calibration and validation of the Bottom-Up cracking transfer function.
- Chapter 7, Local calibration and validation of the Top-Down cracking transfer function.
- Chapter 8, Local calibration of the roughness model.
- Chapter 9, Discussion of the flexible pavement design criteria for Tennessee.
- Chapter 10, Conclusions and Recommendations.
- Chapter 11, References.

CHAPTER 2 LITERATURE REVIEWS

Since its release under NCHRP 1-37A (ARA, 2004) and NCHRP 1-40D (Darter, et al., 2006), the new MEPDG has been seen as a new trend in pavement design and analysis, which will be used as a substitution to the AASHTO 1993 design guide (AASHTO, 1993) in future. It has significantly improved the ability to model and simulate the effects of traffic, material properties, and climate on pavement damage, distress, and smoothness. The long-term pavement performance (LTPP) database in North America was initially utilized as a resource for developing national transfer functions of distresses. Although the transfer functions were nationally calibrated based on LTPP database, local calibrations were strongly recommended due to the variation of traffic, environment, pavement structure and materials through states.

Tremendous efforts have to be put onto the local calibration. Based on the sensitivity analysis, critical properties of materials need to be collected in the laboratory. Then pavement sections from the LTPP database or local PMS databases are selected. And then measured pavement distresses such as rutting, cracking, and international roughness index were used to calibrate the transfer functions in MEPDG. In the final step, extra pavement sections should be used to validate the local calibrated transfer functions.

For those agencies that want to utilize local PMS database to calibrate MEPDG, comparison between data in LTPP and in PMS should be conducted to see if differences exist. Kang and Adams (2007) prepared a regional pavement performance database for a Midwest implementation of the MEPDG from Michigan, Ohio, Iowa and Wisconsin State transportation agencies. They suggested a data cleaning process be conducted before applied to MEPDG calibration. They also found that the default national calibration values do not predict the distresses observed in the Midwest. Souliman, et al. (2010) found the differences between the Arizona Department of Transportation (ADOT) PMS data and the LTPP database used in the original development and national calibration of the MEPDG distress models including rut measurements, asphalt cracking, IRI, and all layer backcalculated moduli found from NDT measurements done by ADOT and those of the LTPP.

Velasquez, et al. (2009) investigated the MEPDG rutting model and the CalME procedure and introduced a procedure incorporating the CalME rutting model into the MEPDG framework for rutting in AC-PCC design and analysis. Gulfam-E-Jannat, et al. (2014) found DARWin-ME overestimated the total rutting in asphalt pavements and they utilized clustering analysis based on functional class and geographical zone to improve the precision of the locally calibrated models. Darter, et al. (2009) utilized LTPP projects in central Ohio to firstly compare the predicted pavement performance with the measured ones and found that hot mix asphalt (HMA) rutting on new flexible pavements and IRI models for both new flexible and rigid pavements need to be calibrated for Ohio conditions. Then the rutting models for the asphalt concrete layers, granular base, and the subgrade were simultaneously calibrated through a simple linear regression. Fair agreement was reached between predicted rutting and the measured data and further comprehensive recalibration was recommended through plenty pavement sections in Ohio. Velasquez, et al. (2009) evaluated MEPDG rutting model with the measured rutting from Minnesota Road Research Project (MnROAD) and offered a novel approach to calibrate the

rutting model: deducting the first month's rutting from the rutting of base. Li, et al. (2009a), Li, et al. (2009b) calibrated transfer functions for AC fatigue cracking, longitudinal cracking, alligator cracking, AC rutting, and subgrade rutting based on data in Washington State Pavement Management System (WSPMS). They established a pavement thickness design catalog for the Washington state Department of Transportation (DOT) based on the calibration of MEPDG software for their state condition. Darter, et al. (2009) calibrated MEPDG for local conditions in Utah State. They claimed that the nationally calibrated rutting model predicted rutting adequately for older pavements constructed using viscosity binder grade (AC-10 and AC-20) and predicted rutting poorly on the new HMA pavements using the Superpave Binders. Therefore, they calibrated the rutting model with the older pavements constructed using viscosity binder grade and offered the locally calibrated coefficients for HMA, Base, and subgrade, respectively. Glover and Mallela (2009) summarized the flexible pavement local calibration value results of the MEPDG from NCHRP project 9-30 (2003), 1-40B (2013), and Montana DOT studies. Muthadi (2007) conducted local calibration on rutting models for North Carolina. Schram and Abdelrahman (2006) conducted local calibration work on MEPDG in the project-level rather than a network level for Jointed Plain Concrete Pavement (JPCP) and HMA overlays of PCC pavements. Results indicate that project-level calibrations reduced default model prediction error by nearly twice that of network-level calibration.

The local calibration on the rutting transfer functions in flexible pavements usually conducted a linear regression on the total measured rutting depth data from predicted rutting depth from sublayers, which failed to indicate the actual part of rutting depth contributed by asphalt layer. Without this information of asphalt layer, the limit on the asphalt layer rutting depth could not be claimed as a firm criterion for asphalt pavement design.

Many states have conducted local calibration to different level and depth. For example, Guo and Timm (2014) in Alabama was able to conduct level-one analysis because of the full-scale test sections at National Center for Asphalt Technology (NCAT) and Ullidtz, et al. (2008) in California was also capable of carrying out the same level of analysis with the help of full-scale test sites (WESTRACK), well characterized traffic, and controlled climate condition. For states have no full-scale test site, data stored in their pavement management system (PMS) and the Long Term Pavement Project (LTPP) database are the main sources for local calibration.

The general procedure for local calibration of the MEPDG has been adequately documented in the Manual of Practice (AASHTO, 2008). However, the huge amount of details on operations, such as transforming the traffic, structure and materials inputs from data stored in PMS into the format required in MEPDG analysis software-AASHTOWare, complicated the problem. In addition, state highway agencies in the US differ in availability of data. The survey, conducted by Pierce and McGovern (2014), shows distresses data are readily available for 32 agencies, but only seventeen of them have easy access to materials data. These make the local calibration of MEPDG simple in idea but difficult in action.

The verification runs with national-default calibration coefficients indicates differences between predicted rutting in MEPDG and measured rutting in PMS in Tennessee (Zhou, et al., 2013a). This suggests an extensive local calibration is needed.

CHAPTER 3 RESULTS FROM THE STATE DOT SURVEY

A questionnaire was generated through the website of the office of information technology (OIT) of the University of Tennessee, in September 2014. In total, 35 survey responses were obtained out of 53 being sent out to the DOTs of United States and several transportation administration agencies in Canada, all the survey responses have been summarized.

3.1 REPORTS ON SURVEY RESPONSES

The main information obtained in the survey is summarized as follows.

Q1. What design procedure is currently used to design asphalt pavements in your state?

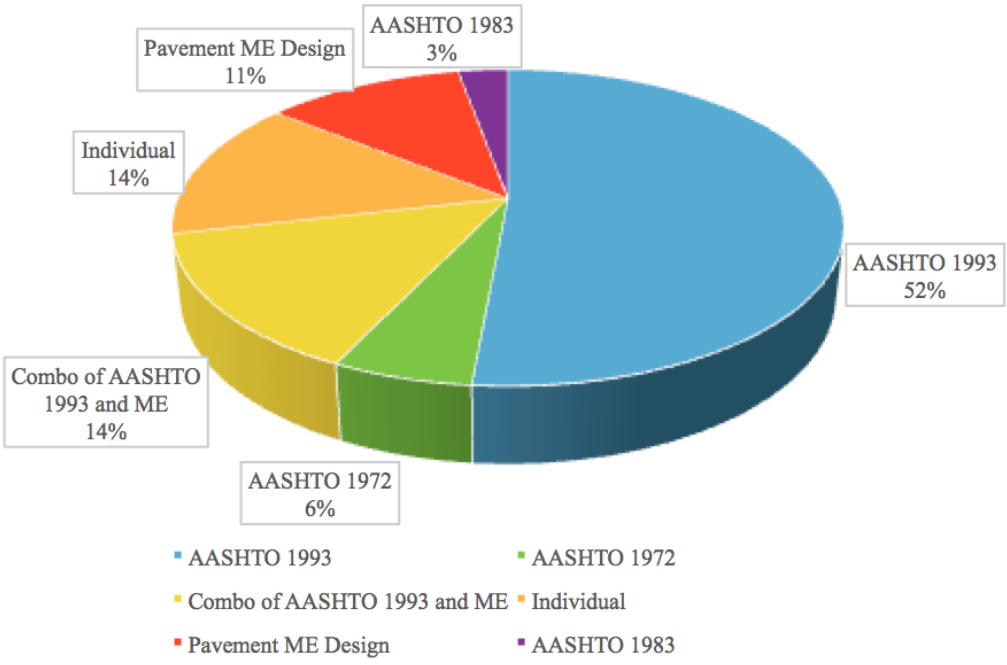

Q2. What design procedure is currently used to design rigid pavements in your state?

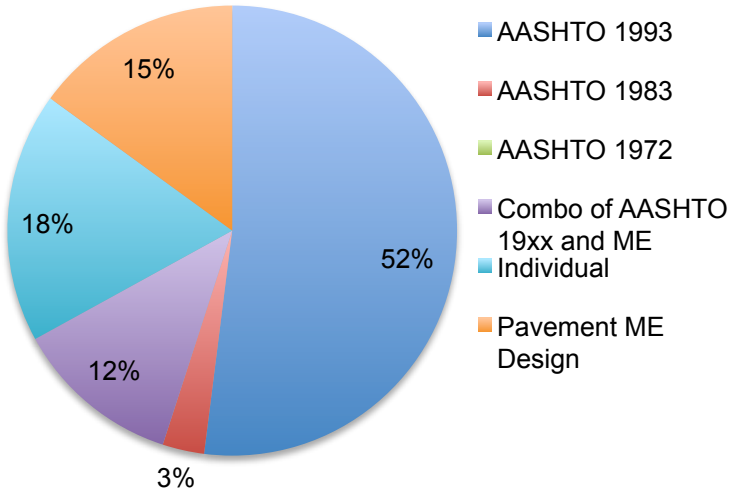

Q3. How soon will your state implement the Pavement ME Design to design pavements?

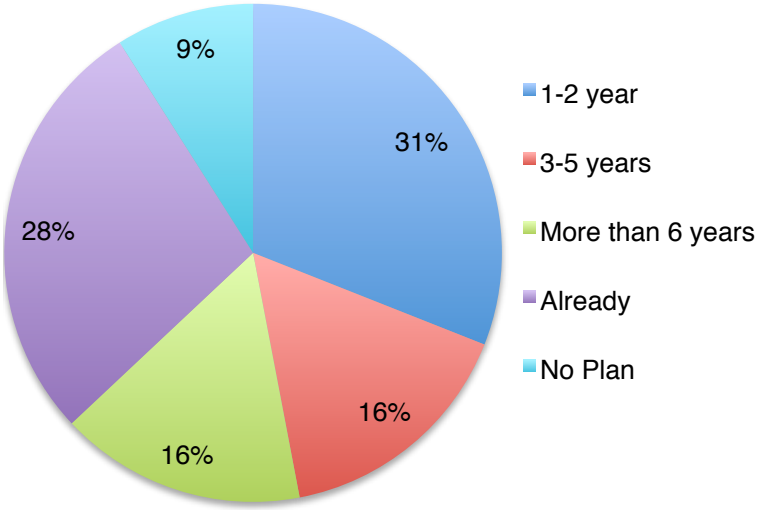

Q4. Which database(s) does your state utilize in the local calibration?

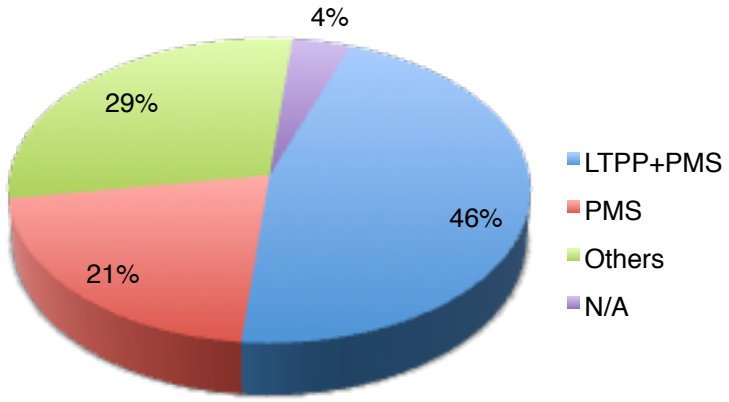

Q5. Are the definitions of distresses from your state different from LTPP? If yes, please tell us which.

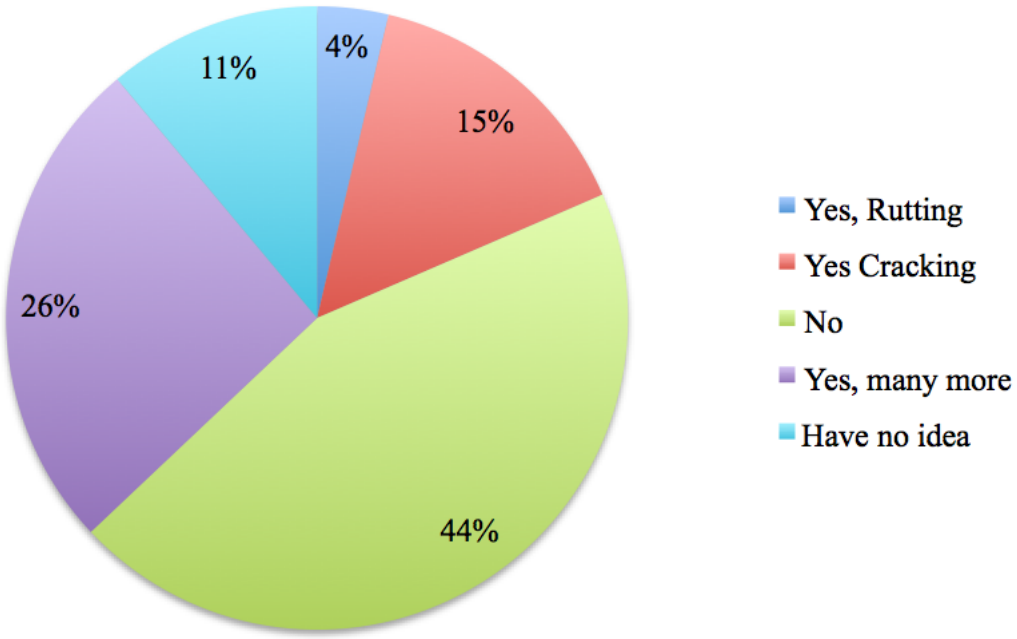

Q6. Has your state developed input database of asphalt materials for Pavement ME Design? If yes, please spell out the specific properties included.

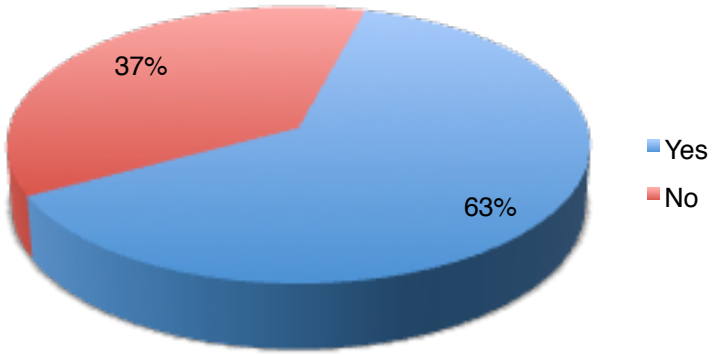

Q7. Has your state developed input database of cement concrete materials for Pavement ME Design? If yes, please spell out the specific properties included.

Yes	13
Not yet	14

For those answered yes, CTE is the one included most frequently.

Q8. Has your state developed input database of base materials for Pavement ME Design? If yes, please spell out the specific properties included.

Yes	14
Not yet	16

Q9. Has your state developed input database of subgrade soil for Pavement ME Design? If yes, please spell out the specific properties included.

Yes	14
Not yet	16

For those who answered yes, resilient modulus was the one most frequently included.

Q10. Is the local loading spectrum available in your state?

Yes	19
No	10
Have no idea	1

Q11. Will your state set up weigh-in-motion station to collect traffic data?

Definitely yes	15
Probably yes	6
Probably no	6

Q12. Has the local calibration been completed for asphalt pavement design in your state?

Yes	12
Local calibration is been conducting	9
No	13

Q13. Generally, how many pavement sections did/has/will your state use(d) in the local calibration of flexible pavement?

10-20	6
20-30	4
More than 30	11

Q14. What distresses of flexible pavements have been locally calibrated in your state?

Rutting	13
Bottom-up cracking	13
Longitudinal cracking	9
Roughness	12
Thermal cracking	6

Since this is a multiple choices question, each distress is counted separately, so the total number is not equal to the total responses.

Q15. What distresses of flexible pavements do you think are most difficult to locally calibrated in your state?

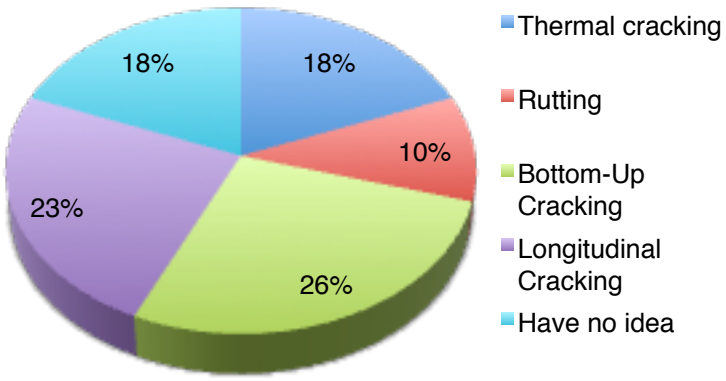

Most of the DOTs think the cracking models are the most difficult to calibrate.

Q16.On the local calibration and design of flexible pavement in your state, are flexible pavements divided into groups due to the variation of inputs, e.g. traffic, climate, and material properties?

Yes	11
No	8
Have no idea	5

There is a strong trend to divide different groups for local calibration, in order to incorporate the effect of traffic, climate and material properties variability.

Q17. According to which factors that the flexible pavements are classified in Pavement ME Design?

Traffic	6
Climate	4
Materials properties	3

Have no idea	5

Q18. Has the local calibration been completed for rigid pavement design in your state?

Yes	6
No	16
Local calibration is been conducting	8

Q19.Generally how many pavement sections did/has/will your state use(d) in the local calibration of rigid pavement?

10-20	5
20-30	3
More than 30	8
Have no idea	5

Similar to sections needed for flexible pavement calibration, more DOTs think more than 30 sections will be appropriate for local calibration.

Q20. What distresses of rigid pavements have been locally calibrated in your state?

Joint faulting	12
Transverse cracking	10
Punch-out's (CRCP)	1
Roughness	12

Q21. What distresses of rigid pavements do you think are most difficult to locally calibrated in your state?

Transverse cracking	8
Joint faulting	3
Roughness	2
All calibrated	1

Q22. On the local calibration and design of rigid pavement in your state, are rigid pavements divided into groups due to the variation of inputs, e.g. traffic, climate, and material properties.

Yes	8
No	9
Have no idea	5

Q23. According to which factors that the rigid pavements are classified in Pavement ME Design?

Materials properties	3
Traffic	3
Climate	3
Have no idea	10

Q24.When designing a pavement section with the same local materials, compared to the AASHTO 1993, the Pavement ME Design gives a _____ flexible pavement structure in your state.

Thicker	2
Thinner	1
Sometimes thicker, sometimes thinner	11

Almost the same	3
Have no idea	12

Q25.When designing a pavement section with the same local materials, compared to the AASHTO 1993, the Pavement ME Design gives a _____ rigid pavement structure in your state.

Thicker	0
Thinner	8
Sometimes thicker, sometimes thinner	7
Almost the same	1
Have no idea	13

There is a trend indicates that the pavement ME design will yield a thicker structure than AASHTO 1993.

Q26. In general, are you satisfied with the AASHTOWare Pavement ME Design software? 5-totally satisfied, 1-not at all

1	1
2	5
3	11
4	6
Have no idea	6

The average score is 3.1.

Q27. In your opinion, what are the shortcomings of the Pavement ME Design?
A lot of feedbacks about this question have been received; here just list a few as an example, the detailed survey results will be presented in a spreadsheet separately.

- We have seen some instances where Pavement ME analysis can provide pavement sections that are significantly different than what we see using current design methods;
- It is difficult to establish standard design policies and procedures given the complexity of the method as well as the vast quantity of input data required to run an analysis;
- Use of the method/software requires extensive training and experience in order to have confidence in the results. (From Arizona DOT).
- The software is not design software. It is a predictive performance modeling tool;
- Many of the unique features of the software will never be known at the stage in the project when the pavement design is being developed. Therefore, generalized data would need to be utilized and/or design at the level-3 design with the default values; This would best be utilized as a forensic investigation tool when a pavement failure is encountered. At that point in time, all the required Level 1 data can be incorporated in the software and the predictive performance can be analyzed. (From Alabama DOT)
- Complexity and data input intensive; A bit of a black box. (From Alberta, Canada)
- For asphalt mixture surfaced pavement, the models overestimated rutting; no top-down cracking models (in the currently version of MEPDG design program-AASHTOWare Pavement M-E Design, top-down cracking model is included); procedure is vague; climate models are too sensitive and results don't make intuitive sense. (From Florida DOT)

3.2 SUMMARY AND CONCLUSIONS

From the responses collected in this survey, it is found that:

1. Most of the states in the United States or provinces in Canada still use AASHTO 1993 for flexible and rigid pavement design.
2. A majority of states in the US or provinces in Canada have plan to make a transition from AASHTO 1993 to the Pavement Mechanistic-Empirical design guide.
3. About half of the responses indicated that LTPP database and data from the pavement management system were employed as the main source of data for local calibration.
4. More than 50% of the responses showed that input database of asphalt materials were developed.
5. Among 27 responses received about setting up weigh-in-motion station to collect traffic data, a total of 15 states have plans to implement this plan.
6. Generally, 10-30 sections were used in the local calibration of flexible pavement.
7. Most of the states reported that the bottom-up cracking (alligator) was the most difficult model to calibration, followed by the longitudinal-cracking and thermal cracking (transverse cracking).
8. Most of the states showed they are not quite satisfied with the current version of AASHTOWare Pavement ME Design software, because there are too many parameters to input and too many information to interpret.

CHAPTER 4 DATA PREPARATION

4.1 CALIBRATION MATRIX

Because the data availability of different types of distresses are different, different calibration plans has been used in this research project. For example, there are more riding quality related data, such as rutting and roughness than cracking data, such as alligator cracking, longitudinal cracking and transverse cracking, especially for the transverse cracking.

4.2 CHARACTERIZATION OF TRAFFIC IN STATE ROUTES

As one of the most important factor, traffic volume influences the performance of pavements and their distress features. Traffic data of each section were collected from PMS for all Interstates in Tennessee. In PMS, only the Annual Average Daily Traffic (AADT), percent truck traffic in the design lane, percent truck traffic in the design direction were recorded. However, the axle load spectrum (ALS) was required in AASHTOWare ME Design package for Hierarchical 1 analysis or the Annual average daily truck traffic (AADTT) for Hierarchical 2 and 3 analyses, which are not available in the current PMS. In order to obtain the AADTT from AADT, the equivalent ESALs within the design life were used. However, further investigation showed AADTTs derived in this manner are too conservative, that is, the number of AADTT converted in this way is too small. With such a small AADTT, AASHTOWare could not yield any noticeable distresses, especially for alligator cracking. Figure 4.1 shows the steps to obtain the AADTT from AADT on the basis of the equivalent ESALs.

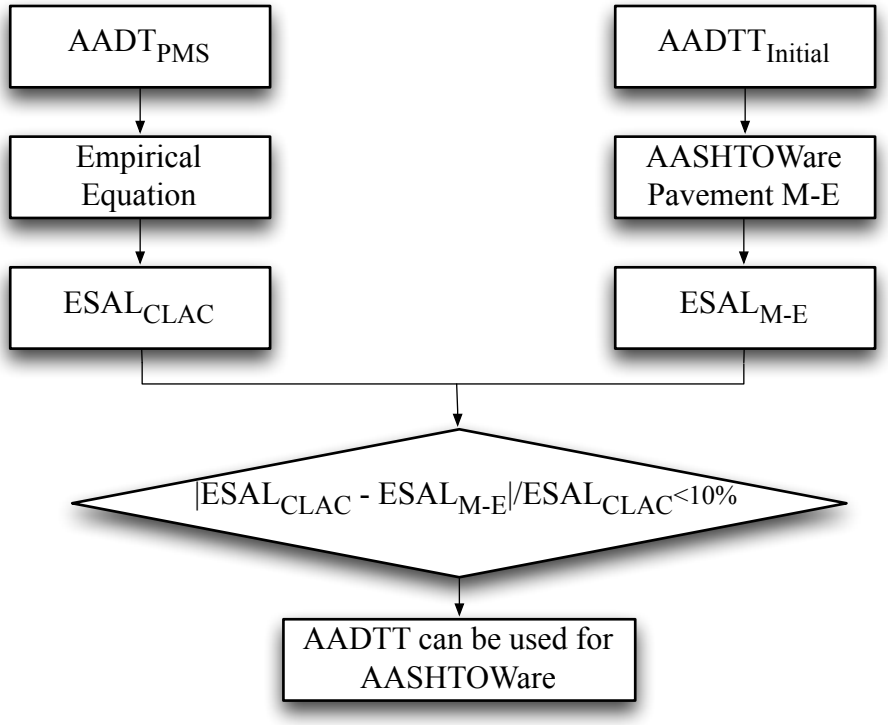

Figure 4.1 Flow Chart of Converting AADT in PMS to AADT Required in AASHTOWare ME Design

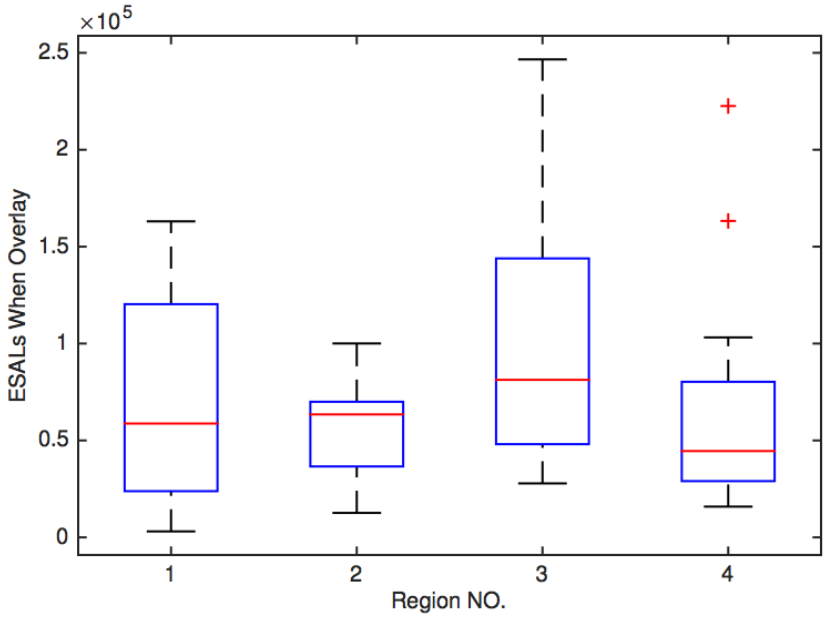

Figure 4.2 Predicted ESALs when overlay (Region NO.=regions in Tennessee)

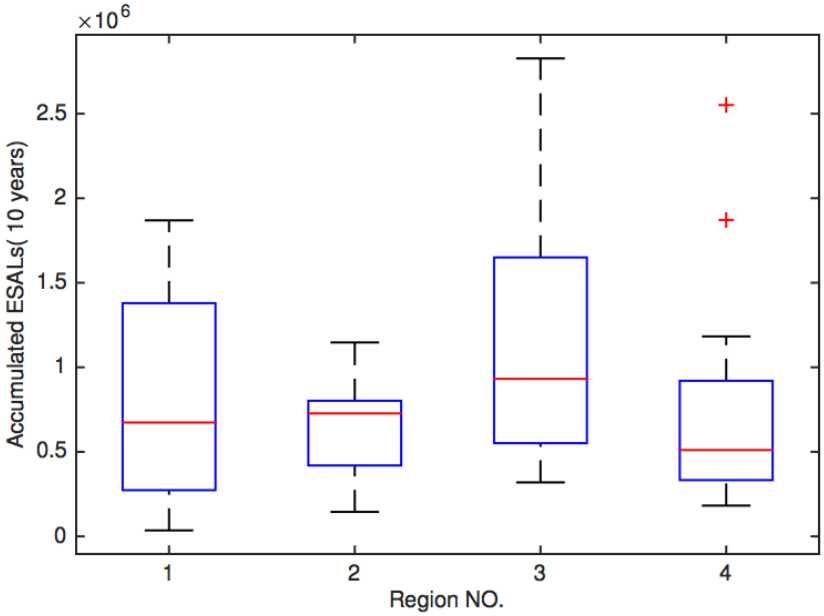

Figure 4.3 Predicted 10 Years accumulated ESALs (Region NO.=regions in Tennessee)

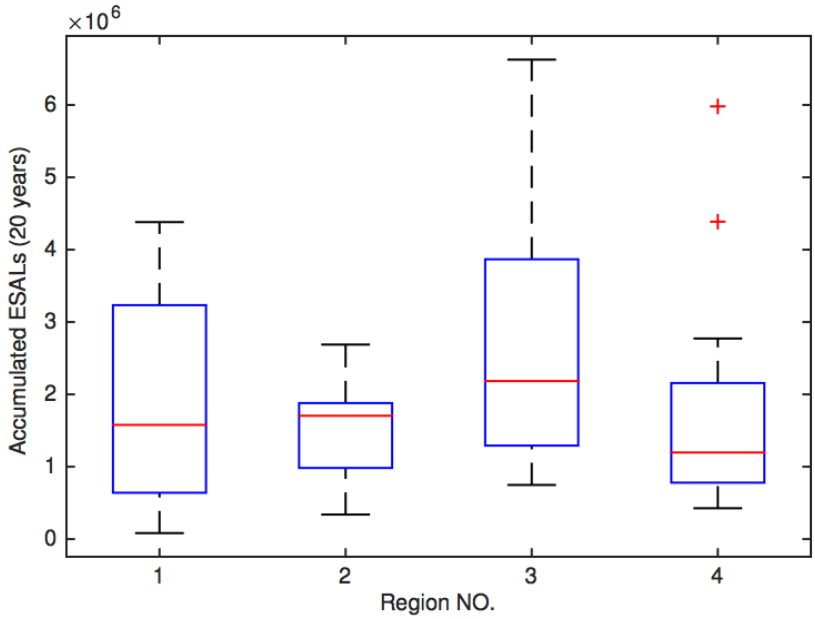

Figure 4.4 Predicted 20 years accumulated ESALs (Region NO.=regions in Tennessee)

Figure 4.2 through Figure 4.4 showed the predicted ESALs from AADT in PMS. As Figure 4.2 through Figure 4.4 indicated, the traffic volume across all four regions is approximately the same. The traffic volume in region III is slightly greater than the other 3 regions, but the data in this region have a larger variation.

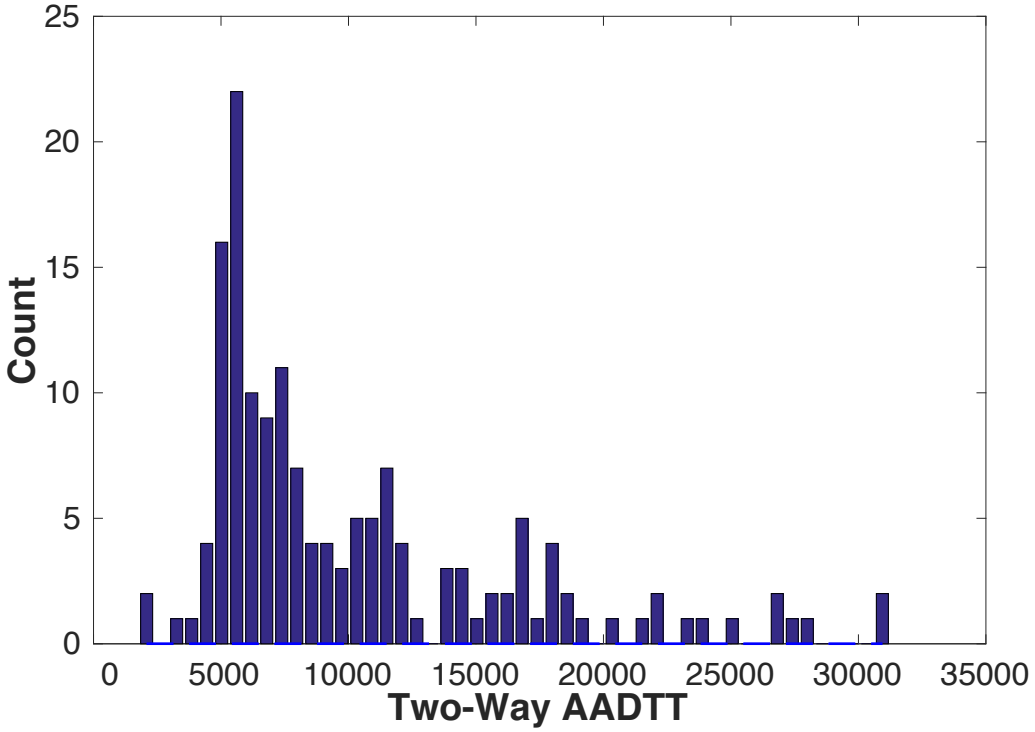

Figure 4.5 DISTRIBUTION of the two-way AADTT in the Interstates of Tennessee

As shown in Figure 4.5, for Interstates in TN, the two-way average annual daily truck traffic (AADTT) of most sections fall in the range of 5000-10000. Because the lane distribution coefficients were not available in PMS, the lane distribution coefficients recommended by Huang (1993) were adopted. Since PMS did not record the AADTT, there are two possible ways could be used to obtain these data, 1) back-calculating from the ESALs predicted by AASHTOWare with assumed annual growth rate; 2) multiplying the AADT by percent truck traffic, which is available in PMS. The former one will yield more conservative amount of AADTT. When these AADTTs are input into AASHTOWare, because the AADTT are too small, generally it will predict no cracking. Thus, the latter one was used to determine the AADTT for AASHTOWare execution.

CHAPTER 5 LOCAL CALIBRATION AND VALIDATION OF RUTTING TRANSFER FUNCTION

Surface distortion in the form of rutting is caused by the plastic or permanent vertical deformation in the HMA, unbound layers, and foundation soil(AASHTO, 2008). The approach used in the MEPDG is based upon calculating incremental distortion or rutting within each sublayer. In other words, rutting is estimated for each sub-season at the mid-depth of each sub-layer within the pavement structure. The plastic deformation for a given season is the sum of the plastic vertical deformations within each layer.

5.1 RUTTING TRANSFER FUNCTIONS

In the Pavement ME Design, the total rut is the sum of ruts from HMA layer, base, and subgrade, as shown in Equation ((2).

$$Rut_{Total} = Rut_{AC} + Rut_{Base} + Rut_{SG} \quad (1)$$

Where, Rut_{Total} = predicted total rutting; Rut_{AC}, Rut_{Base}, and Rut_{SG} = rutting from asphalt layer, base, and subgrade, respectively.

The AASHTOWare Pavement M-E Design version 2.1 nationally calibrated rutting transfer function (Bari and Witczak 2006) is as follows:

$$\Delta_{pac} = \varepsilon_{(pac)} h_{ac} = \beta_{r1} k_z \varepsilon_{rac} 10^{k_1} T^{k_2 \beta_{r2}} n^{k_3 \beta_{r3}} h_{ac} \quad (2)$$

Where Δ_{pac}=Accumulated permanent or plastic vertical deformation in the HMA layer/sublayer, inches; $\varepsilon_{(pac)}$=Permanent or plastic axial strain in the HMA layer/sublayer, inches/inches; ε_{rac}=resilient axial strain in the HMA layer/sublayer, inches/inches; h_{ac}=Thickness of the HMA layer/sublayer, inches; n =Number of axle load repetitions; T=Mix or pavement temperature, ^{o}F; k_z=Depth confinement factor, inches; $k_{1,2,3}$=Global filed calibration parameters (from the NCHRP 1-40D recalibration; $k_1 = -3.35412, k_2 = 1.5606, k_3 = 0.4791$); $\beta_{r1,r2,r3}$=Local or mixture field calibration constants; for the global calibration, these constants were all set to 1.0.

$$\begin{aligned} k_z &= (C_1 + C_2 D) \times 0.328196^{D} \\ C_1 &= -0.1039(H_{ac})^2 + 2.4868 H_{ac} - 17.342 \\ C_2 &= 0.0172(H_{ac})^2 - 1.7331 H_{ac} + 27.428 \end{aligned} \quad (3)$$

Where D=Depth below the surface, inches; H_{ac} = Total HMA thickness, inches.

It is noted that only the asphalt surface layer is divided into two sublayers: the top 0.5 inches and the rest. No layers under the asphalt surface layer are further divided during the calculation.

The rutting transfer function for the unbound pavement layers (Bari and Witczak, 2006) and the subgrade is shown in Equation (4).

$$\delta_a(N) = \beta_{s1} k_1 \varepsilon_v h_{soil} \left(\frac{\varepsilon_0}{\varepsilon_r}\right) e^{-\left(\frac{\rho}{n}\right)^{\beta}} \quad (4)$$

Where $\delta_a(N) =$ Permanent or plastic deformation in a layer/sublayer, inches; n = Number of axle load applications; ε_0 = Intercept determined from laboratory repeated load permanent deformation tests, inches/inches; ε_r =Resilient strain imposed in laboratory test to obtain material properties, i.e., ε_v, β_{s1}, and ρ , inches/inches; h_{soil} = Thickness of the unbound layer/sublayer, inches; $k_1 =$ Global calibration coefficients; $k_1 = 2.03$ for granular materials and $k_1 = 1.35$ for fine-grained materials; β_{s1} = Local calibration constant for the rutting in the unbound layers.

$$\begin{aligned} log\,\beta &= -0.06119 - 0.017638(W_e) \\ \rho &= 10^9 \left(\frac{C_0}{1-(10^9)^{\beta}}\right)^{\frac{1}{\beta}} \\ C_0 &= ln\left(\frac{a_1 M_r^{b_1}}{a_9 M_r^{b_9}}\right) \end{aligned} \quad (5)$$

Where W_e = water content, percent; M_r = resilient modulus of the unbound layer and sublayer, psi; $a_{1,9}$ = regression constants; $a_1 = 0.15, a_9 = 20.0$; $b_{1,9}$ =regression constants, $b_1 = 0, b_9 = 0$.

5.2 CALIBRATION ON AC RUTTING MODEL ON AC OVERLAY UPON AC PAVEMENT

In this study, the asphalt overlay on asphalt pavement is treated as new asphalt pavement. The reason for this treatment is that the asphalt overlay pavements and the new asphalt pavements use the same rutting transfer functions in the Pavement ME Design. Additionally, all the selected overlays are thicker than 10cm. Hence, it is reasonable that the asphalt overlays are treated as new asphalt pavements. For asphalt overlays, the level-2 inputs were adopted for the local calibration. The asphalt layers before overlay are combined together and treated as asphalt bases. There are totally 14 pavement sections selected from the Tennessee PMS, as shown in Figure 5.1. Other information about the selected pavement sections, including pavement structure, materials, and traffic, is listed in Table 5.1 .

Table 5.1 Asphalt overlay on asphalt pavements for local calibration on rutting model

Highway	County	Mileage	Year Built	Year Overlay	Initial AADTT (since Overlay)	Overlay (cm)	Existing AC (cm)	Crushed Stone (cm)
I-40	Knoxville	0-6.9	1986*	2002	250	Mill and Replace 1-2in.	31.1Asphalt Surface+8.9Asphalt Base	20.3
SR-36	Washington	14.4-15.1	1984*	1994	380	Mill and Replace 1-2in.	17.8Asphalt Surface+8.9Asphalt Base	20.3
I-81	Greene	6.0-12.3	1975	1985*	520	13.3Asphalt Surface	5.7Asphalt Surface+26.7Asphalt Base	7.6
I-40	Roane	15.7-22.9	1972	1984*	600	3.2GrD+6.4GrB+7.6GrA	18.4Asphalt Surface+17.8Asphalt Base	25.4
I-40	Benton	0-8	1966	1989*	750	7.6Asphalt Surface+7.6Asphalt Base	25.4Asphalt Base	20.3
I-75	Campell	27-30.4	1981	1993*	750	7.6Asphalt Surface +15.2 Asphalt Base	25.4Asphalt Base	20.3
I-40	Dickson	9.1-17.8	1970	1986*	820	8.3Asphalt Surface +27.9Asphalt Base	17.8Asphalt Base	20.3
I-75	McMinn	10.9-13.4	1974	1986*	870	11.4Asphalt Surface	5.7Asphalt Surface+17.8Asphalt Base	20.3
I-40	Cumberland	6.4-13.5	1968	1986*	950	3.2Asphalt Surface +7.6Asphalt Base	6.4Asphalt Surface+31.8Asphalt Base	20.3
I-40	Davidson	0-4.69	1962	1985*	1100	13.3Asphalt Surface	Milled Asphalt Surface off	35.6
I-75	Anderson	8.3-10.2	1974	1990*	1150	8.3Asphalt Surface +10.2Asphalt Base	17.8Asphalt Base	20.3
I-24	Montgomery	11.7-17.2	1976	1995*	1370	3.2Asphalt Surface +12.1Asphalt Base	19.7Asphalt Surface+8.9Asphalt Base	12.7
I-24	Marion	1.2-6.3	1968	1994*	820	3.2Asphalt Surface+15.2Asphalt Base	4.4Asphalt Surface+8.9Asphalt Base	20.3
I-75	Hamilton	8.5-15.6	1988	1996*	1300	6.4Asphalt Surface+6.4Asphalt Base	7.0Asphalt Surface+10.8Asphalt Base	35.6

Note: *The first years analyzed in Pavement ME Design 2.0 software.

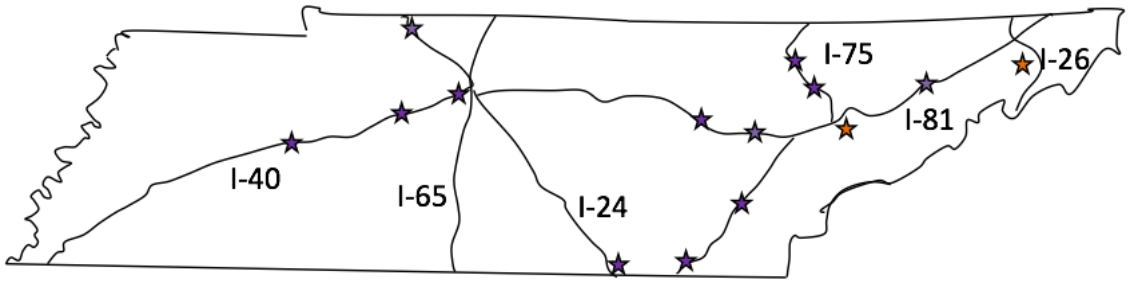

Figure 5.1 Asphalt pavement sections for local calibration on rutting models

Figure 5.2 shows the comparison of the rut measurements and the values predicted from the nationally calibrated model. It shows that the nationally calibrated rutting transfer function over predicted total rutting. Other researchers have drawn similar conclusions as well (Velasquez, et al., 2009, Zhou, et al., 2013b). The Jackknife Statistic resampling method was utilized to determine the local coefficients. The Microsoft Excel Solver was utilized to minimize SEE between measured ruts and $\beta_{r1}, \beta_{BS}, \beta_{SG}$ predicted total ruts. The local coefficients were calculated, as shown in Table 2. With these local calibration coefficients, the SEE decreased from 0.36 cm (national calibration) to 0.15 cm. It can be seen that the locally calibrated rutting transfer functions gave better prediction than the nationally calibrated ones. The scattered data points are due to the error in the field rut measurement.

Table 5.2 Summary of local coefficients of rutting models in AC overlay on asphalt pavements

	β_{r1}	β_{BS}	β_{SG}
Estimated Parameters	1.160	0.144	0.737
Variance of Estimation	1.66	0.10	0.18

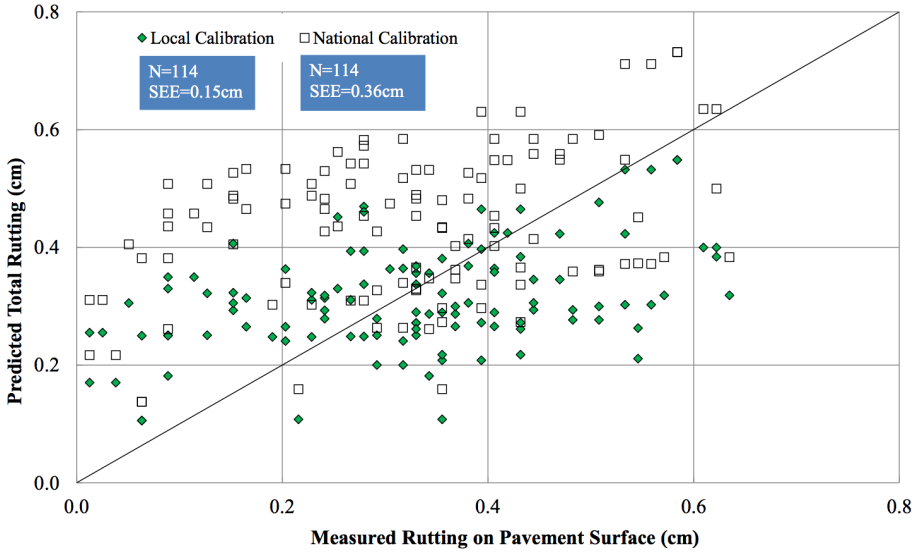

Figure 5.2 Comparison of measured and predicted rutting of the asphalt overlay on asphalt pavements

5.3 Refining of Rutting Transfer Function for Asphalt Overlay on Asphalt Pavements

Additional pavement sections were selected for further local calibration on rutting transfer functions on AC overlay on AC pavements. For asphalt overlays, the level 2 inputs were adopted for the local calibration. There were totally 27 pavement sections selected from the Tennessee PMS, as shown in Figure 5.3 Other information about the selected pavement sections, including pavement structure, materials, and traffic, was listed in Table 3. Climate, traffic, and material inputs were obtained the same way as described in the local calibration on AC overlay on PCC pavements.

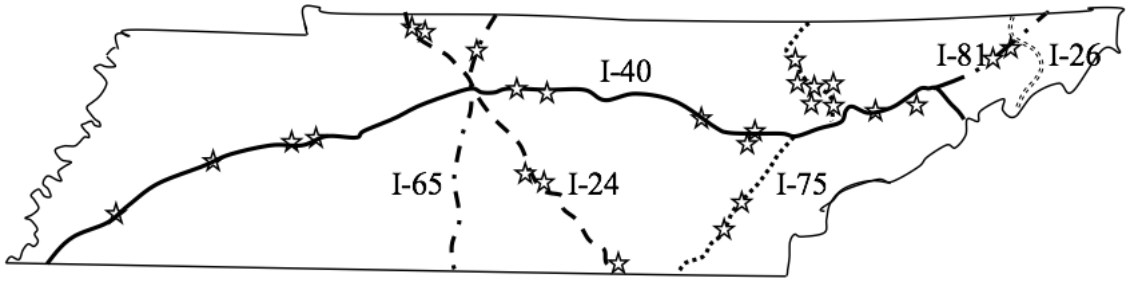

Figure 5.3 Asphalt pavement sections for local calibration on rutting models

Table 5.3 Asphalt overlay on asphalt pavements for local calibration on rutting model

Highway	County	Mileage	Year Built	Year Overlay	Initial AADTT (since Overlay)	Overlay (cm)	Existing AC (cm)	Crushed Stone (cm)	20 years ESALs (Million)
I-40	Knoxville	0-6.9	1973	1986 2002	290	Mill and Replace 1-2in.	31.1Asphalt Surface+8.9Asphalt Base	20.3	1.08
SR-36	Washington	14.4-15.1	1978	1984 2007	440	Mill and Replace 1-2in.	17.8Asphalt Surface+8.9Asphalt Base	20.3	1.63
I-81	Greene	6.0-12.3	1975	1985 2003	610	13.3Asphalt Surface	5.7Asphalt Surface+26.7Asphalt Base	7.6	2.26
I-40	Roane	16.2-22.9	1972	1984 1996	685	3.2GrD+6.4GrB+7.6GrA	18.4Asphalt Surface+17.8Asphalt Base	25.4	2.55
I-40	Benton	0-8	1966	1989 1998	840	7.6Asphalt Surface+7.6Asphalt Base	25.4Asphalt Base	20.3	3.12
I-75	Campell	27-30.4	1981	1993 2000	840	7.6Asphalt Surface +15.2 Asphalt Base	25.4Asphalt Base	20.3	3.16
I-40	Dickson	9.1-17.8	1970	1986 2000	850	8.3Asphalt Surface +27.9Asphalt Base	17.8Asphalt Base	20.3	3.49
I-75	McMinn	10.9-13.4	1974	1986 2000	1025	11.4Asphalt Surface	5.7Asphalt Surface+17.8Asphalt Base	20.3	3.81
I-75	Anderson	8.3-10.2	1974	1990 2000	1330	8.3Asphalt Surface +10.2Asphalt Base	17.8Asphalt Base	20.3	4.95
I-24	Montgomery	11.7-17.2	1976	1995 2003	1585	3.2Asphalt Surface +12.1Asphalt Base	19.7Asphalt Surface+8.9Asphalt Base	12.7	5.89
I-24	Marion	1.2-6.3	1968	1994 2003	1350	3.2Asphalt Surface+15.2Asphalt Base	4.4Asphalt Surface+8.9Asphalt Base	20.3	5.03
I-75	Hamilton	8.5-15.6	1988	1996 2004	1510	6.4Asphalt Surface+6.4Asphalt Base	7.0Asphalt Surface+10.8Asphalt Base	35.6	5.62
I-40	Jefferson	15.17-20.13	1962	1985 2003	670	5.7Asphalt Surface+8.9Asphalt Base	5.7Asphalt Surface+7.6Asphalt Base	20.3	2.48
I-40	Roane	11.35-16.15	1960	1994	1440	Mill and Replace 1-2in.	3.2Asphalt Surface+7.6Asphalt Base	43.2	5.35
I-40	Cumberland	13.54-24.51	1968	1995 2004	1190	Mill and Replace 1-2in.	6.4 Aspahlt Surface+7.6Asphalt Base	20.3	4.44
I-40	Smith	0-8.21	1965	1990 2000	1180	Mill and Replace 1-2in.	14.0Asphalt Surface+20.3Asphalt Base	20.3	4.38
I-40	Wilson	12.71-19.69	1966	1989	1625	Mill 1.5in., 3.2Asphalt Surface+5.1Asphalt Base	13.3Asphalt Surface+20.3Asphalt Base	20.3	6.05
I-40	Henderson	13.24-20.37	1965	1986 1997	830	3.2Asphalt Surface+3.8Aspahlt Base	5.1Aspahlt Surface+17.8Asphalt Base	20.3	3.08
I-75	Campbell	1.87-4.64	1964	1986 2005	1280	6.4Aspahlt Surface+6.4Aspahlt Base	12.1Asphalt Surface+17.8Asphalt Base	25.4	4.76
I-75	McMinn	1.55-4.00	1974	1997 2006	1570	Mill and Replace 1-2in.	5.7Aspahlt Surface+17.8Aspahlt Base	20.3	5.83

5.3.1 CALIBRATION

Rutting data measures at the same sites are potentially correlated across years. Hence, a random effect parameter is included in the linear model to account for this temporal correlation. The random effect linear model can be expressed as Equation (6).

$$\begin{cases} y_{it} \sim Normal(\mu_{it}, \sigma_{it}^2) \\ \mu_{it} = x'_{ijt}\beta_t + \varepsilon_i \\ \varepsilon_i \sim Normal(0.0, \tau_i^2) \\ \beta_j \sim dunif(0.0,100) \end{cases} \quad (6)$$

where y_{it} is the measured total rutting depth; u_{it} is the mean of predicted total rutting of site *i* at time *t* in the linear regression; and σ_{it} is the corresponding variance. ε_{it} is a site specific random effect, which does not change for a site over time. This quantity is assumed to follow normal distribution with mean 0 and variance τ_i^2. x'_{ijt} represents the predicted rutting depths of asphalt layer, base, and subgrade for site *i* at time *t*. β_j is the parameter estimate for variable *j*.

The random effect linear model was estimated using the open source software WinBUGS® 3.0.2 (Windows Bayesian Inference Using Gibbs Sampling). 10,000 iterations were discarded as burn-in, and the 10,000 iterations that followed were used to obtain summary statistics of the posterior inference. Convergence was assessed by visual inspection of the Markov chains for the parameters. Furthermore, the number of iterations was selected so that the Monte Carlo error would be less than 0.05 for each parameter.

Among the 295 observations from the 27 pavement sections, 205 observations were randomly selected with the restriction that at least one observation is selected from each pavement section. The random selected 205 samples were utilized to fit the model. The remaining data were employed to validate the goodness of fit of the model. The circles in Figure 5.4 shows the comparison of the rut measurements and the values predicted from the nationally calibrated model. It shows that the nationally calibrated rutting transfer function over-predicts total rutting. The regressed local coefficients for rutting transfer functions were summarized in Table 5.4. And after local calibration, the comparison between predicted and measured total rutting was shown in Figure 5.4 (the triangles). It can be seen that after local calibration, the predicted total rutting from AASHTOWare Pavement M-E Design version 2.1 has good agreement with the measured total rutting on AC overlay AC pavements. *T*-tests were conducted on the bias between predicted and measured total rutting prior to and after local calibration. The detailed *t*-tests results as well as the goodness of fit were shown in Table 5.5. It indicates that the bias between the predicted and measured total rutting was eliminated after local calibration. SEE decreased from 0.56 cm in national calibration to 0.20 cm in local calibration.

Table 5.4 Parameter estimates of the random effect linear model

Variables	Coefficients	Standard Deviation	0.025	0.975
Rutting of asphalt layer	0.11	0.0864	0.004	0.3249
Rutting of base	0.2	0.1901	0.0052	0.6973
Rutting of subgrade	0.671	0.1104	0.4265	0.8659

(2.5% and 97.5% indicates the 95% confidence interval of the parameter estimates.)

Table 5.5 Goodness of fit and bias test statistics for rutting model of AC overlay on AC pavement in linear regression

Analysis Type	Diagnostic Statistics	Results	
		National Calibration	Local Calibration
Goodness of Fit	R^2	0.64	0.68
	SEE	0.56cm	0.20cm
	N	205	205
Biases	H_0: Slope=1.0	p-value<0.0001	p-value=0.43
	H_0: Predicted-measured rutting depth=0 (paired t-test)	p-value<0.0001	p-value=0.12

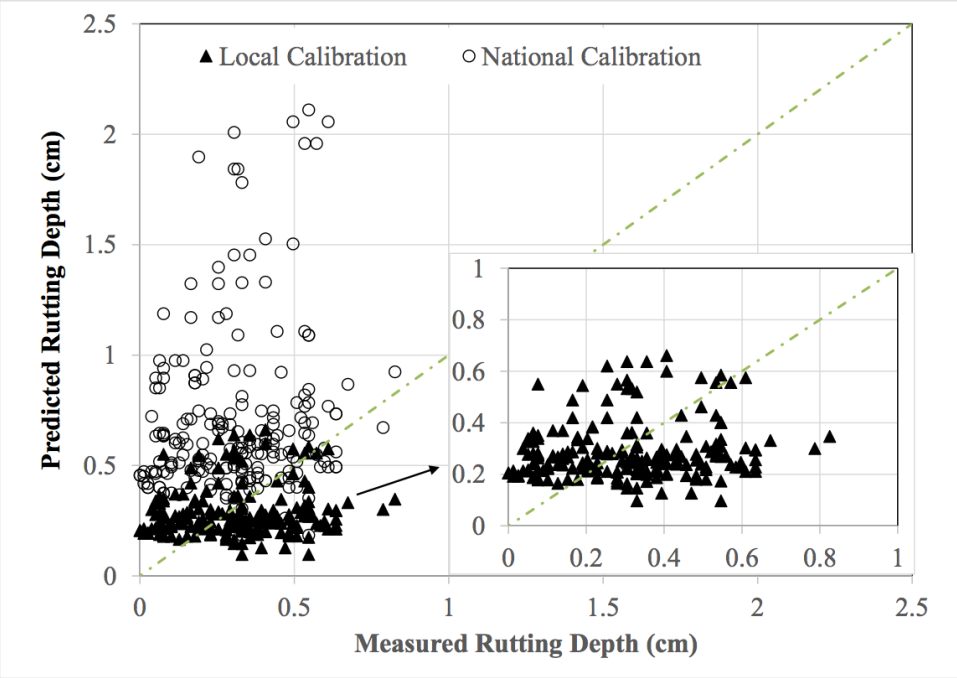

Figure 5.4 Comparison of measured and predicted rutting of asphalt overlay asphalt pavements in linear regression

5.3.2 VALIDATION

The locally calibrated rutting transfer functions were further validated using the resting 90 observations. Similarly, comparison between the predicted and measured total rutting of AC overlay on AC pavements were shown in Figure 5.5. And *t*-tests results for bias between predicted and measured total rutting were summarized in Table 5.6. It can be seen that the goodness of fit between the predicted and the measured total rutting was significantly improved and the bias were eliminated as well. Therefore, the local calibration for AC overlay on AC pavements was validated. SEE decreased from 0.62 cm in national calibration to 0.19 cm in local calibration.

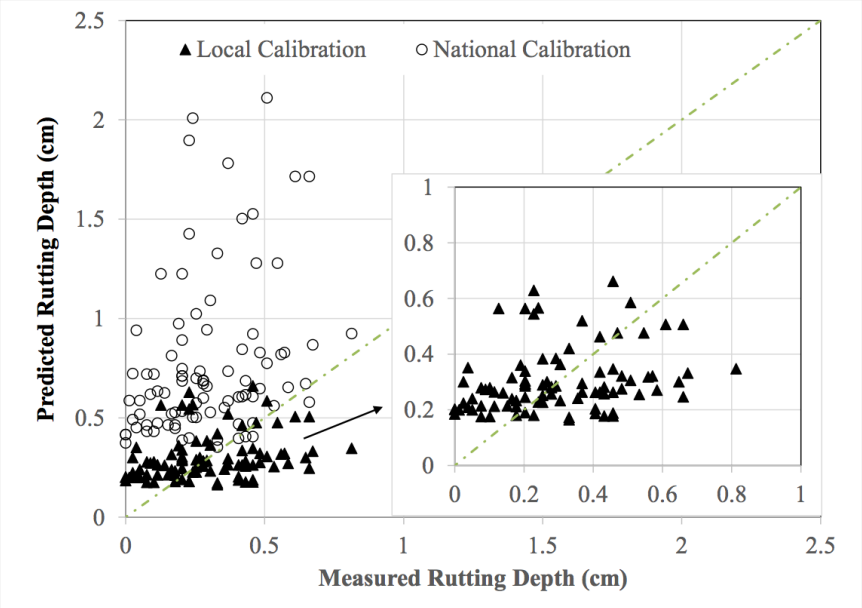

Figure 5.5 Comparison of measured and predicted rutting of asphalt overlay asphalt pavements for validation

Table 5.6 Goodness of fit and bias test statistics for rutting model of AC overlay on AC pavement in validation

Analysis Type	Diagnostic Statistics	Results	
		National Calibration	Local Calibration
Goodness of Fit	R^2	0.68	0.72
	SEE	0.62cm	0.19cm
	N	90	90
Bias	H_0: Slope=1.0	p-value<0.0001	p-value=0.20
	H_0: Predicted-measured rutting depth=0 (paired t-test)	p-value<0.0001	p-value=0.76

5.4 RECALIBRATING THE RUTTING MODEL

5.4.1 GROUPS OF INTERSTATES HIGHWAYS FOR LOCAL CALIBRATION

Asphalt Overlay on Asphalt Pavements

Geographically, Tennessee is narrow in longitudinal direction while very long in latitudinal direction. The monthly average and maximum temperatures of main areas in TN cited from *climate-zone.com* are shown in Figure 5.6. It can be seen that the annual temperatures of main areas in Tennessee are very close. Actually, the mountainous areas (1800-6000ft in elevation) were avoided when Interstates were built except one case, i.e., I-40 Interstates in Cumberland county. Therefore, due to the similarity in temperatures, all the Interstates were treated as the one group in the local calibration on rutting models, except for the I-40 Interstates in Cumberland county which was treated as another group. The total length of Interstates I-40 in Cumberland County is less than 40 miles. Totally, there were 25 pavement sections selected in plain areas from the PMS of Tennessee, as shown in Figure 5.7. The information of the selected pavement sections, including pavement structure, materials, and traffic, was listed in Table 5.7. Similarly, 5 pavement sections were selected from I-40 Interstates in Cumberland County, as shown in Table 5.8.

Table 5.7 Asphalt overlay on asphalt pavements in plain for local calibration on rutting model

Highway	County	Mileage	Year Built	Year Overlay	Initial AADTT (since Overlay)	Overlay (cm)	Existing AC (cm)	Crushed Stone (cm)	20 years of ESALs (Million)
I-40	Knoxville	0-6.9	1973	1986 2002	290	Mill and Replace 1-2in.	31.1Asphalt Surface+8.9Asphalt Base	20.3	1.08
I-81	Greene	6.0-12.3	1975	1985 2003	610	13.3Asphalt Surface	5.7Asphalt Surface+26.7Asphalt Base	7.6	2.26
I-40	Roane	16.2-22.9	1972	1984 1996	685	9.6Asphalt Surface+7.6Asphalt Base	18.4Asphalt Surface+17.8Asphalt Base	25.4	2.55
I-40	Benton	0-8	1966	1989 1998	840	7.6Asphalt Surface+7.6Asphalt Base	25.4Asphalt Base	20.3	3.12
I-75	Campell	27-30.4	1981	1993 2000	840	7.6Asphalt Surface +15.2 Asphalt Base	25.4Asphalt Base	20.3	3.16
I-40	Dickson	9.1-17.8	1970	1986 2000	850	8.3Asphalt Surface +27.9Asphalt Base	17.8Asphalt Base	20.3	3.49
I-75	McMinn	10.9-13.4	1974	1986 2000	1025	11.4Asphalt Surface	5.7Asphalt Surface+17.8Asphalt Base	20.3	3.81
I-75	Anderson	8.3-10.2	1974	1990 2000	1330	8.3Asphalt Surface +10.2Asphalt Base	17.8Asphalt Base	20.3	4.95
I-24	Montgomery	11.7-17.2	1976	1995 2003	1585	3.2Asphalt Surface +12.1Asphalt Base	19.7Asphalt Surface+8.9Asphalt Base	12.7	5.89
I-24	Marion	1.2-6.3	1968	1994 2003	1350	3.2Asphalt Surface+15.2Asphalt Base	4.4Asphalt Surface+8.9Asphalt Base	20.3	5.03
I-75	Hamilton	8.5-15.6	1988	1996 2004	1510	6.4Asphalt Surface+6.4Asphalt Base	7.0Asphalt Surface+10.8Asphalt Base	35.6	5.62
I-40	Jefferson	15.17-20.13	1962	1985 2003	670	5.7Asphalt Surface+8.9Asphalt Base	5.7Asphalt Surface+7.6Asphalt Base	20.3	2.48
I-40	Roane	11.35-16.15	1960	1994	1440	Mill and Replace 1-2in.	3.2Asphalt Surface+7.6Asphalt Base	43.2	5.35
I-40	Smith	0-8.21	1965	1990 2000	1180	Mill and Replace 1-2in.	14.0Asphalt Surface+20.3Asphalt Base	20.3	4.38
I-40	Wilson	12.71-19.69	1966	1989	1625	Mill 1.5in., 3.2Asphalt Surface+5.1Asphalt Base	13.3Asphalt Surface+20.3Asphalt Base	20.3	6.05

Table 5.8 Asphalt overlay on asphalt pavements in mountainous areas for local calibration on rutting model

Highway	County	Mileage	Year Built	Year Overlay	Initial AADTT (since Overlay)	Overlay (cm)	Existing AC (cm)	Crushed Stone (cm)	20 years of EASLs (Million)
I-40	Cumberland	0-6.42	1968	1978/1993/2001/2008	1430	3.2	10.8 Asphalt Surface +27.9 Asphalt Base	20.3	5.30
I-40	Cumberland	7.18-13.52	1968	1978//1993/2001/2008	1620	3.2	10.8 Asphalt Surface+27.9 Asphalt Base	20.3	6.00
I-40	Cumberland	24.84-34.16	1969	1988/1998/2007	1510	3.2	10.8 Asphalt Surface +26.0 Asphalt Base	20.3	5.62
I-40	Cumberland	13.54-18.8	1968	1995/2004	1380	3.2	10.8 Asphalt Surface + 8.9 Asphalt Base	20.3	5.12
I-40	Cumberland	18.8-24.51	1968	1995/2004	1350	3.2	10.8 Asphalt Surface+ 17.8 Asphalt Base	20.3	5.01

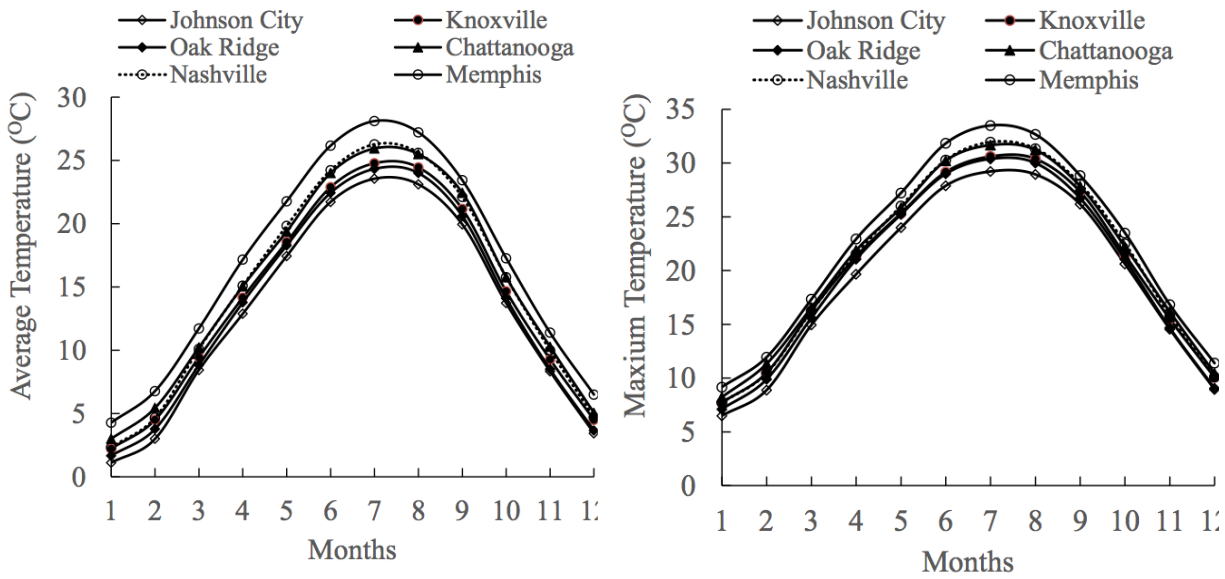

a) Average temperature b) Maximum temperature

Figure 5.6 Monthly temperature in main areas through Tennessee

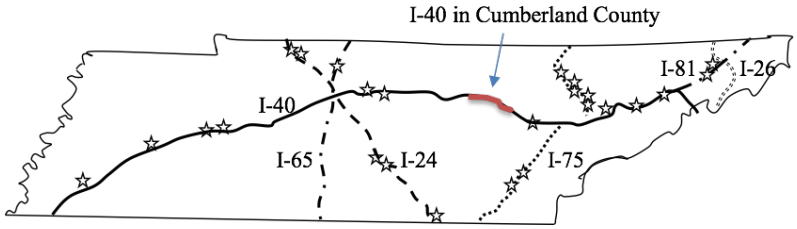

Figure 5.7 Selected AC overlays on AC pavements in plain in TN

Asphalt Overlay on PCC Pavements

The amount of cement concrete pavements is much less than those of asphalt pavements in Tennessee. Six representative sections of asphalt overlays on PCC pavements were selected from the PMS of Tennessee, as shown in Figure 5.8. The information was shown in Table 5.9, including pavement structure, materials, and traffic. The same methodologies were utilized on selecting inputs for asphalt layers, base materials, and soils in AC overlay on PCC pavements as AC overlay on AC pavements. The national default values for PCC slab were adopted.

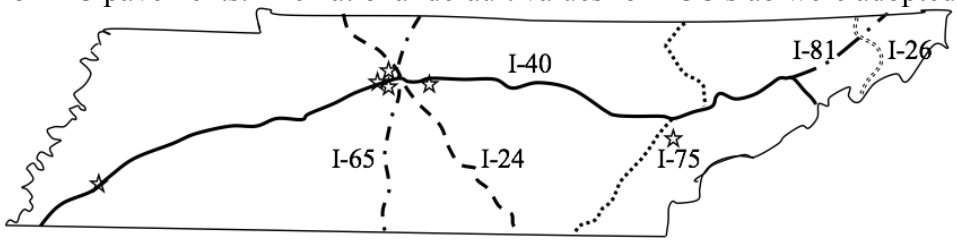

Figure 5.8 AC overlay on PCC pavements sections for local calibrations on rutting models

Table 5.9 Details of AC overlay on PCC pavements Sections

Highway	County	Mileage	Year Built	Year Overlay	Initial AADTT (Since Overlay)	Asphalt Overlay (cm)	Concrete Slab (cm)	Stone Base (cm)
I-40	Madison	7.4-12.4	1965	1988	710	3.2Asphalt Surface +15.2Asphalt Base	22.9	15.2
I-40	Davidson	9.6-13.2	1965	1988	1550	9.5Asphalt Surface+8.9Asphalt Base	25.4	15.2 CTB
I-65	Davidson	0.4-3.5	1964	1992	2350	13.3Asphalt Surface+7.6Asphalt Base	22.9	22.9
I-65	Davidson	20.9-22.9	1970	1982	1120	7Asphalt Surface+14Asphalt Base	22.9	22.9
I-75	Knoxville	8.8-13.7	1972	1993	590	7.6Asphalt Surface +26.7Asphalt Base	22.9	41.9
I-40	Haywood	2.9-10.1	1963	1992	420	7.6Asphalt Surface+8.9Asphalt Base	22.9	15.2CTB

Note: CTB stands for cement treated base.

5.4.2 GROUPS OF STATE ROUTES FOR LOCAL CALIBRATION

Local materials are prone to be used in state routes. In order to address the material variation in Tennessee for state routes, four groups of state routes were divided in this research, basically following the division of Region I, Region II, Region III, and Region IV in Tennessee except that the counties in Region II located in Appalachian valley were classified to Region I, which including Rhea, Meigs, McMinn, Hamilton, Bradley, and Polk. Specifically, the pavement sections from the state routes in each region were selected, as shown in Table 5.10 through Table 5.13 (please see in the following pages).

Table 5.10 State routes sections selected for local calibration in Region I

Highway	County	Mileage	Year Built	Year Overlay	Overlay (in.)	Existing AC (in.)	Crushed Stone (in.)
SR-1	Hawkins	0-1.190	1994	2005	Mill and replace 1-2”	1.25GrD+2.5GrB+7GrA+6CTB	4+6SLP
SR-1	Hawkins	3.53-7.87	1986	1996	Mill and Replace 1-2in.	1GrD+1.25GrC+6GrB+3.5GrA	5
SR-1	Hawkins	31.76-36.05	1970	1985/2002	Mill and Replace 1-2in.	1GrD+1.5GrC+2GrD+4GrB	14
SR-29	Hamilton	25.77-27.93	1994	2008	Mill and replace 1-2”	1.25GrD+2GrB+7.5GrA	12
SR-29	Hamilton	27.93-30.83	1994	2004	Mill and replace 1-2”	1.25GrD+2GrB+7.5GrA	10
SR-29	Morgan	0-7.3	1970	1994	Mill and replace 1-2”	6.75GrD	14
SR-29	Rhea	0-4.2	1992	2004	Mill and replace 1-2”	1.25GrD+2GrB+7GrAs	10
SR-29	Roane	7.78-9.29	1990	2000	Mill and replace 1-2”	1.25GrD+1.25GrC+4GrB+3.5GrAs	10
SR-29	Scott	21.74-27	1962	1992/2000	Mill and replace 1-2”	1.25GrD+3.5GrB+0.75sbst	14
SR-30	Polk	8.4-12.4	1981	1996	Mill and replace 1-2”	1GrD+1.25GrB+2GrA	3
SR-32	Claiborne	0-3.06	1983	1993	Mill and replace 1-2”	1GrD+1.25GrB+3GrC+3.25GrA	10
SR-32	Claiborne	3.06-4.45	1983	1996	Mill and replace 1-2”	1GrD+1.25GrB+3GrC+3.25GrA	10
SR-34	Sullivan	0-5	1986	2001	Mill and replace 1-2”	1GrD+1.25GrC+7GrB+3.5GrA	5
SR-34	Sullivan	5.75-9.21	1976	1986	1.25GrD+1.25GrC	1GrD+3.5GrB	8
SR-34	Washington	0-4.57	1988	1991/2002	Mill and replace 1-2”	1.25GrD+1.25GrC+3GrB+3.5GrA	8
SR-34	Washington	21.83-23.78	1988	2003	Mill and replace 1-2”	1.25GrD+1.25GrC+4GrB+3.5GrA	5
SR-40	Polk	20.11-26.5	1970	1978/1991	Mill and replace 1-2”	1.25GrD+2.25GrB+0.75GrD+1GrC+2.5GrB	8
SR-40	Polk	26.5-30.3	1970	2001	Mill and replace 1-2”	2.5GrD+1GrC+2.5GrB	8
SR-61	Anderson	15.13-16.06	1987	2000	Mill and replace 1-2”	1.25GrD+1.25GrC+2.5GrB	8.5
SR-67	Carter	0-2.77	1988	2004	Mill and replace 1-2”	1.25GrD+1.25GrC+4.5GrB+3.5GrA	9
SR-67	Carter	2.79-3.44	1988	1997	Mill and replace 1-2”	1.25GrD+1.25GrC+2.75GrBm+5.5GrB+3.25GrA	5.5
SR-67	Carter	5.94-7.36	1987	2002	Mill and replace 1-2”	1.25GrD+1.25GrC+1GrB+4GrA	11.5
SR-93	Sullivan	6.1-11.3	1980	1992/2007	Mill and replace 1-2”	1.25GrD+1.5GrB+1.5GrC+1GrD+6GrB	12GrA
SR-111	Hamilton	.9-3.69	1995	2002	Mill and replace 1-2”	1.25GrD+1.25GrC+2GrB+9GrA	18
SR-123	Polk	0-1.23	1987	1995/1999	Mill and replace 1-2”	1.25GrD+1.25GrC+6.5GrA	8
SR-158	Knox	1.47-2.58	1974	1993/2003	Mill and replace 1-2”	1GrD+5.5GrB	6
SR-302	Rhea	0-5.67	1987	2000	Mill and replace 1-2”	2GrD+0.75 SBST	6
SR-302	Rhea	8.91-12.27	1988	2003	Mill and replace 1-2”	1.25GrD+2GrB	6
SR-313	Polk	0-1.79	1991	2001	Mill and replace 1-2”	1.25GrD+1.25GrC+1GrA	6

Table 5.11 State route sections selected for local calibration in Region II

Highway	County	Mileage	Year Built	Year Overlay	Overlay (in.)	Existing AC (in.)	Crushed Stone (in.)
SR-1	Cannon	0-6.06	1990	2001	Mill and replace 1-2”	1.25GrD+4GrB+4GrA	12in
SR-1	Cannon	8.01-9.63	1984	1998	Mill and replace 1-2”	1.25GrD+2GrC+2GrB	13.5
SR-8	Sequatchie	19.05-23.31	1966/1977	1995	2GrD+1.25GrB	1GrD+2.5GrB+0.75 GrD+3.5GrB	8
SR-8	Sequatchie	23.31-30.06	1976/1986/1994	2002	Mill and replace 1-2in.	1.25GrD+2GrB+1GrD+3.5GrB	8
SR-10	Bedford	10.74-11.92	1994	2001	Mill and replace 1-2in.	1.25GrA+1GrC+3.5GrB+3GrC+4GrA	6
SR-55	Warren	1.09-4.76	1992	2001	Mill and replace 1-2”	1.25GrD+2GrB+7.5GrA	10
SR-55	Warren	4.76-8.33	1992	2002	Mill and replace 1-2”	1.25GrD+2GrB+7.5GrA	10
SR-55	Warren	8.6-12.63	1992	2005	Mill and replace 1-2”	1.25GrD+1.75GrB+6GrA	5CTB+4stone+6SLP
SR-111	Overton	0-3.7	1993	1996	Mill and replace 1-2”	1.5GrD+1.75GrB+6GrAs	10
SR-111	Putnam	2-5.27	1990	1993/2004	Mill and replace 1-2”	1.25GrD+2GrB+3.5GrAs	10
SR-111	Sequatchie	9.4-10.4	1976	1993	1.25GrD+1.75GrB	1GrD+2.5GrB	8.5

Table 5.12 State route sections selected for local calibration in Region III

Highway	County	Mileage	Year Built	Year Overlay	Overlay (in.)	Existing AC (in.)	Crushed Stone (in.)
SR-1	Rutherford	19.12-28.35	1993	2006	Mill and Replace 1-2in.	1.25GrD+6GrA+3.5GrAS	5
SR-1	Rutherford	28.35-29.65	1990	2002	Mill and Replace 1-2in.	1.25GrD+4GrB+4GrA	12
SR-6	Sumner	26.79-31.76	1965/1987	2001	Mill and replace 1-2in.	1.25GrD+0.75sbst+1.5GrC1.25GrD+2.5GrB+7GrAs	8
SR-10	Rutherford	5.24-10.25	1994	2007	Mill and replace 1-2in.	1.25GrD+2GrB	10.5+6LFAB
SR-13	Wayne	21.6-26.7	1972/1993	2006	Mill and replace 1-2in.	2.25GrD+3.5GrB	8
SR-76	Stewart	11.38-13.28	1934	1960/1980/1995	1.25GrD+1.5GrB	1GrD+1.5GrB+2.5GrD+3MIP	3.5
SR-76	Stewart	14.6-22.09	1979	1993	1.25GrD+0.5LvCC	1GrD	6
SR-96	Rutherford	0-2.1	1974	1996/1998	Mill and replace 1-2”	2.25GrD+5.75GrB	10
SR-96	Rutherford	0-6.3	1973	1996/1998	Mill and replace 1-2”	2.25GrD+1GrC+4.75GrB	10
SR-96	Rutherford	9.25-11.51	1975	1991	Mill and replace 1-2”	1GrD+5.5GrB	8
SR-99	Maury	16.94-18.33	1982	1990/1994/2007	Mill and replace 1-2”	1.25GrD+0.5GrC+2.5GrD	8
SR-155	Davidson	17-18.4	1988	2000/2008	Mill and replace 1-2”	1.25GrD+1.25GrC+6GrB+3.5GrA	8
SR-254	Davidson	8.24-13.97	1991	2008	Mill and replace 1-2”	1.25GrD+6GrB+3.5GrA	10
SR-374	Montgomery	0-2.66	1987	1995	Mill and replace 1-2”	2.25GrD+2GrC	6

Table 5.13 State route sections selected for local calibration in Region IV

Highway	County	Mileage	Year Built	Year Overlay	Overlay (in.)	Existing AC (in.)	Crushed Stone (in.)
SR-3	Dyer	2.37-6.73	1968/1981/1990	2005	Mill and Replace 1-2in.	1.25GrD+1.25GrC+2GrD+1GrC+4GrB+0.5SBST	14
SR-3	Lauderdale	20.5-25	1968/1972/1992	2008	Mill and Replace 1-2in.	1GrD+1.25GrC+1GrD+1GrC+4GrB	14
SR-5	Chester	4.26-9.63	1989	1996/2005		1.25GrD+1GrC+2.5GrB+3.5GrA	5
SR-5	Madison	0-5	1976	1996	1.25GrD+2gr-b	1GrD+4GrB	8
SR-5	Madison	5-8.21	1977/1986	1996	Mill and replace 1-2in.	1.25GrD+1.25GrB+1.25GrD+1.25GrB	14Gravel
SR-14	Shelby	2.69-5.72	1991	2006	Mill and replace 1-2”	1.25GrD+1.25GrC+4GrB+3.5GrA	5CTB
SR-14	Shelby	5.72-7.26	1990	2006	Mill and replace 1-2”	1.25GrD+1.25GrC+4GrB+3.5GrA	5CTB
SR-20	Dyer	.81-6.48	1995	2002/2008	Mill and replace 1-2”	1.25GrD+1.75GrB+6GrA	6
SR-20	Dyer	7.78-12.36	1971	1974/1987/2006	Mill and replace 1-2”	**1.25GrD+1.25GrC**+2GrD+0.5SBST	14
SR-20	Madison	0-1.76	1992	2004	Mill and replace 1-2”	1.25GrD+2GrB+6GrA	10
SR-20	Madison	1.77-6.62	1970	1998/2009	Mill and replace 1-2”	2.25GrD+5GrB	6CTB
SR-22	Weakley	0-4.86	1959	1963/1985	1.25GrD+1.25GrC	1.25GrD+2.5GrB+0.75SBST	14
SR-22	Weakley	4.86-9.93	1959	1963/1986	1.25GrD	1.25GrD+2.5GrB+0.75SBST	14
SR-22	Weakley	9.93-14.6	1959	1963/1987	1.25GrD+1.25GrC	1.25GrD+2.5GrB+0.75SBST	14
SR-Dyer	Shelby	0-2.1	1994	2001	Mill and replace 1-2”	1.25GrD+1.5GrC+1.5GrB	6
SR-69	Benton	1.5-8.92	1991	2004	Mill and replace 1-2”	1.25GrD+1.5GrB+1.75GrC+3.5GrA	8
SR-69	Henry	1.2-6.13	1970	1986/1995	In 1995 Overlay 200-400PSY	1GrD+1GrB+3.5GrC+0.75GrD+4GrB	8
SR-69	Henry	12.04-13.02	1976	1992	Mill and replace 1-2”(add 1.25GrD+1.5GrB)	1GrD+4.75GrB	8
SR-76	Henry	0-4.27	1972	1982/1991	Mill and replace 1-2” (Overlay 200-400psy)	1.25GrD+1.5GrB+1GrD+1.25GrC+2.75GrB+2.75GrA (already considered mill)	6
SR-76	Henry	4.27-7	1972	1982/1991/2002	Mill and replace	1.25GrD+1.5GrB+1GrD+1.25GrC+2.75GrB+2.75GrA (already considered mill)	6
SR-76	Henry	25.72-30.54	1964	2002	Mill and replace 1-2”	.75GrD+2GrB+3.75GrC	8GrC
SR-215	Obion	0.86-2.06	1985	1987/1994	Mill and replace 1-2”	1.25GrD+1.5GrC+2.5GrB+1.25GrA	8
SR-86	Fayette	0-1.9	1974	1987/1998	Mill and replace 1-2”	2GrD+2GrB+2GrC	8gravel
SR-86	Shelby	0-3.29	19774	1987/1998	Mill and replace 1-2”	7GrD	8gravel

5.4.3 LOCAL CALIBRATION ON RUTTING MODELS ON INTERSTATE HIGHWAYS

The local calibration coefficients of the rutting model for Interstates highways have been determined, as shown Table 5.14.

Table 5.14 Summary on local coefficients of rutting models on Interstates highways

Local coefficients	AC overlay on AC pavements		AC overlay on PCC pavements
	Mountain areas	Plain areas	
Asphalt layer	0.177	0.111	1.70
Base layer	1.034	0.196	-
Subgrade	0.159	0.722	-

5.4.4 CALIBRATING THE RUTTING MODEL FOR STATE ROUTES

As stated in the previous quarter report, more than 70 sections across the whole state were collected, 29 sections in region I, 11 sections in region II, 13 sections in region III and 23 section in region IV (only 15 sections presented in this report).

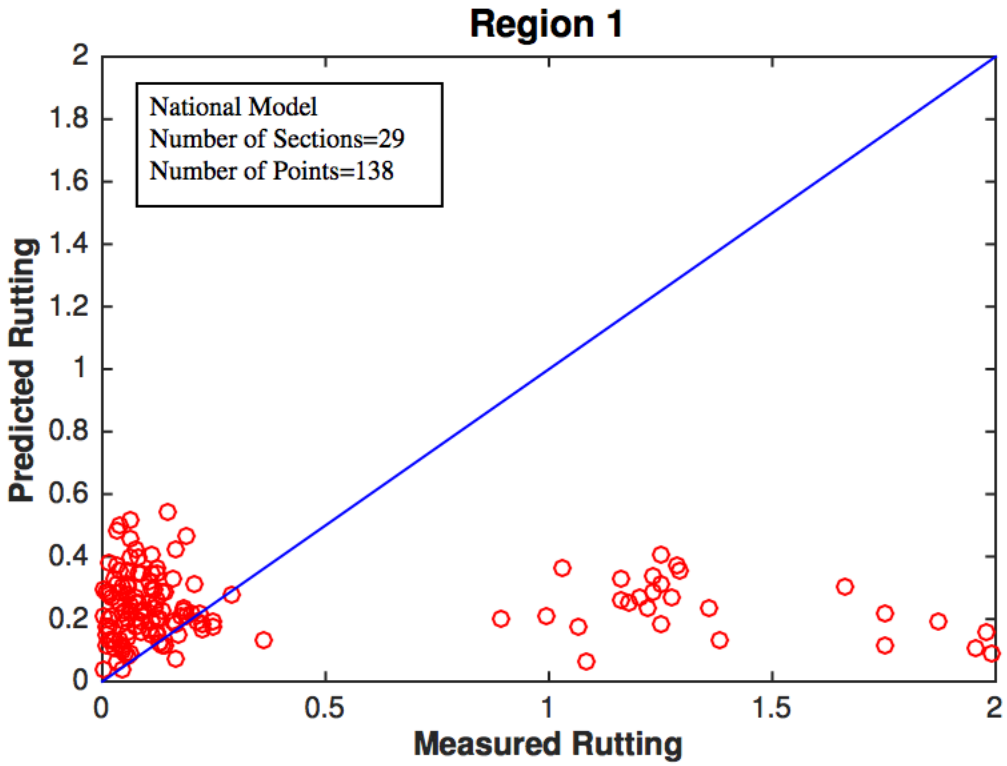

Figure 5.9 Comparison of Measured Rutting with Predicted Rutting in Region I

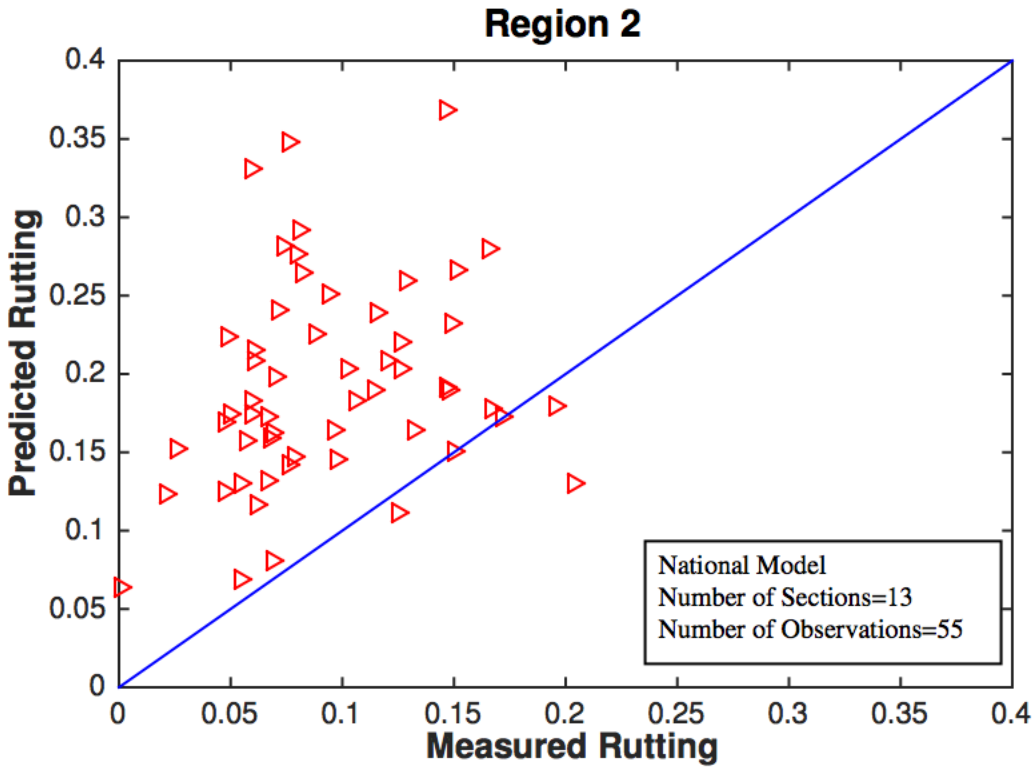

Figure 5.10 Comparison of Measured Rutting with Predicted Rutting in Region II

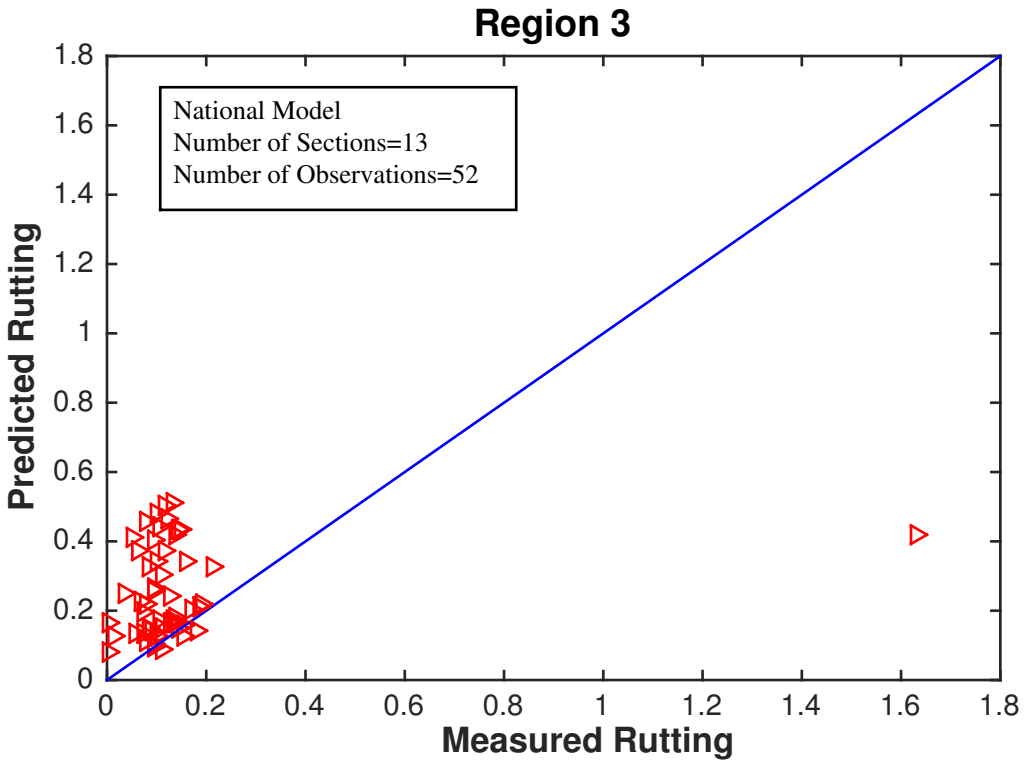

Figure 5.11 Comparison of Measured Rutting with Predicted Rutting in Region III

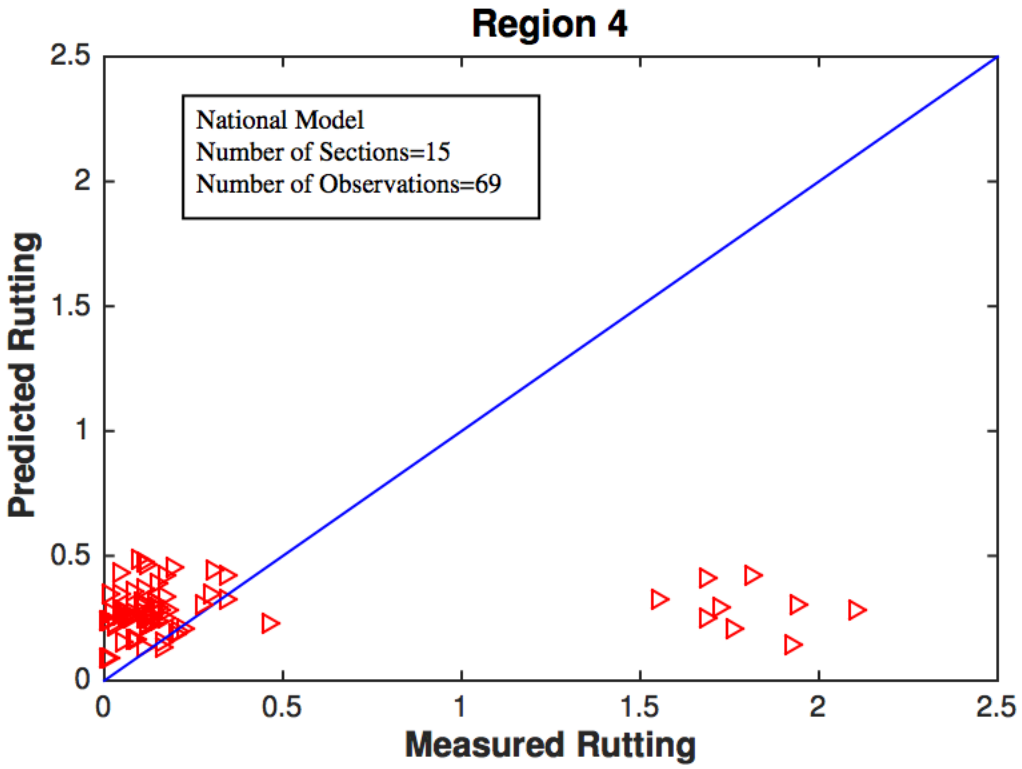

Figure 5.12 Comparison of Measured Rutting with Predicted Rutting in Region IV

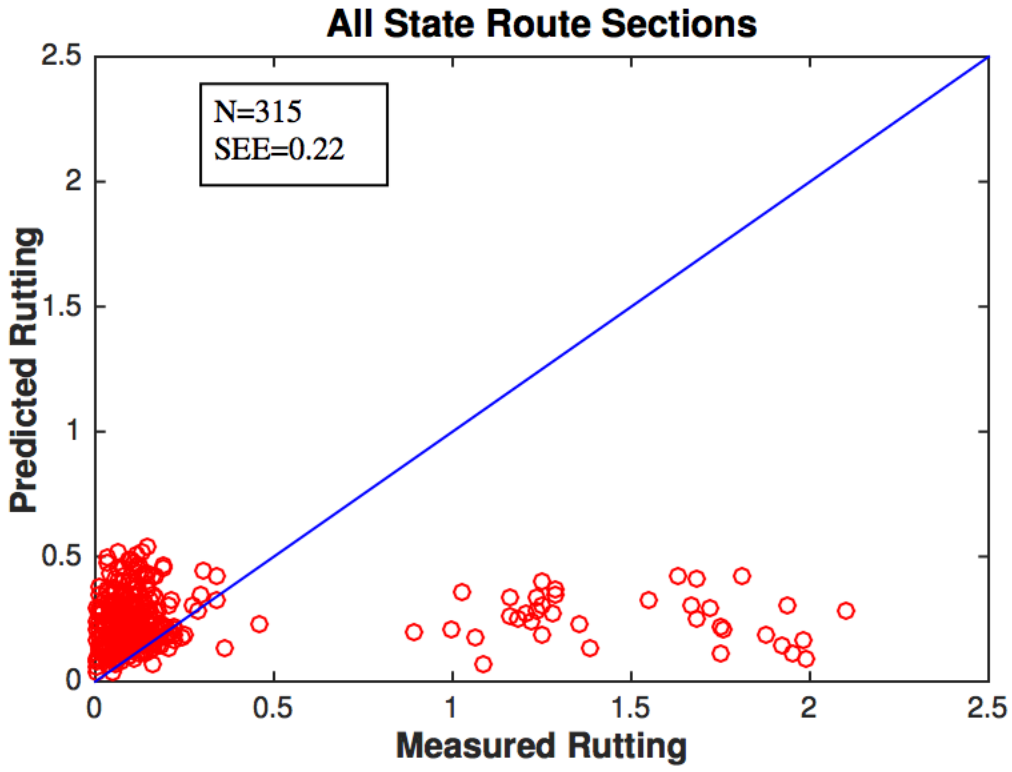

Figure 5.13 Comparison of Measured Rutting with Predicted Rutting

As Figure 5.9 through Figure 5.12 showed, for all 4 regions, the global model generally over predicted the rutting. However, for region I, there are more than 20 observations fall below the line of equity, this part of these observations were identified as outliers, and was later removed for calibration. For region III, there is only one observation fall below the line of equity, this should be probably also an outlier, in the later calibration process, and it was removed as well. Figure 5.13 showed all the observations in one plot. As indicated in Figure 5.13, compared to the plot for each region, the sum of squared error (SEE) of all the observations much greater. Therefore, calibrate the rutting model for each region seems to be able to improve the accuracy of the prediction.

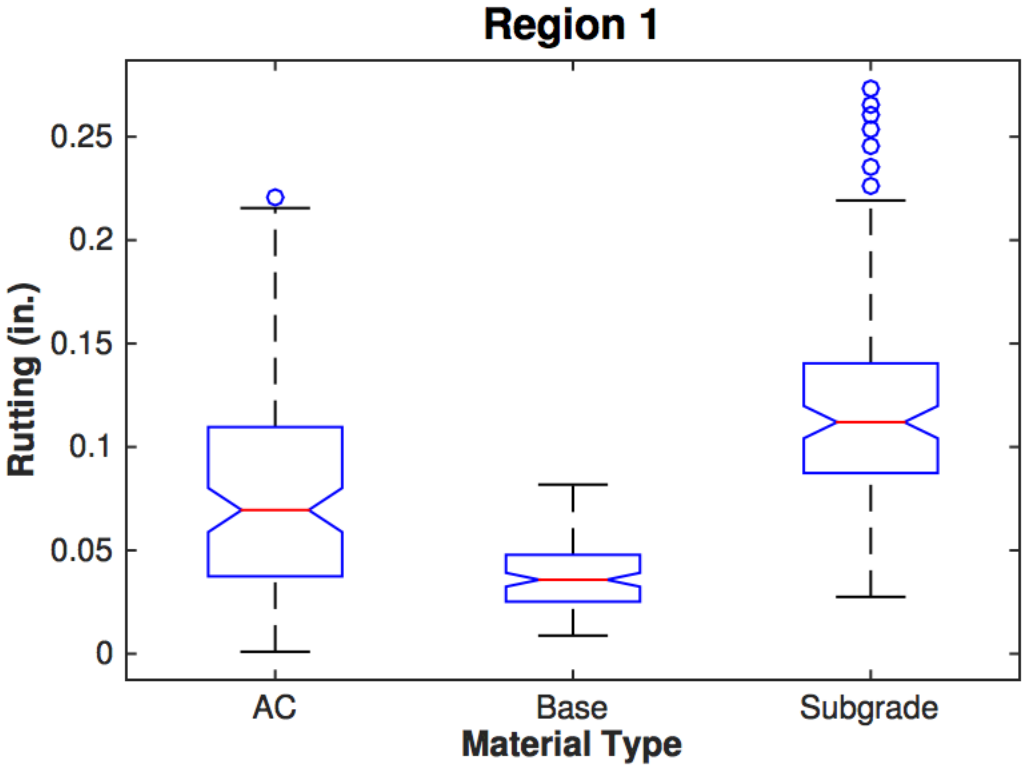

Figure 5.14 Predicted rutting in each layer

Figure 5.14 showed predicted rutting from each type material in pavement. As Figure 5.14 indicated, the part of rutting from subgrade is the largest, followed by rutting from asphalt mixtures layer, the part from base materials are the smallest. To simplify the calibration process, (Hall et al. 2011) assumed the calibration coefficient for unbounded base material is the same as national model, this assumption is also adopted in this report.

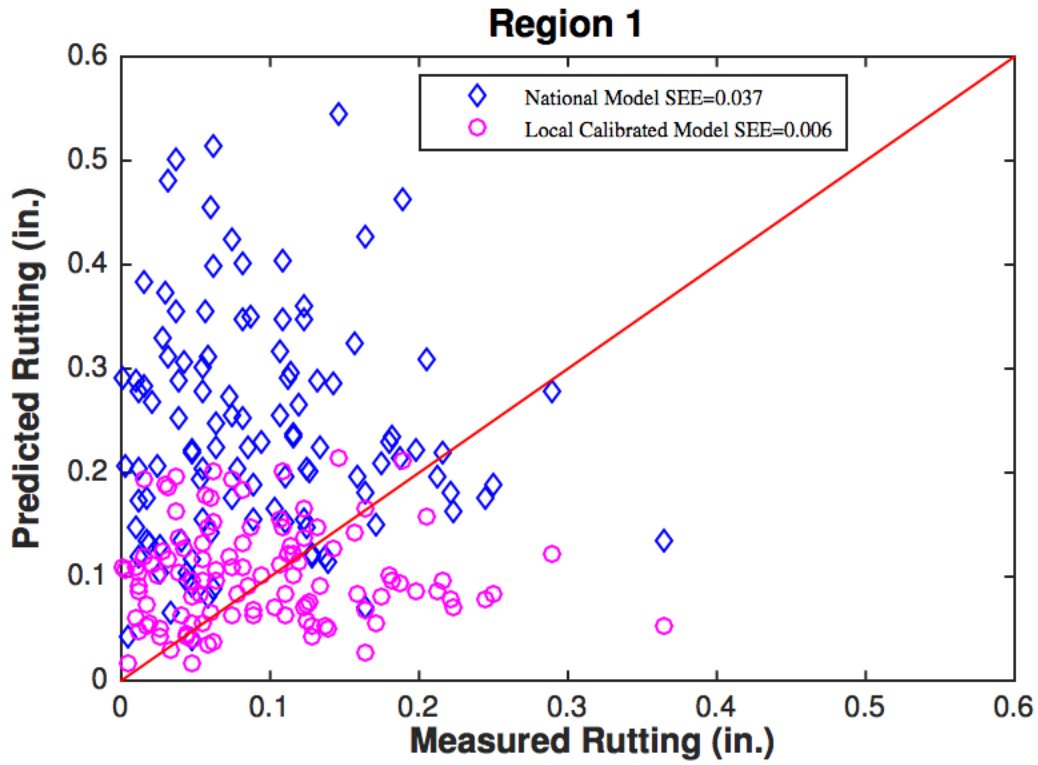

Figure 5.15 Comparison of calibrated model with global model for region I

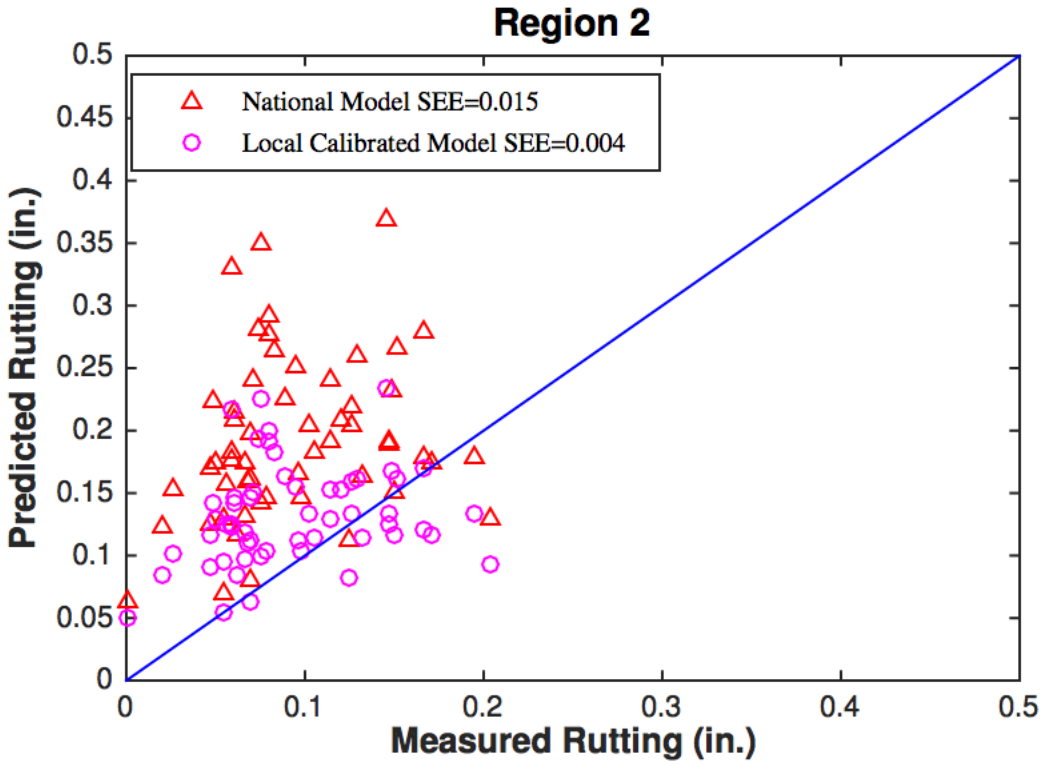

Figure 5.16 Comparison of calibrated model with global model in region II

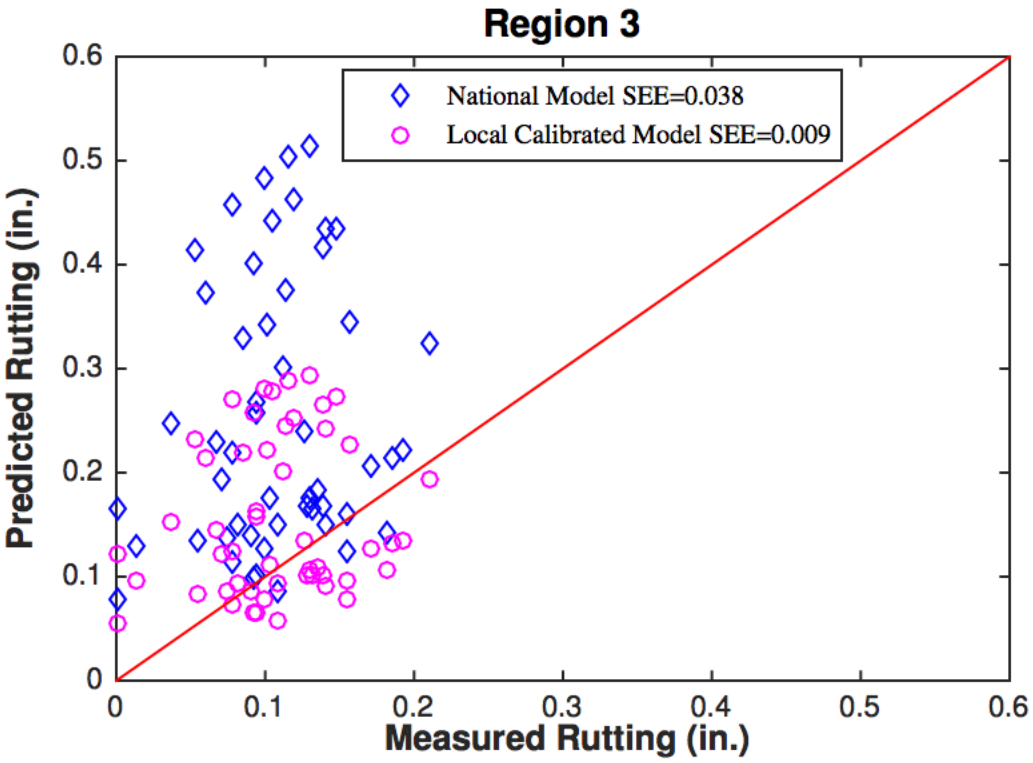

Figure 5.17 Comparison of calibrated model with global model in region III

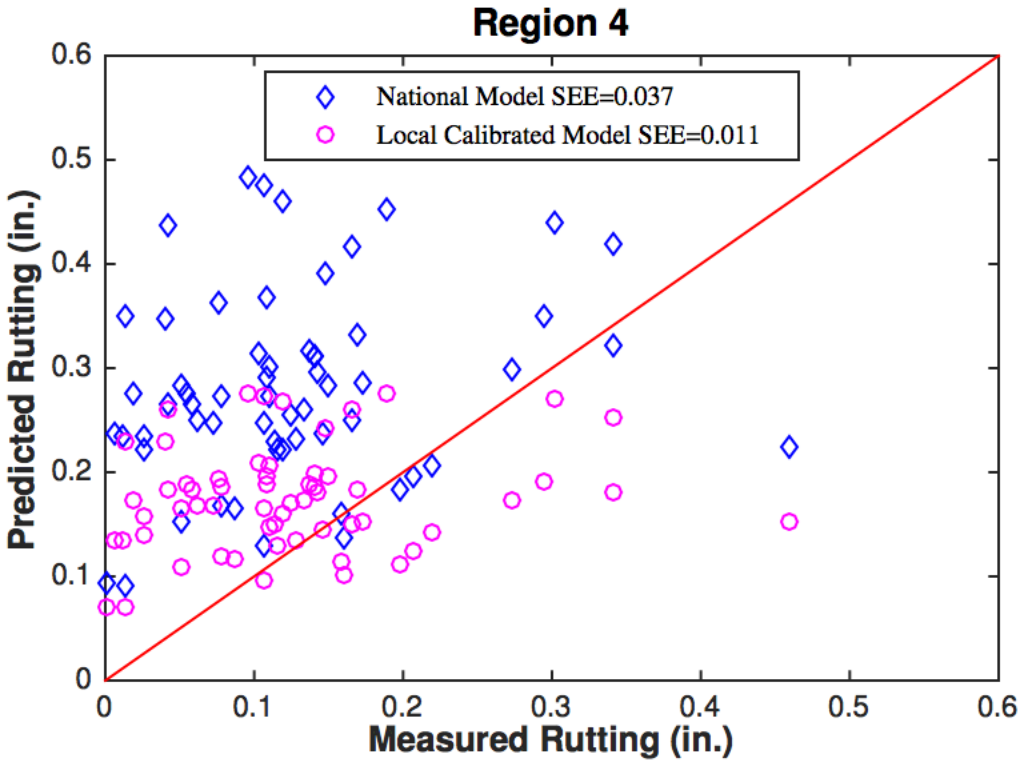

Figure 5.18 Comparison of calibrated model with global model in region IV

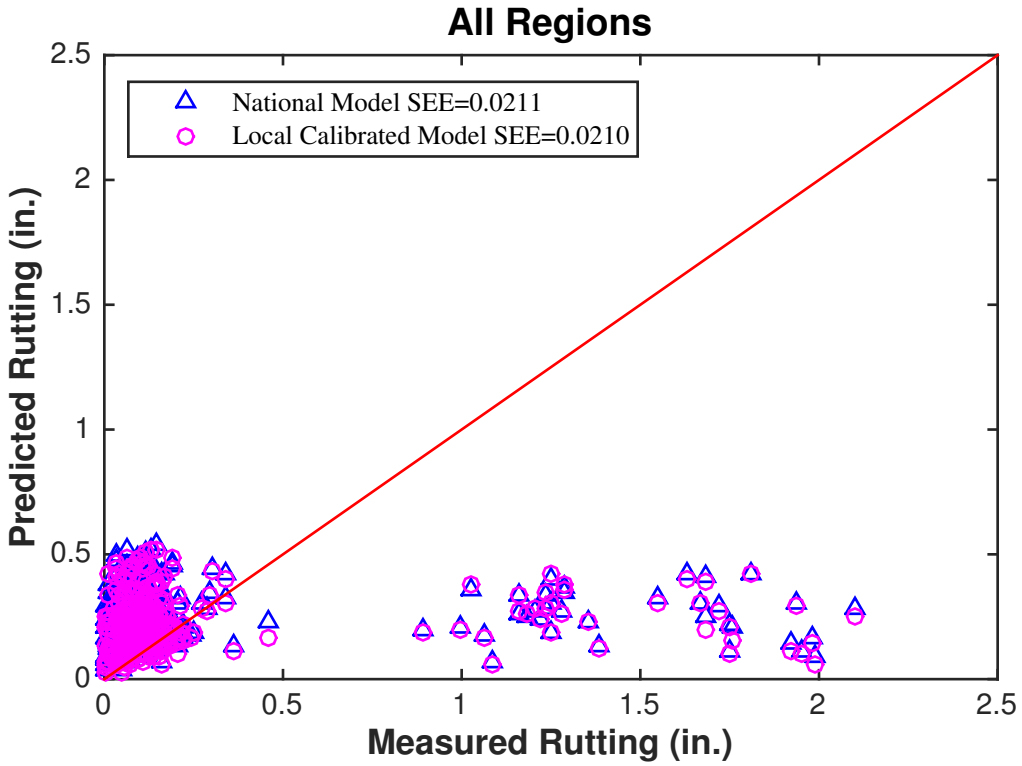

Figure 5.19 Comparison of calibrated model with global model in all regions

Figure 5.15 through Figure 5.18 showed the comparison of calibrated rutting with rutting predicted from global model. As can be observed from Figure 5.15 through Figure 5.18, after calibration, all the points were draw from over the line of equity to the line itself. Meanwhile, the sum of estimate error (SEE) was also significantly reduced. Of all the 4 regions, rutting model for region 1 seems to be calibrated best. This is probably because more sections are collected and thus more observations, collecting more sections from other 3 regions should also help to increase the quality of calibration. Figure 5.19 showed the prediction from model calibrated by observations combined with all 4 regions. When data in all 4 regions were combined, as can be seen from Figure 5.19, the locally calibrated model does not help to improve the accuracy of prediction. Therefore, calibrating all the transfer functions by their geographical feature could help to improve the accuracy of prediction. All the local calibration coefficients are presented Table 5.15.

Table 5.15 Local calibration coefficients for the four regions in TN

Region Number	AC	Unbounded Base	Subgrade	SEE
I	0.0476	1	0.366	0.006
II	0.112	1.000	0.817	0.004
III	0.236	1.000	0.674	0.009
VI	0.026	1.000	0.781	0.011

CHAPTER 6 LOCAL CALIBRATION AND VALIDATION OF BOTTOM-UP CRACKING TRANSFER FUNCTION

6.1 INTRODUCTION

Fatigue cracking is one of the major distresses that directly related to traffic loading of pavement system during a specific service period. The action of repeated traffic loads would induce tensile stress and shear stress at the bottom of asphaltic mixture or PCC layers, which will finally make micro-damage develop into macro-cracking, thus causing the bounded layer losing integrity (El-Basyouny and Witczak 2005). Generally, Miner's law was use to predict fatigue cracking, which is based on the concept of accumulated damage (Huang 1993). A survey (Pierce and McGovern, 2014) on the implementation of MEPDG in North America shows that most States in US consider the alligator cracking model in Pavement ME to be the most challenging one to calibrate. It is known that automatic image identification vehicles collect the cracking data, such as alligator and longitudinal cracking. These data are usually high in variability. One of the purposes for local calibration was to deal with these problems. Local calibration is a process to remove the bias and minimize the variability of the prediction in the national models. Several methods can be used to achieve this goal. The gradual reduced gradient (GRG), genetic algorithm, and curve fitting are among the most popular methods. The gradual reduced gradient method can be readily brought about with the Excel® Solver in a more straightforward but effort-costing way which starts with running a serial of combination of coefficients iteratively and finishes with finding the best combination of coefficients that have the minimum standard error of estimate (SEE) or sum of squared error (SSE). However, there are disadvantages in these methods. The GRG and genetic algorithm are unable to use robust statistics to exclude the effect of potential outliers. The trial-and-error method is too time-consuming and it may only find the combination of coefficients that has minimum SEE or SSE in a specific experiment. However, for curve fitting, more controls are allowed to consider the impacts of potential outliers. It can also be fast when the experiments are coded to execute in a batch. In this study, this method was implemented through the curve fitting procedure in the MATLAB. This procedure uses a trust-region optimization algorithm and robust least square implemented by bisquare weights. Trust region algorithm, also known as restricted step methods, denotes the subset of the region of objective function that is approximated using a model function. If a proper model in the subset region is found, then the region is expanded. Otherwise, the subset region needs to be contracted until an adequate model is found. The bisquare weight minimizes a weighted sum of squares, where the weight given to each data point depends on how far the point is from the fitted line. The closer the point is to the fitting line, the higher weight it gains. Thus, it minimizes the effect of the outliers.

6.2 DATA PREPARATION

Although there are 114 LTPP test sites in Tennessee, some sites seem to be in good condition or maintenance was applied before severe deterioration occurred, in addition to that a lot of the test sites are absent of detailed materials and maintenance records, which are required to conduct analyses in MEPDG. Therefore, only twelve sites were found suitable for validation of the alligator-cracking model for Tennessee in the LTPP database.

6.2.1.1 Materials

Asphalt and Asphalt Mixture

The properties of asphalt can be found in the INV_PMA_ASPHALT table of Inventory module. Information about asphalt contained in this table include asphalt grade (ASPHAT_GRADE) in penetration, the source of asphalt, asphalt specific gravity, original asphalt viscosity at 140 and 275 and original penetration. Two types of asphalt were recorded in TN LTPP database, grade 14 (penetration grade 85-100 PEN) and grade 4 (AC-20).

Base

Only two sections in Tennessee LTPP database with full descriptions of rehabilitation activities were identified in the Info-Pave database. Both inputs for bounded (chemical stabilized), such as cement stabilized, lime stabilized and unbounded base materials were referred to (NCHRP 2004).

Subgrade

Since only four sections located in Tennessee in LTPP database are available, all the inputs for subgrade were obtained from the literature. According to the coordinate of location provided in the Administration module of the LTPP online database, the resilient modulus data of subgrade were obtained from Shu and Huang (2009).

6.2.1.2 Structure

Pavement structure information is included in the Administration module (Administration.mdb), pavement structure (LAYER_NO), the layer thicknesses (REPR_THICKNESS), materials (LAYER_TYPE and MATL_CODE) are included in the SECTION_LAYER_STRUCTURE table, other information included in the calibration process in this table is the maintenance information, i.e. CONSTRUCTION_NO, with a value of 1, means never been overlaid, with a value of 2, means it has been overlaid once, which can be used to differentiate whether the pavement is a new flexible pavement or an overlay in creating projects in AASHTOWare. When the layer thickness is less than one inch (the minimum layer thickness allowed in AASHTOWare), it will be combined with adjacent layer. Table 6.1 gives an example of how pavement structure data were recorded in the LTPP database named Info-Pave.

Table 6.1 Example of pavement structure data in LTPP Info-Pave

SHRP_ID	STATE_CODE	CONSTRUCTION_NO	LAYER_NO	DESCRIPTION	LAYER_TYPE	REPR_THICKNESS	MATL_CODE
1023	47	1	1	7	SS		120
1023	47	1	2	6	GS	6	303
1023	47	1	3	5	TB	6.1	321
1023	47	1	4	4	AC	3.4	1
1023	47	1	5	4	AC	1.5	1
1023	47	1	6	3	AC	0.4	1
1023	47	3	1	7	SS		120
1023	47	3	2	6	GS	6	303
1023	47	3	3	5	TB	6.1	321
1023	47	3	4	4	AC	3.4	1
1023	47	3	5	4	AC	1.5	1
1023	47	3	6	3	AC	0.4	1
1023	47	3	7	8	AC	0.5	84
1023	47	3	8	1	AC	1.2	1

Note: LAYER-NO indicate the number of layers in a structure; LAYER_TYPE indicates the materials used for a layer; REPR_THICKNESS is the representative thickness of a layer; MATL_CODE is an index used in LTPP to describe the materials.

6.2.1.3 Traffic

Traffic data was collected from the Traffic module (Traffic.mdb) in LTPP database, when traffic data began to record, the estimated two-way annual average daily traffic in all lanes, estimated two-way annual daily traffic number of trucks in all lanes were provided in the TRF_HIST_EST_EASL table. The TRF_ESAL_COMPUTED table gives the ESAL computed corresponding to a certain year. The vehicle class data was included in the TRF_HIST_CLASS_DATA table.

6.2.1.4 Distresses

Distress data were obtained in the MON_DIS_AC_REV of the Monitoring module (Monitoring.mdb). Only alligator cracking (GATOR_CRACKING) data were used in this study. Refer to (El-Basyouny and Witczak 2005), an assumption was also made here that bottom-up cracking is the only cracking results from repeated traffic load, even though longitudinal cracking is also a type of fatigue cracking, but it is counted as a separate type. There are three different levels of alligator cracking in the LTPP database, all three levels of cracking were summed up without any weight coefficients included, as was used in previous research (El-Basyouny and Witczak 2005). Figure 3 showed seven sections collected from the MON_DIS_AC_REV table with full distress history records, which are required during the calibration process. As indicated in Figure 3, the levels of alligator crack in TN LTPP test sites are relatively low. This could be attributed to that all the sites were maintained very well, or alligator cracking has been converted into other type of cracking, such as block cracking.

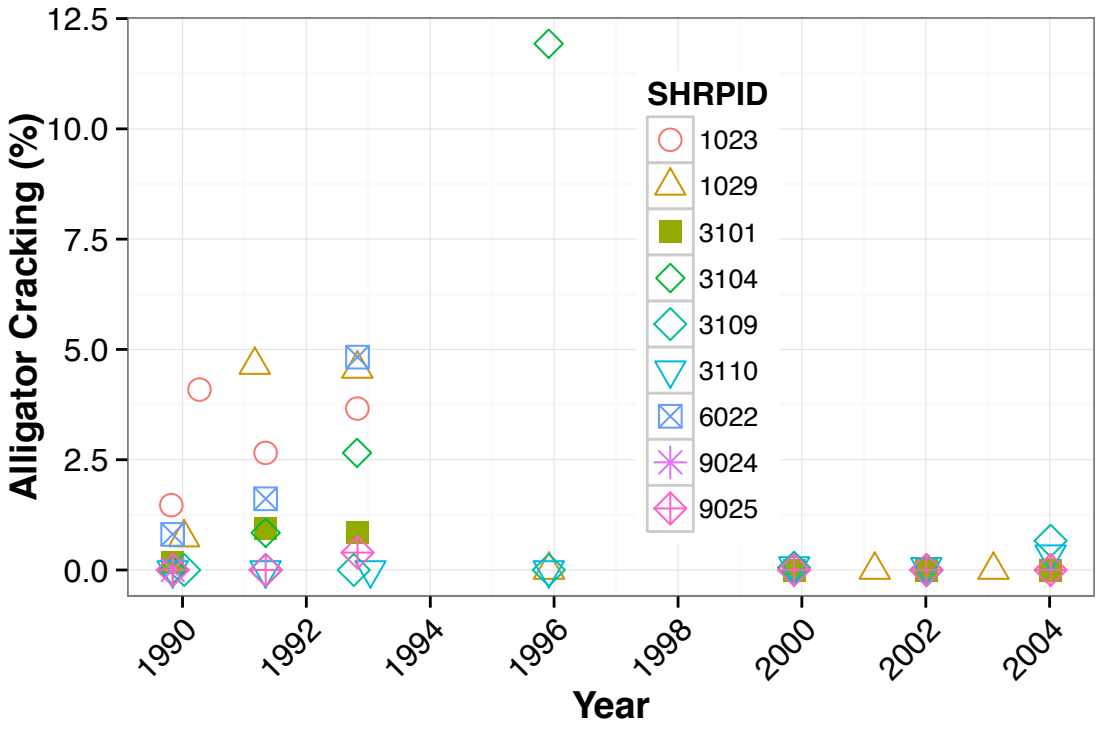

Figure 6.1 Alligator cracking time history

6.3 CALIBRATION PLAN

Table 6.2 Fatigue cracking model calibration coefficients in other States

Washington State (Li et al. 2009b)	C1=1.071;C2=1;C3=6000
North Carolina (Kim and Muthadi 2007)	C1=0.437;C2=0.151;C3=6000
Arkansas (Kang and Adams 2007)	C1=0.688;C2=0.294;C3=6000
New Mexico (Tarefder and Rodriguez-Ruiz 2013)	C1=0.625;C2=0.25;C3=6000
National Calibration (ARA 2004)	C1=1;C2=1;C3=6000

Table 6.2 shows the local calibration coefficients identified in the literature, it can be observed that C_3 is held constant as 6000. Therefore, in our calibration process, this method was also used in the initial attempts to verify the national model.

Several combinations of C_1 and C_2 were set to find the one that could minimize the SSE (standardized square error). By referring to method of (Tarefder and Rodriguez-Ruiz 2013), an experiment matrix was designed, as indicated in Table 6.3, 36 combinations of C_1, C_2, C_3 were designed.

Table 6.3 Experiment matrix design

Set number	C1	C2	C3
1	0.2	0.2	6000
2	0.2	0.6	6000
3	0.2	1	6000
4	0.2	1.4	6000
5	0.2	1.8	6000
6	0.2	2.2	6000
7	0.6	0.2	6000
8	0.6	0.6	6000
9	0.6	1	6000
10	0.6	1.4	6000
11	0.6	1.8	6000
12	0.6	2.2	6000
13	1	0.2	6000
14	1	0.6	6000
15	1	1	6000
16	1	1.4	6000
17	1	1.8	6000
18	1	2.2	6000
19	1.4	0.2	6000
20	1.4	0.6	6000
21	1.4	1	6000
22	1.4	1.4	6000
23	1.4	1.8	6000
24	1.4	2.2	6000
25	1.8	0.2	6000
26	1.8	0.6	6000
27	1.8	1	6000
28	1.8	1.4	6000
29	1.8	1.8	6000
30	1.8	2.2	6000
31	2.2	0.2	6000
32	2.2	0.6	6000
33	2.2	1	6000
34	2.2	1.4	6000
35	2.2	1.8	6000
36	2.2	2.2	6000

However, this method is only applicable for illustration purpose, due to the tremendous number of runs needed to implement this matrix. That is, each section needed to be run 36 times. It usually takes about 10 minutes to finish a run even for a fast-configured desktop. It is

impossible to execute all the sections collected for calibration, which are more than 100 sections. Therefore, the Excel Solver® method was used to minimize the difference between the measured cracking and predicted cracking, and to determine the local coefficients of alligator cracking and longitudinal cracking model.

6.4 CALIBRATION OF BOTTOM-UP FATIGUE CRACKING MODEL

The final number of the load repetition fatigue model (2002 D-G model) is given as

$$\begin{aligned} N_f &= 0.00432 \times k_1 \times C \left(\frac{1}{\varepsilon_t}\right)^{1.9492} \left(\frac{1}{E}\right)^{1.281} \\ C &= 10^M \\ M &= 4.84\left(\frac{V_b}{V_a + V_b} - 0.69\right) \end{aligned} \tag{7}$$

where:
N_f = Number of repetitions to fatigue cracking;
ε_t= Tensile strain at the critical location,
C=correction factor;
V_a = Effective binder content (%);
V_b=Air voids (%).

$$FC = \left(\frac{6000}{1 + e^{C_1 - C_2 \times \log DI}}\right) \times \left(\frac{1}{60}\right) \tag{8}$$

where,
FC = fatigue cracking (% of the lane area);
$C_1 = -2 \times C_2$;
$C_2 = -2.40874 - 29.748 \times (1 + h_{ac})^{-2.856}$;
D = Miner's Law damage, $D = \sum_{i=1}^{T} \frac{n_i}{N_j}$, n_i =actual traffic for period i. N_i = Traffic allowed under conditions prevailing in i; T = total number of periods.

The Miner's damage D is one of the most important outputs of AASHTOWare can get from the resulted PDF or excel report, once the fatigue cracking damage has been obtained from AASHTOWare, the fatigue cracking could be predicted with Equation 8, then compare the predicted and measured fatigue cracking in LTPP database. After obtaining all these data, calibration could then be carried out, Figure 6.2 gives an illustration of the output of bottom-up cracking obtained from the AASHTOWare.

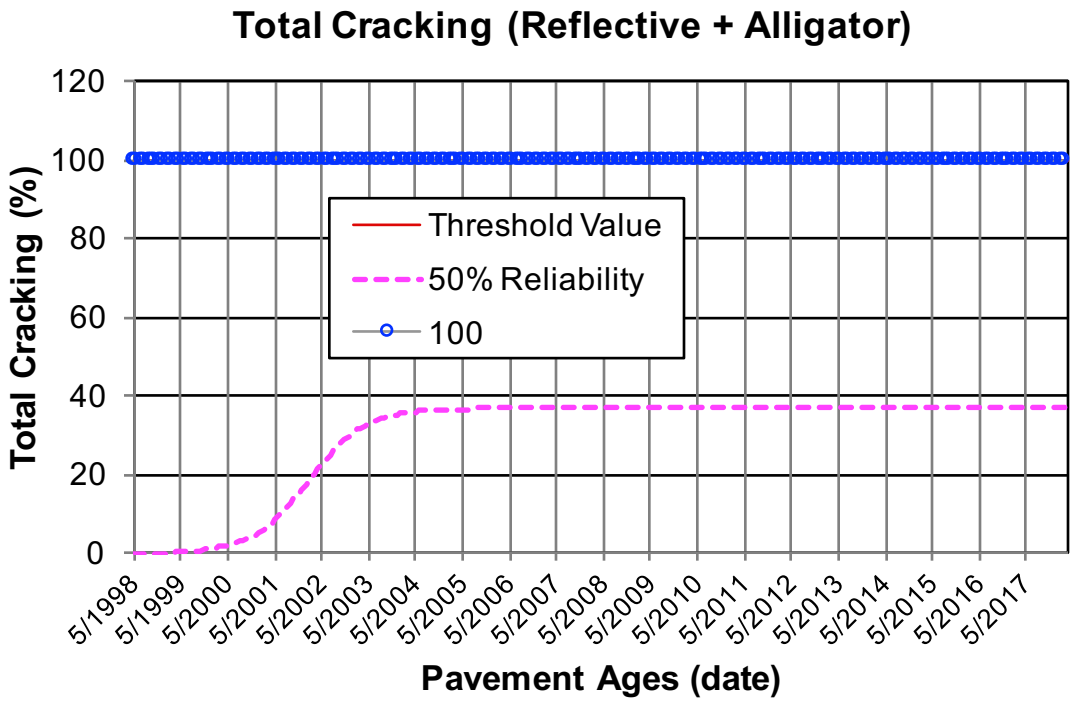

Figure 6.2 AASHTOWare Alligator Cracking damage output

COLLECTING BASIC INFORMATION AND DISTRESSES INFORMATION OF PAVEMENT SECTIONS FROM LTPP

A total of 20 pavement sections from LTPP database were collected. After examining these sections, 5 sections were found to have full records of construction history (construction date), comprehensive traffic (AADDT), materials properties, such as asphalt binder grade and type, subgrade type (coarse or fine), pavement structural information including layer thickness, noticeable distress level, and climate record. Climate information was obtained from adjacent climate monitoring station in LTPP database. For example, for the section with a SHRP ID 1023, the climate module in LTPP has a record of location for this section, Latitude = 36.18705, Longitude = −84.09882. It is close to the weather monitoring station in Jackson (Latitude = 36.18705, Longitude = −84.09882), and therefore Jackson was selected as the climate station in AASHTOWare. Five sections were selected to verify whether the national default coefficients for fatigue cracking on asphalt pavements are appropriate for Tennessee conditions. Basic information including pavement structure, materials, and traffic were collected from LTPP. Additionally, the fatigue cracking data was mined from the LTPP. The basic information of the pavement section selected was shown in Table 19.

Table 6.4 Basic information of selected sections to verify the fatigue cracking model

SHRP ID	Asphalt layers (in.)	Base layer (in.)	Subgrade	Traffic (AADTT)
1023	(1.9+3.4+6.1)	6 (Crushed stone)	A-1-a	4000
1028	7.0+5.1	10(Crushed stone)	A-1-a	560
1029	2.8+8.9+4.0	6.1 (Crushed gravel)	A-4	300
3075	5.0	9.2	A-1-a	1000
3101	5.6+3.3	5.5(A-1-a)	A-4	150

Note: There is no specific asphalt mixture information for the asphalt layers in LTPP. Typical asphalt mixture types were adopted in Pavement ME Design software according to the routine in Tennessee.

RESULTS FROM THE EXPERIMENT MATRIX

The predicted fatigue cracking on the pavement section 1023 was compared with the measured data from LTPP, as shown Figure 27. It can be seen from these two plots that, with the default global calibration coefficient input, when the time is around 1990, the predicted damage was just slightly greater than 4%. However, for measured damaged as showed in Figure 6.3, when the time is around 1990, the damage was as large as 24%, which was 6 times greater than the predicted one. It is seen in Figure 6.3, as the time increases, bottom up cracking increases as well. Due to a maintenance or rehabilitation applied at the end of 1990, the fatigue cracking began to decrease at the end of 1990.

Therefore, local calibration is necessary for the fatigue-cracking model in Pavement ME Design. The following part focused on local calibration on the fatigue-cracking model. The local calibration coefficients were changed to determine the optimal combination, as shown in Table 6.5. The comparisons between the predicted fatigue cracking corresponding to the local coefficients Table 6.5 and the measured fatigue cracking data were shown in Table 6.5 and Figure 6.4. It indicates that when the default calibration coefficients were utilized, for the 5 sections collected, except for section 3101, poor agreements were reached between the predicted and the measured fatigue cracking. What's more, the differences between predicted and measured alligator cracking showed no definite pattern, as indicated in Figure 2. For instance, the predicted alligator cracking in section 1023, 1028, and 3075, 3101 were greater than the measured ones while the predicted alligator cracking in section 1029 is smaller than the measured one.

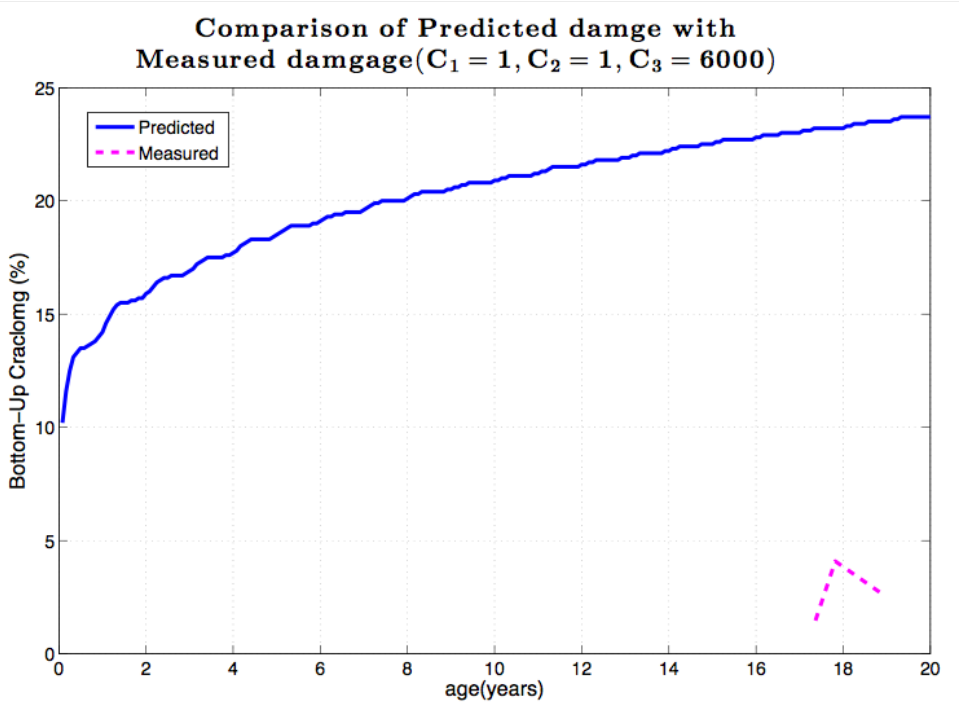

Figure 6.3 Predicted Bottom-up fatigue cracking development curve for section 1023

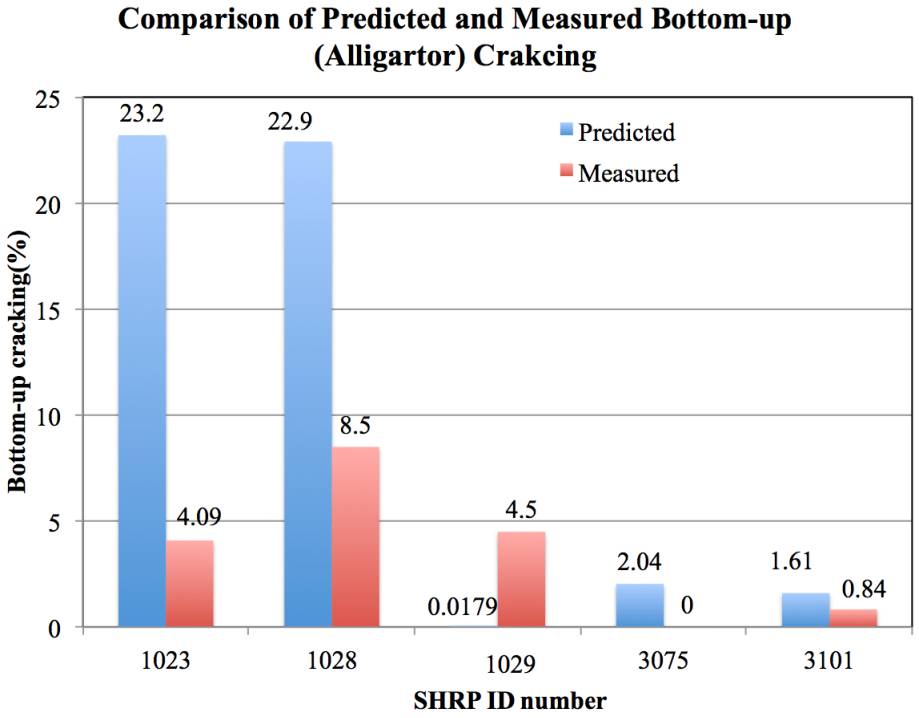

Figure 6.4 Comparisons between Predicted and Measured Bottom-Up Cracking

According to (Li et al. 2009b) and the model in (AASHTO 2008) local calibration guide (Equation 9), Table 6.5 was designed to determine the optimal calibration coefficient for a certain section, for example, section with SHRP ID 1023. It can be observed from Table 6.5, when default calibration coefficients were utilized (set 1), the relative difference between the predicted damage and the measured one is greater than 6 times. Therefore, in order to ensure the designed pavements will not experience too high damage than allowable alligator cracking. In this case, pavement should be designed thicker than it should be or to use better materials than it needs. This will result in wasting of the always-limited budget for rehabilitating existing pavements or constructing new pavements. After 36 run of analyses, as indicated in Table 6.5, when C_1=0.6, C_2=0.6, C_3=6000, as showed in Table 6.5, the difference between the predicted alligator cracking and measured alligator cracking is the smallest. Though only one section is used to determine the optimal calibration coefficients, this method could also be used to verify and validate the alligator-cracking model calibrated with much more sections, which is our next step of work.

$$FC = \frac{6000}{1 + e^{C_1 \times C_1^* + C_2 \times C_2^* \, log_{10}(DI \times 100)}} \tag{9}$$

Where, $C_2^* = -2.40874 - 49.748 \times (1 + h_{ac})^{-2.856}$, $C_1^* = -2C_2^*$

It is worth noting that the activities on calibrating fatigue cracking is not that valid yet, due to the limited number of pavement sections investigated. More pavement sections will be covered in the following work, as well as statistical methodologies. The target for this local calibration is to remove the bias between the predicted and measured fatigue cracking data and to minimize the variance of the prediction from the fatigue-cracking model.

Table 6.5 Experiment matrix (Section 1023, when section received a rehabilitation)

Set number	C1	C2	C3	Predicted damage	Measured damage	Difference
1	0.2	0.2	6000	23.2	4.09	19.1
2	0.2	0.6	6000	16.2	4.09	12.1
3	0.2	1	6000	11.1	4.09	7.0
4	0.2	1.4	6000	7.41	4.09	3.3
5	0.2	1.8	6000	4.89	4.09	0.8
6	0.2	2.2	6000	3.19	4.09	0.9
7	0.6	0.2	6000	4.12	4.09	0.03
8	0.6	0.6	6000	2.68	4.09	1.4
9	0.6	1	6000	1.74	4.09	2.4
10	0.6	1.4	6000	1.12	4.09	3.0
11	0.6	1.8	6000	0.725	4.09	3.4
12	0.6	2.2	6000	0.467	4.09	3.6
13	1	0.2	6000	0.607	4.09	3.5
14	1	0.6	6000	0.39	4.09	3.7
15	1	1	6000	0.251	4.09	3.8
16	1	1.4	6000	0.1601	4.09	3.9
17	1	1.8	6000	0.104	4.09	4.0
18	1	2.2	6000	0.066	4.09	4.0
19	1.4	0.2	6000	0.0878	4.09	4.0
20	1.4	0.6	6000	0.0557	4.09	4.0
21	1.4	1	6000	0.0358	4.09	4.1
22	1.4	1.4	6000	0.023	4.09	4.1
23	1.4	1.8	6000	0.0147	4.09	4.1
24	1.4	2.2	6000	0.0095	4.09	4.1
25	1.8	0.2	6000	0.0123	4.09	4.1
26	1.8	0.6	6000	0.0079	4.09	4.1
27	1.8	1	6000	0.0051	4.09	4.1
28	1.8	1.4	6000	0.0033	4.09	4.1
29	1.8	1.8	6000	0.0021	4.09	4.1
30	1.8	2.2	6000	0.0014	4.09	4.1
31	2.2	0.2	6000	0.0018	4.09	4.1
32	2.2	0.6	6000	0.0007	4.09	4.1
33	2.2	1	6000	0.0006	4.09	4.1
34	2.2	1.4	6000	0.0005	4.09	4.1
35	2.2	1.8	6000	0.0003	4.09	4.1
36	2.2	2.2	6000	0.0002	4.09	4.1

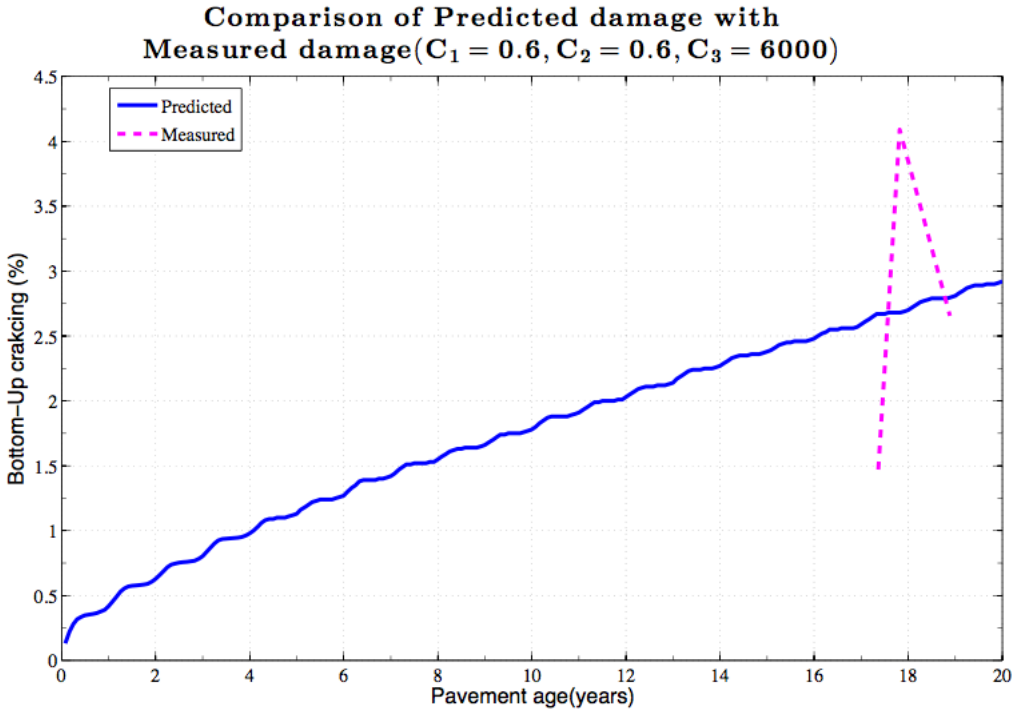

Figure 6.5 Measured bottom-up fatigue cracking development curve for section 47-1023

METHODOLOGY FOR ALLIGATOR CRACKING MODEL CALIBRATION

As has been used in the rutting model, the Microsoft Excel® Solver is a simple but powerful tool to determine the coefficients of a model with restraints, and minimizing the estimated square error (SEE) between the predicted distress and measured distress in our case. A lot of researches in other States have confirmed the feasibility of using this tool for calibration efforts (Kang and Adams 2007; Kim and Muthadi 2007; Aguiar-Moya et al. 2009). Therefore, Microsoft Excel® Solver will be used to calibrate the Bottom-Up cracking (alligator) model, Top-Down cracking (wheel-path longitudinal cracking) and the roughness predicting (IRI) model for our later calibration work.

6.4.1 CALIBRATION OF THE FATIGUE CRACKING MODEL

6.4.1.1 Alligator transfer function

Two types of load-related cracking are predicted in the MEPDG, namely, the alligator cracking and longitudinal cracking. The MEPDG assumes that alligator or area crack initiated at the bottom of the HMA layers and propagated to the surface with continued truck traffic, while longitudinal cracks are assumed to initiate at the surface (AASHTO 2008). The allowable number of axle-load applications needed for the incremental damage index approach to predict both types of load related cracking (alligator and longitudinal) are shown in Equation 10.

$$N_{(f-HMA)} = k_{(f1)}(C)(C_H)\beta_{f1}(\varepsilon_r)^{(k_{f2}\,\beta_{f2})}\,(E_{HMA})^{k_{f3}\beta_{f3}} \quad (10)$$

where:

$N_{f\text{-}HMA}$ = Allowable number of axle-load applications for a flexible pavement and HMA overlays,

ε_r = Tensile strain at critical locations, calculated by the structural response model, in./in.,

E_{HMA} = Dynamic compressive modulus of the HMA, psi,

k_{f1}, k_{f2}, k_{f3} = Global field calibration parameters (from the NCHRP 1-40D re-calibration; k_{f1}=-0.007566, k_{f2}=-3.9492 and k_{f3}=-1.281), and

β_{f1}, β_{f2}, β_{f3} = Local or mixture specific field calibration constants; for the global calibration effort, these constants were set to 1.0.

$$C = 10^M, M = 4.84\left(\frac{V_{be}}{V_a + V_{be}} - 0.69\right) \quad (11)$$

where V_{be} = Effective asphalt content by volume, %; V_a = Percent air voids in the HMA, and C_H = Thickness correction term, dependent on type of cracking.

MEPDG calculates the incremental damage indices on a grid pattern including the whole HMA layers at their critical depths. According to Minor's Law, the incremental damage index (ΔDI) is calculated by dividing the actual number of axle loads by the allowable number of axle load ($N_{f\text{-}HMA}$ in Equation 10) within a certain time increment and axle-load interval for each axle type. The cumulative damage index (DI) for each critical location is determined by summing the incremental damage indices over time, as shown in

$$DI = \sum(\Delta DI)_{j,m,l,p,T} = \sum\left(\frac{n}{N_{f-HMA}}\right)_{j,m,l,p,T} \quad (12)$$

where: n = Actual number of axle-load application within a specific time period, j= axle-load interval, m = axle-load type (single, tandem, tridem, quad, or special axle configuration, l = Truck type using the truck classification groups included in the MEPDG, p = Month, and T = Median temperature for the five temperature intervals or quintiles used to subdivide each month).

Sections from PMS were collected to verify fatigue cracking model in MEPDG. The area of alligator cracking and length of longitudinal cracking are calculated from the total damage over time, as shown in Equation 11, using different transfer functions. Equation 12 is the relationship used to predict the amount of alligator cracking on an area basis.

$$FC_{Bottom} = \frac{1}{60}\frac{C_4}{1 + e^{(C_1C_1^* + C_2C_2^* \log(DI*100)}} \quad (13)$$

where:

FC_{Bottom} = Area of alligator cracking that initiates at the bottom of the HAM layer, % of total lane area,

DI = Cumulative damage index at the bottom of the HMA layers, and

C_1, C_2, C_4 - Transfer function regression constants; C_4=6000; C_1=1.00; C_2=1.00.

C_2^* = -2.40874-49.748×$(1+H_{HMA})^{-2.856}$, C_1^* = -2C_2^*, H_{HMA} = Total HMA thickness, in.

6.5 VERIFY FATIGUE TRANSFER FUNCTION WITH PMS DATA

Figure 6.8 showed the distribution of total thickness of asphalt mixture layer (H_{ac}) used for calibration. This graph represented the typical total thickness of asphalt mixture layer of Interstates in Tennessee. As indicated in Figure 6.8, more than 80% of the sections with total thickness of asphalt mixture greater than 10 inches. About 16% of the sections with H_{ac} fall in the range of 4-10 inches. Overall, the total thicknesses of asphalt pavements in Interstates of Tennessee are relatively thick.

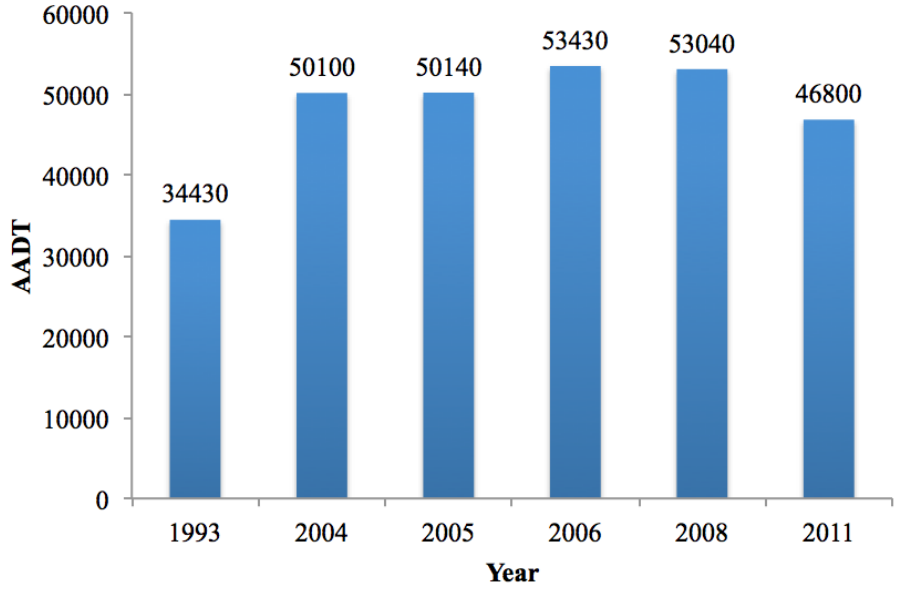

Figure 6.6 AADT vs. time (I40-CN11 (Cheatham)-Plus)

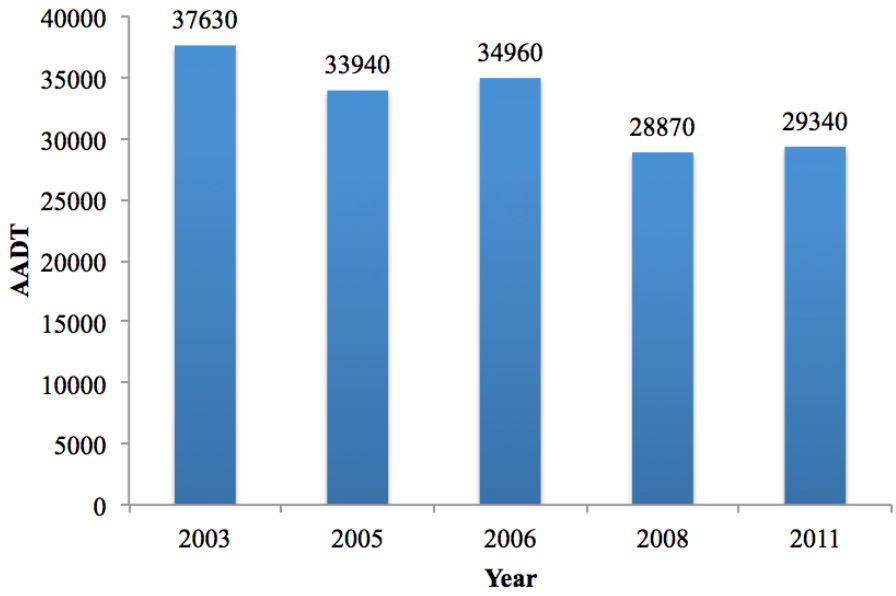

Figure 6.7 AADT vs. time (I40-CN18 (Cumberland)-Plus)

Table 6.6 Basic information of the sections to verify the fatigue cracking model on asphalt pavement

Highway	County	Mileage	Year Built	Year Overlay	Initial AADTT (Since overlay)	Overlay (cm)	Existing AC (cm)	Crushed Stone (cm)	20 year ESALs (Million)
I-40	Knoxville	0-6.9	1973	1986 2002	290	Mill and Replace 1-2in.	31.1Asphalt Surface+8.9Asphalt Base	20.3	1.08
I-81	Greene	6.0-12.3	1975	1985 2003	610	13.3Asphalt Surface	5.7Asphalt Surface+26.7Asphalt Base	7.6	2.26
I-40	Roane	16.2-22.9	1972	1984 1996	685	9.6Asphalt Surface+7.6Asphalt Base	18.4Asphalt Surface+17.8Asphalt Base	25.4	2.55
I-40	Benton	0-8	1966	1989 1998	840	7.6Asphalt Surface+7.6Asphalt Base	25.4Asphalt Base	20.3	3.12
I-75	Campell	27-30.4	1981	1993 2000	840	7.6Asphalt Surface +15.2 Asphalt Base	25.4Asphalt Base	20.3	3.16
I-40	Dickson	9.1-17.8	1970	1986 2000	850	8.3Asphalt Surface +27.9Asphalt Base	17.8Asphalt Base	20.3	3.49
I-75	McMinn	10.9-13.4	1974	1986 2000	1025	11.4Asphalt Surface	5.7Asphalt Surface+17.8Asphalt Base	20.3	3.81
I-75	Anderson	8.3-10.2	1974	1990 2000	1330	8.3Asphalt Surface +10.2Asphalt Base	17.8Asphalt Base	20.3	4.95
I-24	Montgomery	11.7-17.2	1976	1995 2003	1585	3.2Asphalt Surface +12.1Asphalt Base	19.7Asphalt Surface+8.9Asphalt Base	12.7	5.89
I-24	Marion	1.2-6.3	1968	1994 2003	1350	3.2Asphalt Surface+15.2Asphalt Base	4.4Asphalt Surface+8.9Asphalt Base	20.3	5.03
I-75	Hamilton	8.5-15.6	1988	1996 2004	1510	6.4Asphalt Surface+6.4Asphalt Base	7.0Asphalt Surface+10.8Asphalt Base	35.6	5.62
I-40	Jefferson	15.17-20.13	1962	1985 2003	670	5.7Asphalt Surface+8.9Asphalt Base	5.7Asphalt Surface+7.6Asphalt Base	20.3	2.48
I-40	Roane	11.35-16.15	1960	1994	1440	Mill and Replace 1-2in.	3.2Asphalt Surface+7.6Asphalt Base	43.2	5.35
I-40	Smith	0-8.21	1965	1990 2000	1180	Mill and Replace 1-2in.	14.0Asphalt Surface+20.3Asphalt Base	20.3	4.38
I-40	Wilson	12.71-19.69	1966	1989	1625	Mill 1.5in., 3.2Asphalt Surface+5.1Asphalt Base	13.3Asphalt Surface+20.3Asphalt Base	20.3	6.05

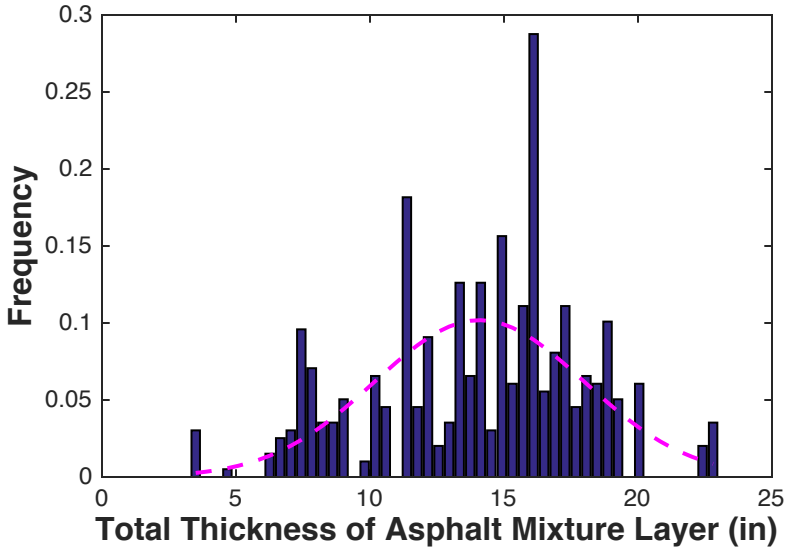

Figure 6.8 Distribution of total thickness of asphalt mixture layer

6.5.1.1 Calibrating the Alligator Cracking Model with PMS Distress Data

Due to the deficiency in LTPP distress data, the maintenance records, distress data, traffic data in PMS were used as the main source of inputs for local calibration. As shown in Figure 6.9, about 40% of the alligator cracking is less than 5% of lane area, less than 10% of the alligator cracking is greater than 10% of the lane area. However, due to the scarcity in maintenance records of newly constructed pavements, most of the sections used for calibration were asphalt mixture overlays. Meanwhile, because the number of sections of concrete pavement and PCC overlaid with asphalt mixture are very low and the level of alligator cracking in all sections are very low, the alligator cracking model for PCC pavements and asphalt mixture overlays on PCC pavements were not considered for calibration. As shown in Figure 6.10, the level of predicted alligator cracking is much lower than those recorded in PMS. Most of the predicted alligator cracking is less than 1%, which was hugely deviated from the measured ones. This entails strong needs to shorten the gap between the predictions and the measurements, thus to improve the accuracy of prediction or future design practice.

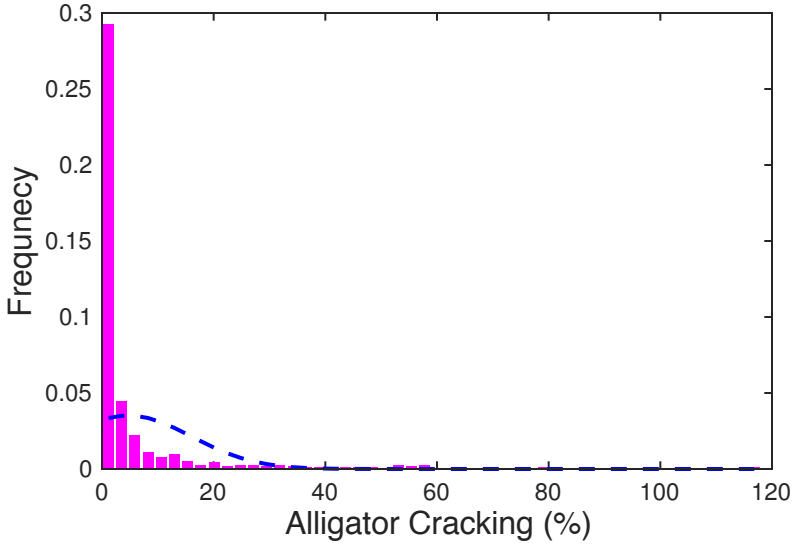

Figure 6.9 Distribution of measured alligator cracking from PMS

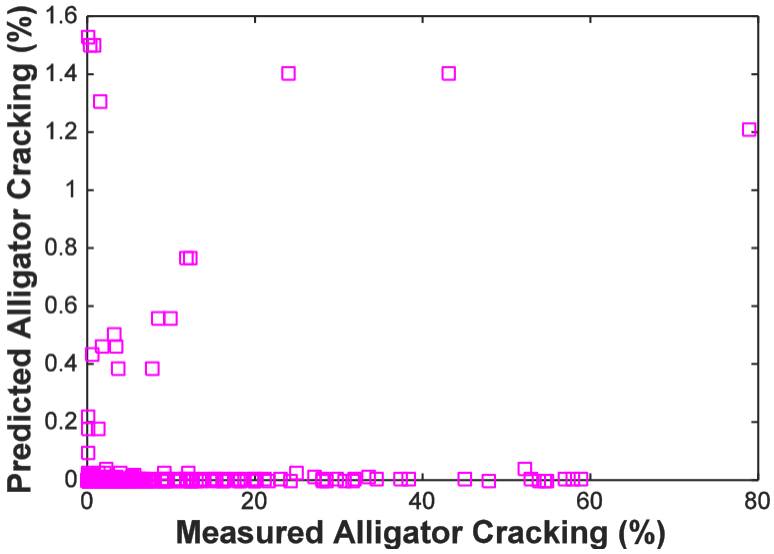

Figure 6.10 Comparison of measured alligator cracking with predicted alligator cracking

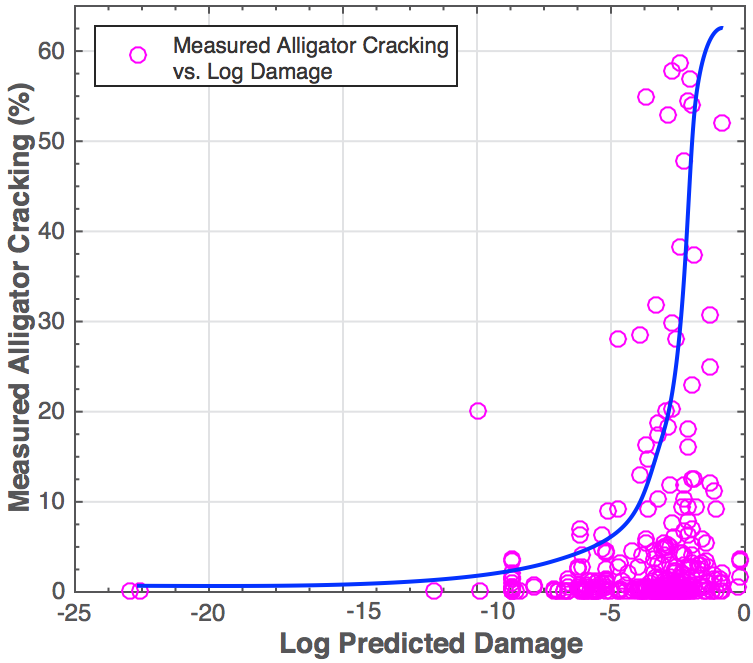

Figure 6.11 Measured alligator cracking versus predicted cumulative damage

The transfer function for alligator cracking is

$$FC_{Bottom} = \frac{1}{60}\frac{C_4}{1 + e^{C_1 C_1^* + C_2 C_2^* log(DI*100)}} \quad (14)$$

where C_1, C_2, and C_4 are the calibration coefficients to be determined, H_{HMA} is the total thickness of the pavement, DI is the cumulative damage index. $C_1 = -2C_2^*$ and $C_2 = -2.40874 - 39.748(1 + H_{HMA}) - 2.85$, Equation 1 can be rewritten into simpler form as follows,

$$y = \frac{A}{1 + e^{Bx_1 + Cx_2}} \quad (15)$$

where $A = \frac{C_4}{60} = \frac{6000}{60} = 100, B = -2(C_1 - C_2), C = C_2, x = C_2^*, x_2 = C_2^* \log(DI)$.

These parameters were obtained through the curve fitting procedure in MATLAB.

$$B = -1.961 \qquad C = 0.045$$

$$R^2 = 0.9825 \qquad SSE = 628.6$$

Therefore, for the transfer function of the alligator cracking, the local calibration coefficients that minimized the sum of squared error (SSE) were C_1=1.023, C_2=0.045, and C4=6000. Figure 6.11 shows the measured cracking varied with the predicted damage. Figure 6.12 shows the national model underestimated the alligator cracking in Tennessee, but the standard error of estimates (SEE) of the national model (SEE=11.16) appeared to be lower than that from the locally calibrated model, as shown in Figure 6.13 (SEE=19.57). However, because the extent of alligator cracking predicted by AASHTOWare was so low, which was less than 2% in average, approximately all the points were grouped upon the *x*-axis (the measured alligator cracking). This made the SEE of the national model predictions seem to be lower than those from the calibrated model. As Figure 6.13 shows, after the calibration, the alligator-cracking model

produced more accurate predictions, although the dispersion was high. This was caused by the high variability in the performance data.

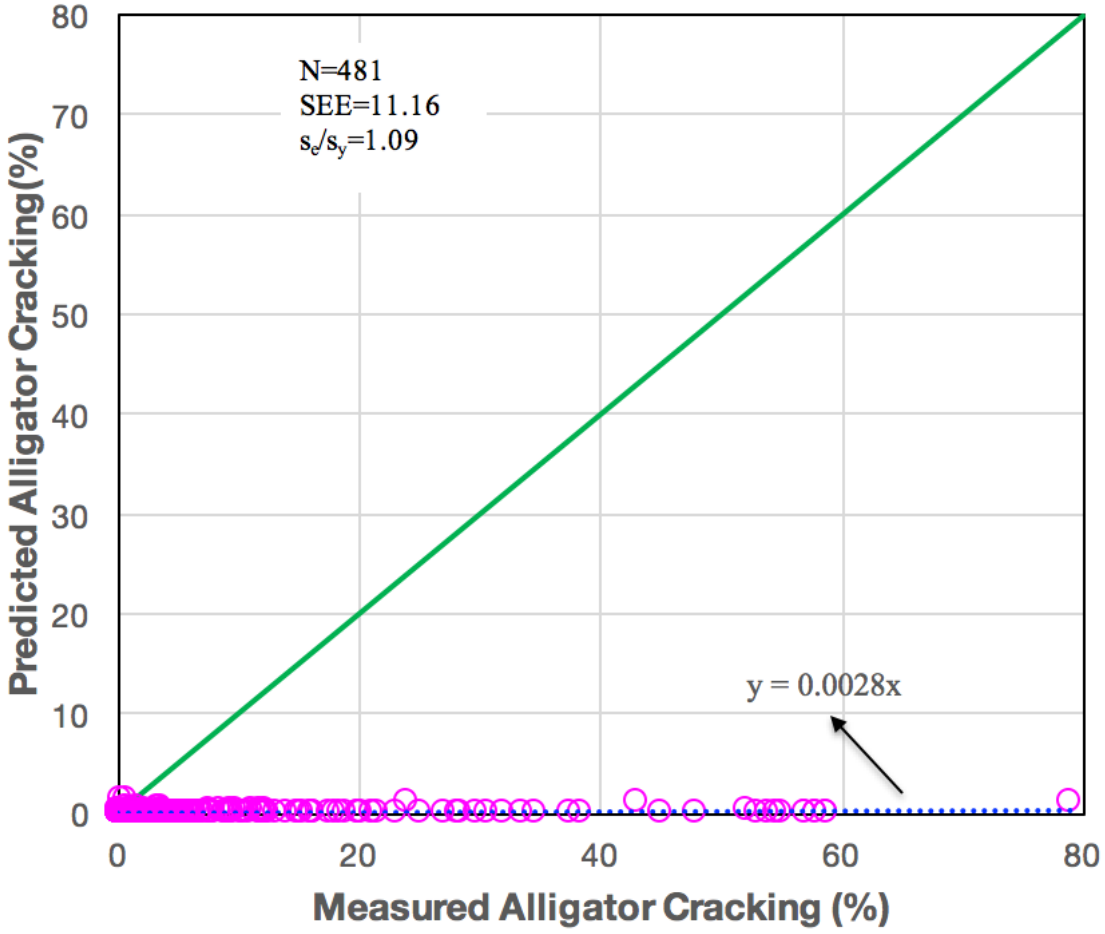

Figure 6.12 Measured alligator cracking versus predicted alligator cracking using the national model

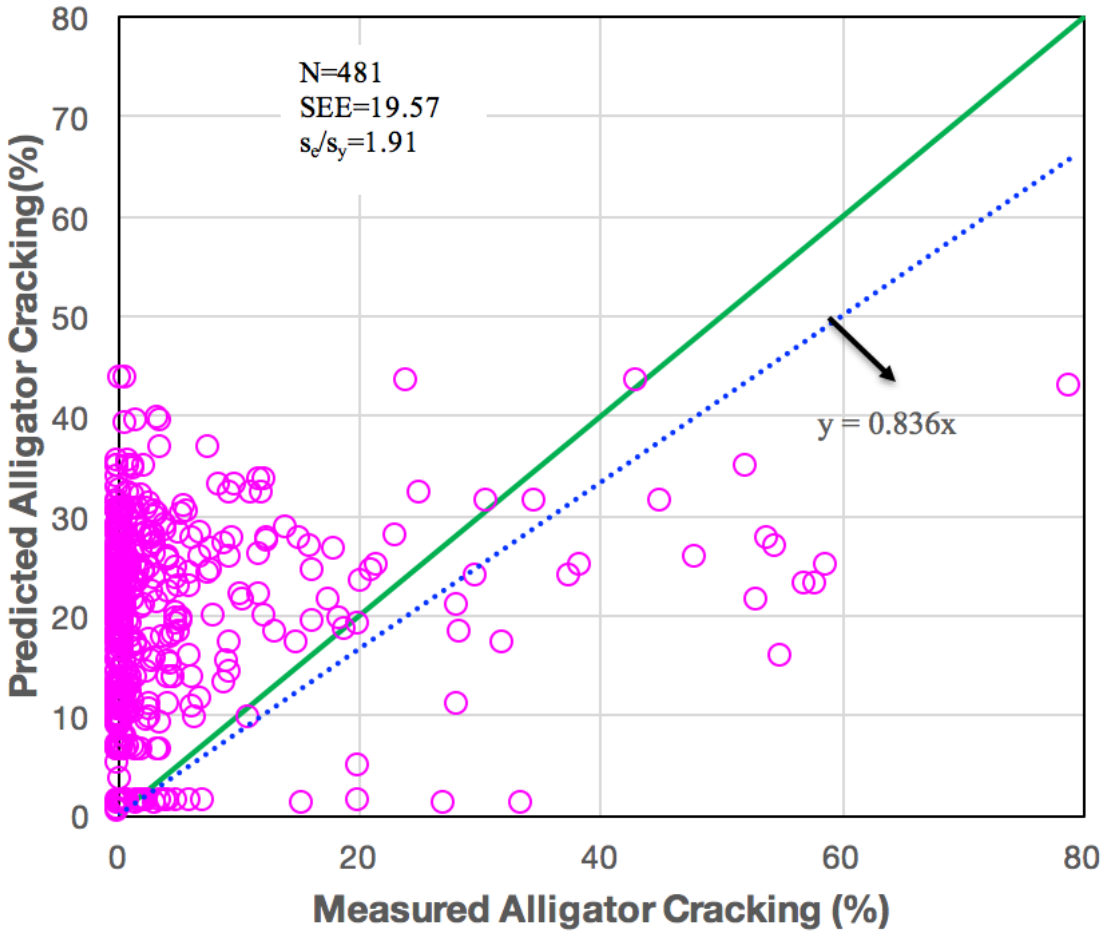

Figure 6.13 Measured alligator cracking versus predicted alligator cracking using the calibrated model

Table 6.7 shows the local calibration coefficients and the national default coefficients for the alligator-cracking model. It is seen in Table 6.7, C_2 is much more sensitive than C_1 to the local condition in Tennessee.

Table 6.7 Local calibration coefficients for alligator cracking model

Calibration Coefficients	C_1	C_2	C_4	SEE	s_e / s_y
National Model	1	1	6000	11.16	1
Local Model	1.023	0.045	6000	19.57	0.996

6.6 VALIDATION OF THE CALIBRATED ALLIGATOR CRACKING MODEL

In many situations, it is not always possible to collect new data for validation. Under such a circumstance, a reasonable way is to split the available data into two parts, the estimation data and the validation data (Snee, 1977). The estimation data are used to determine the coefficients of the model, and the validation data are used to test the extrapolation capability the model. A negative impact of using data splitting is loss of information, especially when the sample size of the observations is small. Jackknife is a special case of data splitting. It takes just one sample out of the whole observations each time, and then uses the rest of the observations to validate the developed model. The losing of information is thus reduced to the least degree.

Among several methods in the fields of estimating bias and standard error of estimate, Jackknife is one of the most popular one. The manual of practice published by AASHTO also recommends calibrating the transfer functions in MEPDG with Jackknife method(AASHTO, 2008). In addition, the jackknife is also useful in outlier detection and it provides a nearly unbiased estimate using only the original data.

A total of 97 sections were used to calibrate the alligator-cracking model. In validating the calibrated alligator-cracking model by jackknife method, each section was taken out once. Thus, 97 samples were used to obtain 97 combinations of calibration coefficients. Figure 6.14 shows the validation of alligator cracking model by jackknife method. As Figure 6.14 indicates, for alligator cracking, C_1 was quite stable for all the samples, with a median of 1.064. The variation in estimating C_2 was larger than C_1. Overall, the sum of squared error (SSE) of the model was stable, which demonstrated that the calibrated model could be applied to different conditions. As can also be observed in Figure 6.14**b**, jackknife was able to detect potential outliers, which resulted in the abnormal values of C_2, such as the negative values in Figure 6.14**b**. Data from this susceptible section should be excluded or used with caution.

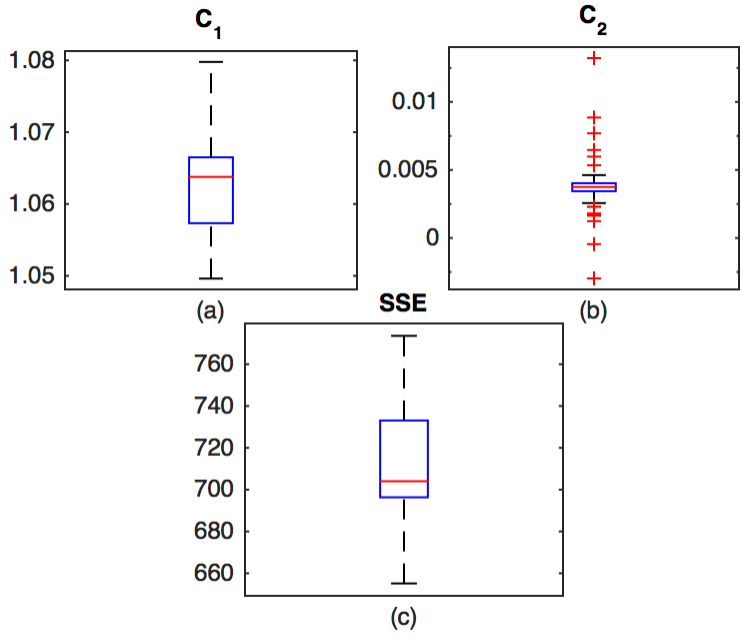

Figure 6.14 Validation of the calibrated alligator cracking model using jackknife method

CHAPTER 7 LOCAL CALIBRATION AND VALIDATION OF TOP-DOWN CRACKING TRANSFER FUNCTION

7.1 INTRODUCTION

Longitudinal cracking is a form of fatigue or wheel load related cracking that occurs within the wheel path and is defined as cracks predominately parallel to the pavement centerline. Longitudinal cracks initiate at the surface of the HMA pavement and initially show up as short longitudinal cracks that become connected longitudinally with continued truck loadings. Raveling or crack deterioration may occur along the edge of these cracks but they do not form an alligator-cracking pattern. The unit of longitudinal cracking calculated by the MEPDG is total feet per mile (meters per kilometer), including both wheel paths. Equation (16) is the default transfer function in MEPDG. It is seen in Equation (16), the form of this function is essentially a sigmoid function. Therefore, similar to the method used to calibrate the alligator-cracking model, a curve fitting procedure based on the form of sigmoid function in the MATLAB is employed.

$$\mathrm{FC_{Top}} = 10.56\left(\frac{C_4}{1+e^{C_1-C_2Log(DI_{Top})}}\right) \quad (16)$$

where:
FC_{Top} = Length of longitudinal cracks that initiate at the top of the HMA layer, ft./mile,
DI_{Top} = Cumulative damage index near the top of the HMA surface, and
$C_{1,2,4}$ = Transfer function regression constants; C_1=7.00; C_2=3.5; and C_4=1,000.

7.2 CALIBRATION

The level of longitudinal cracking on the Interstates of Tennessee is relatively low compared to the corresponding design criterion (2000 ft./mile). The average length of this type of cracking was only about 8 ft./mile, but it could still be used to adapt the transfer function into the local condition in Tennessee. This model was calibrated with a procedure similar to the alligator-cracking model above. Since this model also had a sigmoid-like form, it could be fitted easily by the curve fitting procedure in MATLAB. Figure 7.1 shows the measured longitudinal cracking varied with the damage in logarithm. As indicated in Figure 7.2, the fitted curve followed the overall trend of the sigmoid-like function pretty well. As Figure 7.2 shows, AASHTOWare generally overestimated the longitudinal cracking in Tennessee. Meanwhile, a large amount of biases and dispersion (a large SEE) were also found in Figure 7.2 and Figure 7.3. As Figure 7.3 indicates, after calibration, the bias was greatly reduced, the slope of the fitting line changed from 18.565 to 1.141. Meanwhile, the calibration also reduced the dispersion in the predictions.

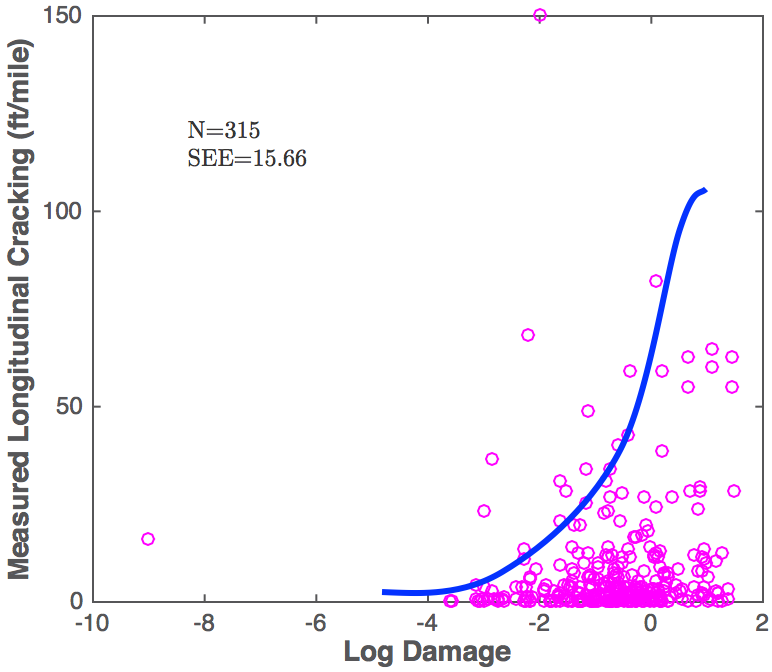

Figure 7.1 Comparison of measured longitudinal cracking versus log damage index

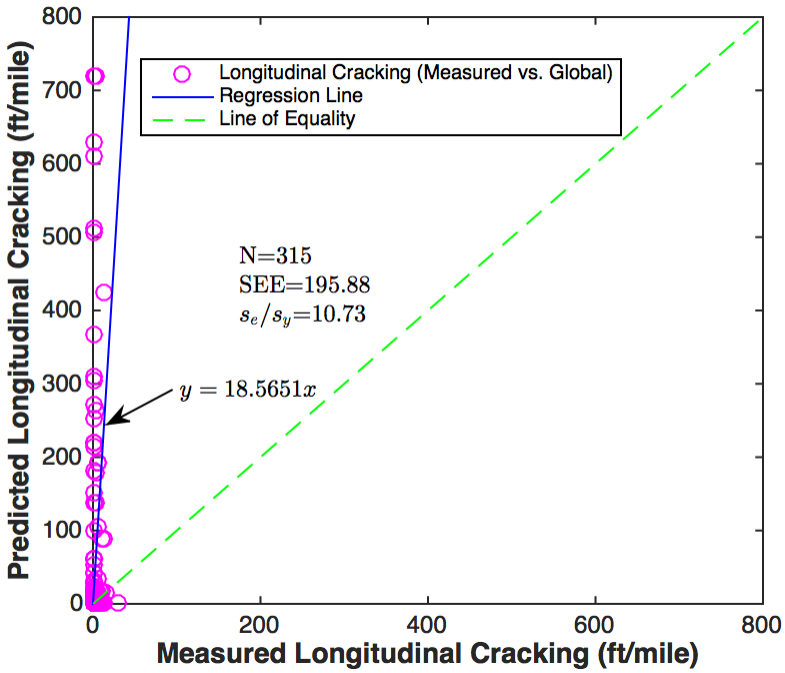

Figure 7.2 Comparison of the measured and national model predicted wheel-path longitudinal cracking

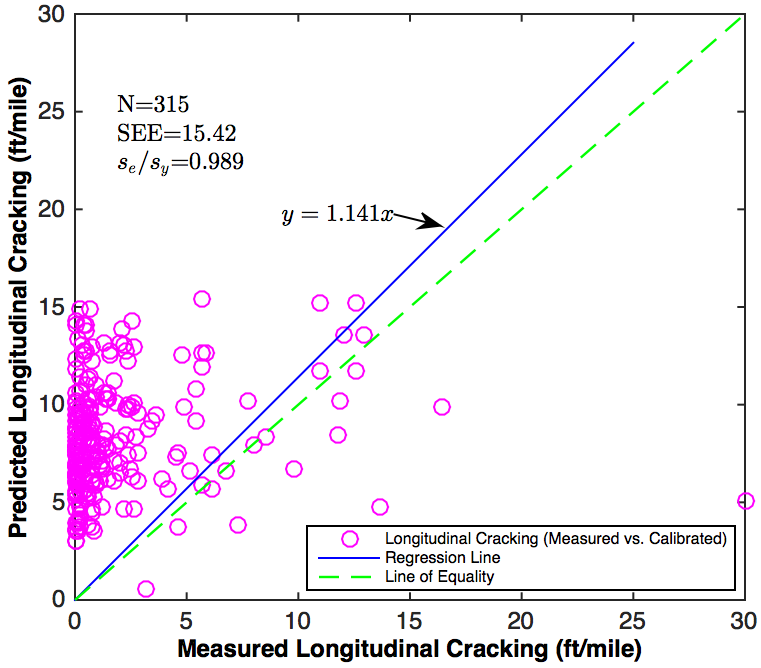

Figure 7.3 Comparison of the calibrated and measured wheel-path longitudinal cracking

7.3 VALIDATION

There are 72 sections involved in calibrating the longitudinal cracking model. Similar to the procedure used for calibrating the alligator-cracking model, 72 combinations of coefficient are determined. Figure 7.4 shows the validation of longitudinal cracking model through jackknife method. As can be observed, C_2 seemed to be insensitive to the resampling process. An extreme value of C_2 in Figure 7.4 (b) indicates an abnormal observation in a section.

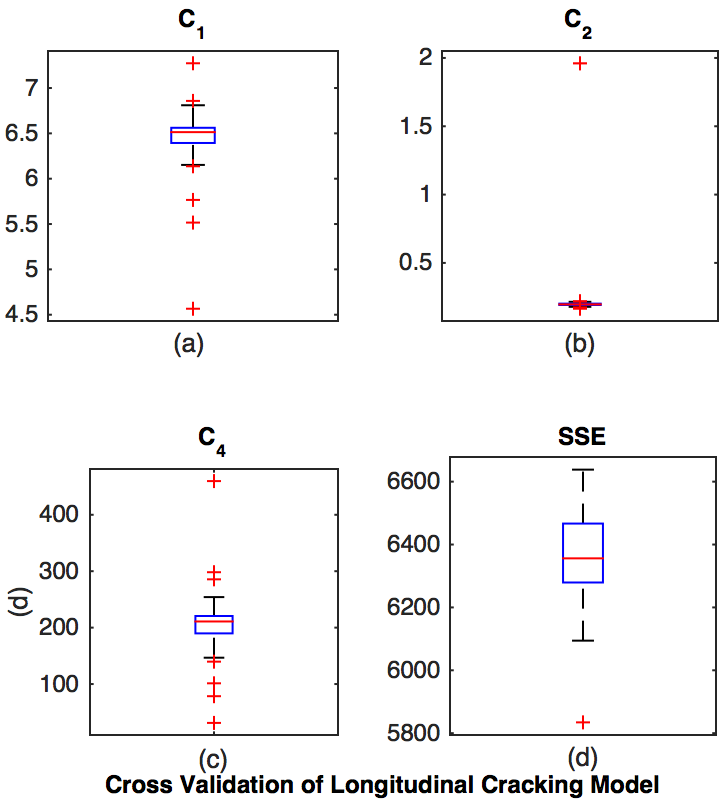

Figure 7.4 Validation of the calibrated wheel-path longitudinal cracking model with jackknife method

CHAPTER 8 LOCAL CALIBRATION OF THE ROUGHNESS MODEL

8.1 INTRODUCTION

The design premise included in the MEPDG for predicting smoothness degradation is that the occurrence of surface distress will result in increased roughness (increasing IRI value), or in other words, a reduction in smoothness. Equation (17) and (18) were developed from data collected within the LTPP program and are embedded in the MEPDG to predict the IRI over time for HMA-surface pavements.

$$IRI = IRI_0 + 0.0150(SF) + 0.400(FC_{Total}) + 0.0080(TC) + 40.0(RD) \quad (17)$$

where:
IRI_0 = Initial IRI after construction, in./mile
SF = Site factor, refer to Equation (18),
FC_{Total} = Area of fatigue cracking (combined alligator, longitudinal, and reflection cracking in the wheel path), percent of total lane area. All load related cracks are combined on an area basis-length of cracks is multiplied by 1 to convert length into an area basis,
TC = Length of transverse cracking (including the reflection of transverse cracks in existing HMA pavements), ft./mile, and,
RD = Average rut depth, in.

The site factor (SF) is calculated accordance with the following equation.

$$SF = Age(0.02003(PI + 1) + 0.007947(Precip + 1) + 0.000636(FI + 1)) \quad (18)$$

where:
Age = Pavement age, year;
PI = Percent plasticity index of the soil,
FI = Average annual freezing index, ºF day, and
$Precip$ = Average annual precipitation or rainfall, in.

The IRI model is built upon all other distresses models, thus all other models should be calibrated prior to the calibration of the IRI model. With the rutting, alligator cracking, and longitudinal cracking models being calibrated, the research team was able to calibrate the IRI model at this stage. It was noted that due to the scarcity in transverse cracking data, the transverse cracking model was not calibrated to the local conditions of Tennessee. However, transverse cracking contributes only marginally to the total roughness in Tennessee. Thus it will not cause significant increase of IRI prediction errors.

8.2 CALIBRATION

Figure 8.1 and Figure 8.2 show comparisons of measured and predicted roughness. It was observed from Figure 8.1 that, unlike the alligator cracking and the longitudinal cracking, the national model for roughness gave more realistic predictions for Tennessee. Still, there were more biases and dispersion in the predictions from the national model than the locally calibrated one. As shown in Figure 8.2, even no adjustment was made to the national model, with all the distresses model calibrated, the bias and dispersion in this model reduced appreciably.

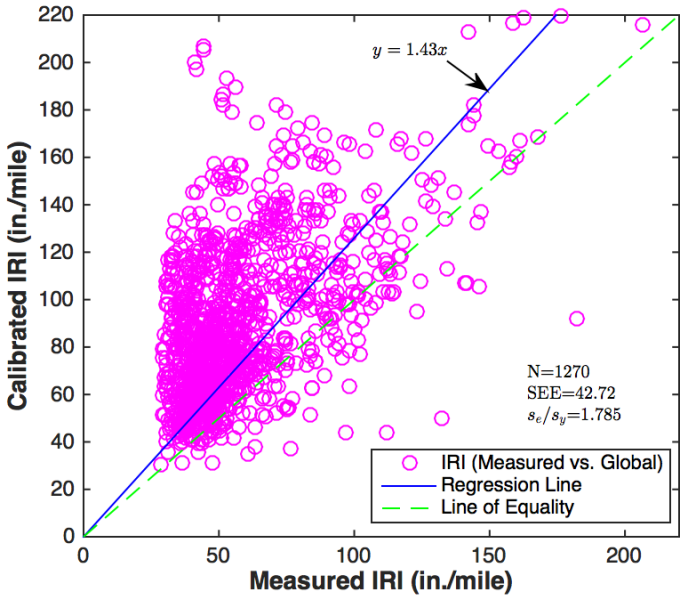

Figure 8.1 Comparison of the measured IRI and IRI prediction from national model

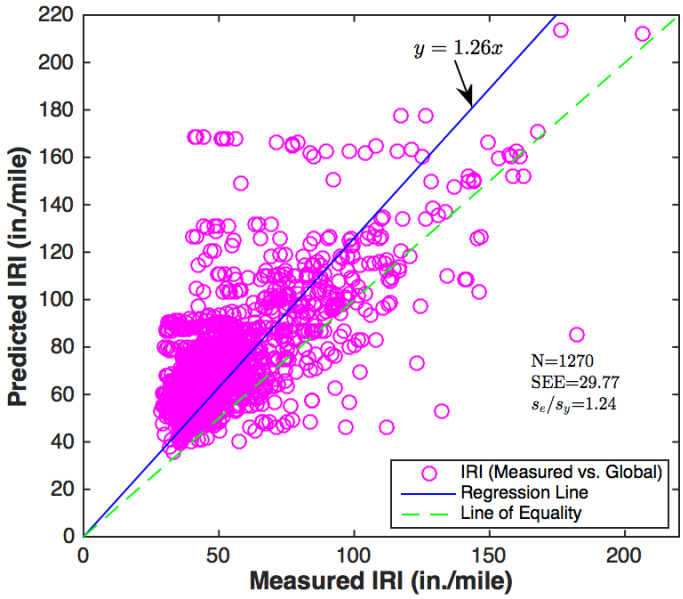

Figure 8.2 Measured IRI versus Predicted IRI using the calibrated model

CHAPTER 9 DISCUSSION OF THE FLEXIBLE PAVEMENT DESIGN CRITERIA FOR TENNESSEE

Design performance criteria and design reliability affect construction costs and performance. The design criteria and design reliability levels could be selected in balance with each other. A low level of distress should not be selected in conjunction with a high level of reliability because this may make it impossible or costly to obtain an adequate design. These levels could become policy values that are usually fixed for routine designs.

Performance criteria are used to ensure that a pavement design will perform well over its design life with satisfaction. The designer selects critical limits or threshold values to judge the adequacy of a design. These criteria or threshold values could represent agency policies regarding the condition of the pavements that trigger some type of major rehabilitation activity or reconstruction. In addition, these values could represent the average values along a project. Two ways could be used to determine these criteria. One is to select by visualizing the pavement condition and its impact on safety, maintenance needs (amount of lane closure), ability to rehabilitate the pavement in that condition, and the realization that this level is set at a given level of design reliability (e.g., 90%). The other one is to select by analyzing the agency's pavement management data through the use of survivability analyses, or based on user considerations and for safety reasons. For this research project, the latter one is used. As a reference, Table 1 shows the recommended design performance criteria value from the Manual of Practice (MOP) of AASHTO pavement design guide(AASHTO, 2008).

Table 9.1 Design Criteria Recommended in the AASHTO Manual of Practice (AASHTO, 2008)

Performance Criteria	Maximum Value at End of Design Life
Alligator cracking (HMA bottom up cracking)	Interstate: 10% lane area Primary: 20% lane area Secondary: 35% lane area
Longitudinal cracking length (HMA top down cracking)	**Interstate**: 2000 ft./mile (90% reliability) (From AASHTOWare®)
Transverse cracking length (thermal cracks)	Interstate: 500 ft./mile Primary: 700 ft./mile Secondary: 700 ft./mile
Rut depth	Interstate :0.40 in. Primary: 0.50 in. Others (<45mph) : 0.65 in.
IRI (Smoothness)	Interstate: 160 in./mile Primary: 200 in./mile Secondary: 200 in./mile

As indicated in Table 9.1, the MOP provides no criteria for the wheel-path longitudinal cracks on all highways including the Interstates. The critical length of wheel-path longitudinal cracking in Table 9.1 was retrieved from the documentation of AASHTOWare Pavement Design software.

9.1 International Roughness Index

9.1.1 Interstates

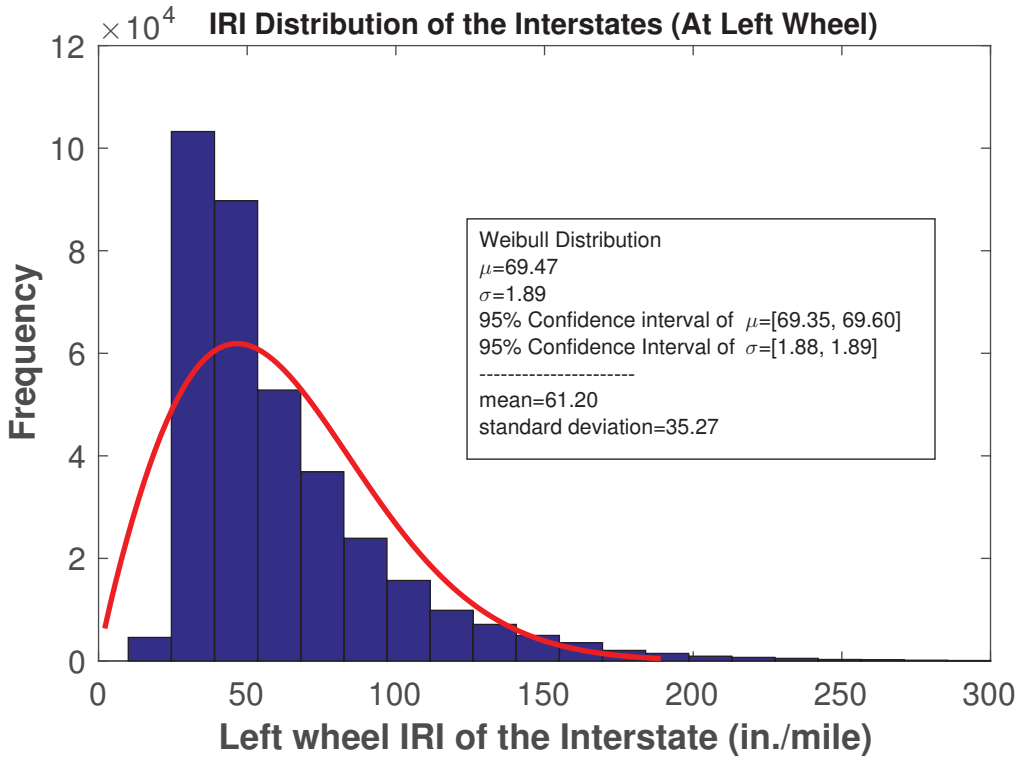

Figure 9.1 Distribution of IRI on Interstates (Left Wheel)

As shown in Figure 9.1, the mean of the left wheel IRI on Interstates is 61.20 in./mile, and the corresponding standard deviation is 35.27. In addition, several distribution models were used to fit the data, the Weibull distribution was found to fit the data best. Once the best distribution was found, it can be used to predict the amount of IRI or distresses under a certain probability. As shown in Figure 1, two parameters were fitted for the Weibull distribution, the location parameter μ=72.23, and the shape parameter σ=1.83. This is reasonable, because most of the survival analyses using Weibull distribution to characterize the data of interest. A 95% confidence level of the location parameter μ is [72.09, 72.37], whereas a 95% confidence level of the shape parameter σ is [1.82, 1.83]. The confidence intervals for both parameters are narrow, which indicates that the Weibull distribution fit the data well. Compared to the initial IRI recommended in the MOP (65 in./mile), the average value of the left wheel IRI is small. This indicates the Interstates in Tennessee are in excellent condition. As presented in Figure 9.1, 90% of the observations are lower than 112.5 in./mile, 85% of them are lower than 103.1 inch/mile,

50% are lower than 63.65 in./mile, 25% are lower than 37.9 in./mile, 10% are lower than 14.8 in./mile.

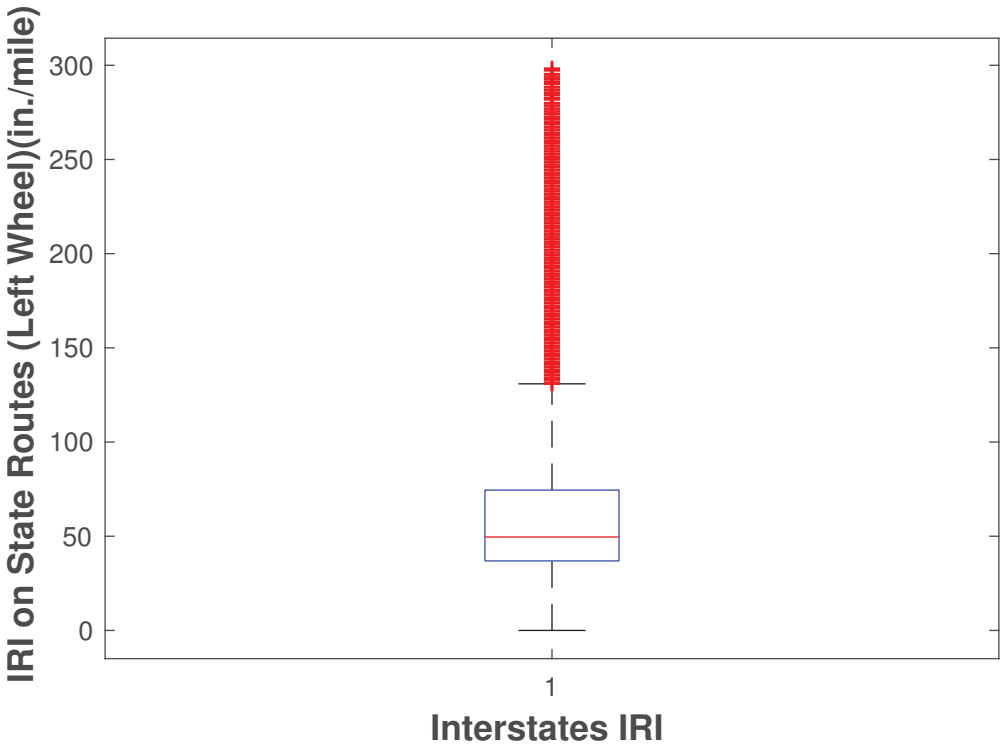

Figure 9.2 Box-plot of IRI on Interstates (Left Wheel)

Figure 9.2 shows a box plot of the left wheel IRI on the Interstates of Tennessee. As indicated in Figure 9.2, the maximum left wheel IRI goes as high as 300 in./mile, but most of the observations are smaller than 150 in./mile. The median of this data set is close to 50 in./mile.

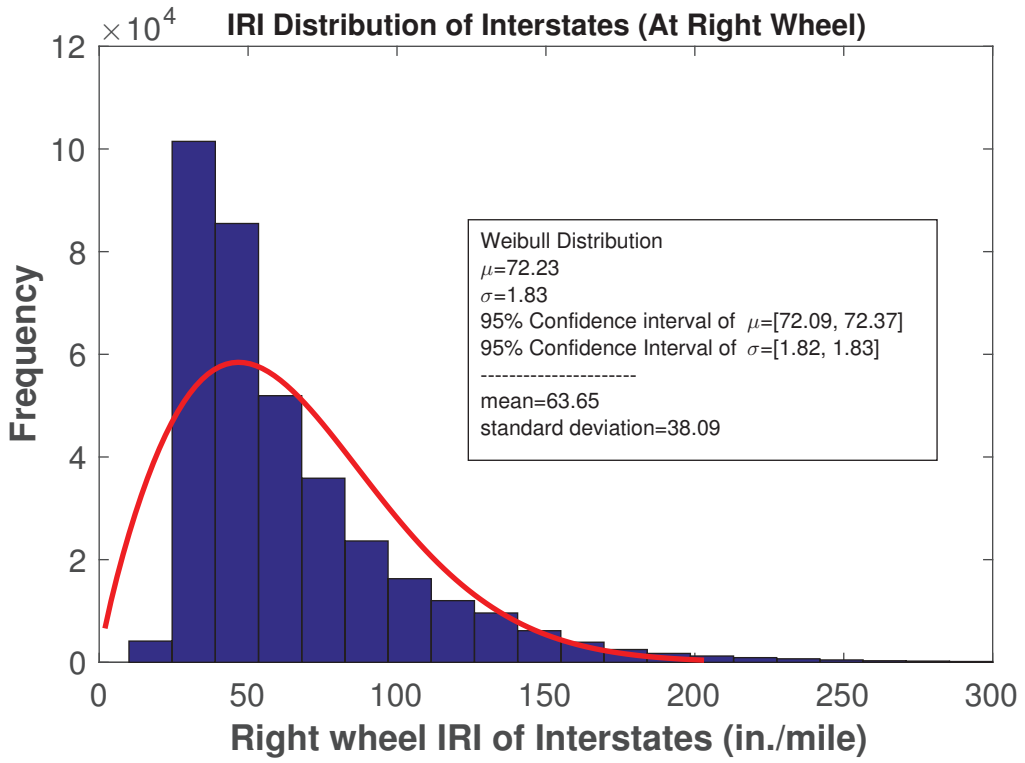

Figure 9.3 Distribution of IRI on Interstates (Right Wheel)

Figure 9.3 shows the distribution of right wheel IRI on Interstates of Tennessee. Similar to its left-wheel counterpart, Weibull distribution rather than normal distribution fits the data best. The fitted location parameter and shape parameter are μ= 72.23 in./mile, σ = 1.83, respectively. The mean value of the right wheel IRI on Interstates of Tennessee is 63.65 in./mile, with a standard deviation of 38.09. The confidence interval for the location and shape parameter are, [72.09, 72.37], and [1.82, 1.83], respectively. Both confidence intervals are narrow, which indicates the Weibull distribution fits the data quite well. It is observed from Figure 3, as presented in Figure 1, 90% of the observations are lower than 106.4 in./mile, 85% of them are lower than 97.8 inch/mile, 50% are lower than 61.2 in./mile, 25% are lower than 37.4 in./mile, 10% are lower than 16 in./mile.

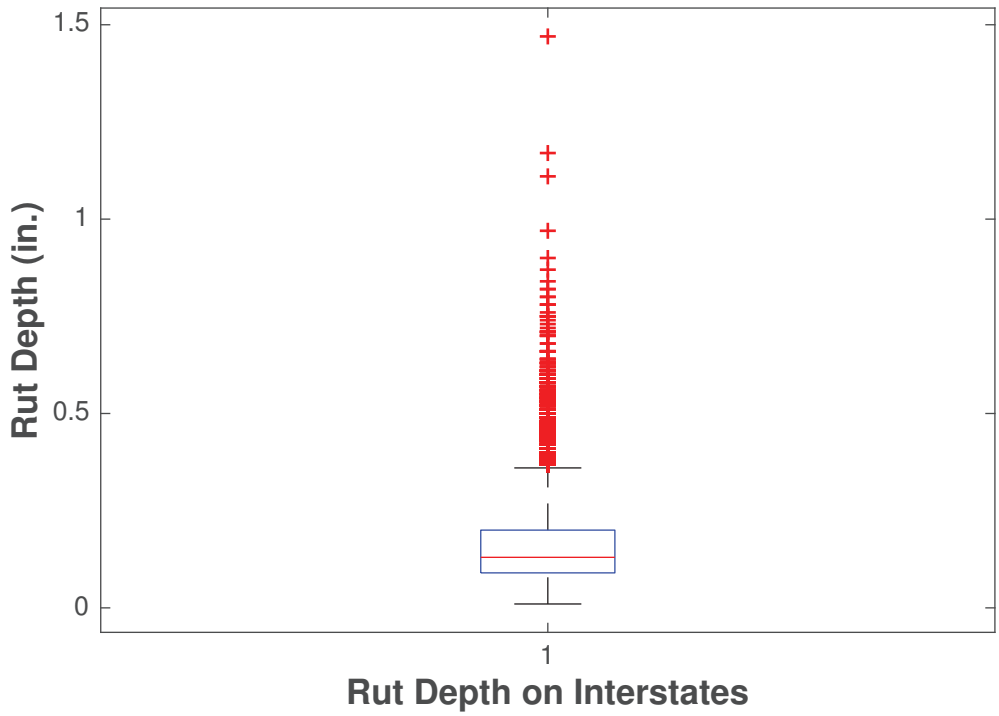

Figure 9.4 Box-plot of IRI on Interstates (Right Wheel)

As indicated in Figure 9.4, the maximum right wheel IRI on the Interstates goes as high as 300 in./mile. Similar to the information presented in Figure 3, most of the data are lower than 150 inch/mile. The median of the right wheel IRI is close to 50 inch/mile.

To summarize, at a probability of 90%, both left-wheel IRI and right-wheel IRI are lower than 115 in./mile, which is much smaller than the value recommended in the MOP (160 in./mile for Interstates, 200 in./mile for other roadways). Owing to the well being of the pavement in Tennessee, a small loosing of the smoothness criterion may result in a large reduction in construction cost of pavement yet induce no sacrifice in the pavement service quality. It is noted that this observation only applies to HMA overlays. For new asphalt pavement design, due to limited data available, no suggestion could be made for revising this criterion, and the recommended values from the MOP are preferable.

9.1.2 STATE ROUTES

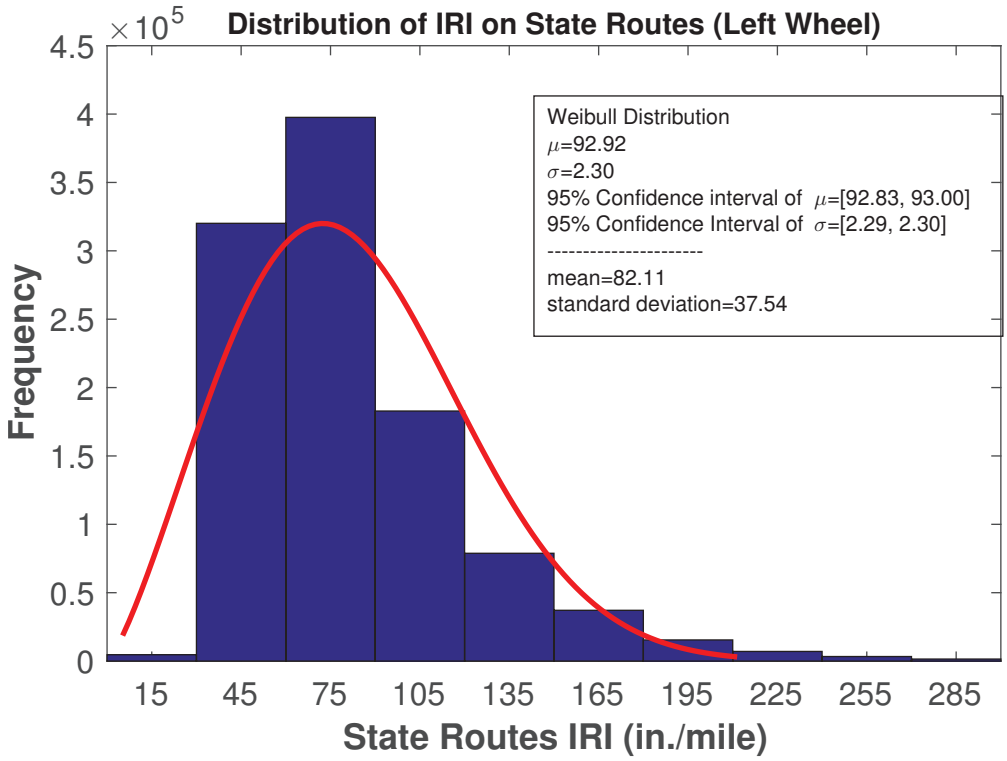

Figure 9.5 Distribution of IRI on State Routes (Left Wheel)

Figure 9.5 shows a distribution of the left wheel IRI on the State Routes of Tennessee. After a comparison with the normal, gamma, and beta distribution, Weibull distribution fits the data best. The fitted location and shape parameters are, $\mu = 92.92$, $\sigma = 2.3$, respectively. The mean left wheel IRI on State Routes is 82.11 in./mile; its corresponding standard deviation is 37.54. As shown in Figure 5, 90% of the observations are lower than 130.2 in./mile, 85% of them are lower than 121.0 in./mile, 50% are lower than 82.1 in./mile, 25% are lower than 56.8 in./mile, 10% are lower than 34 in./mile.

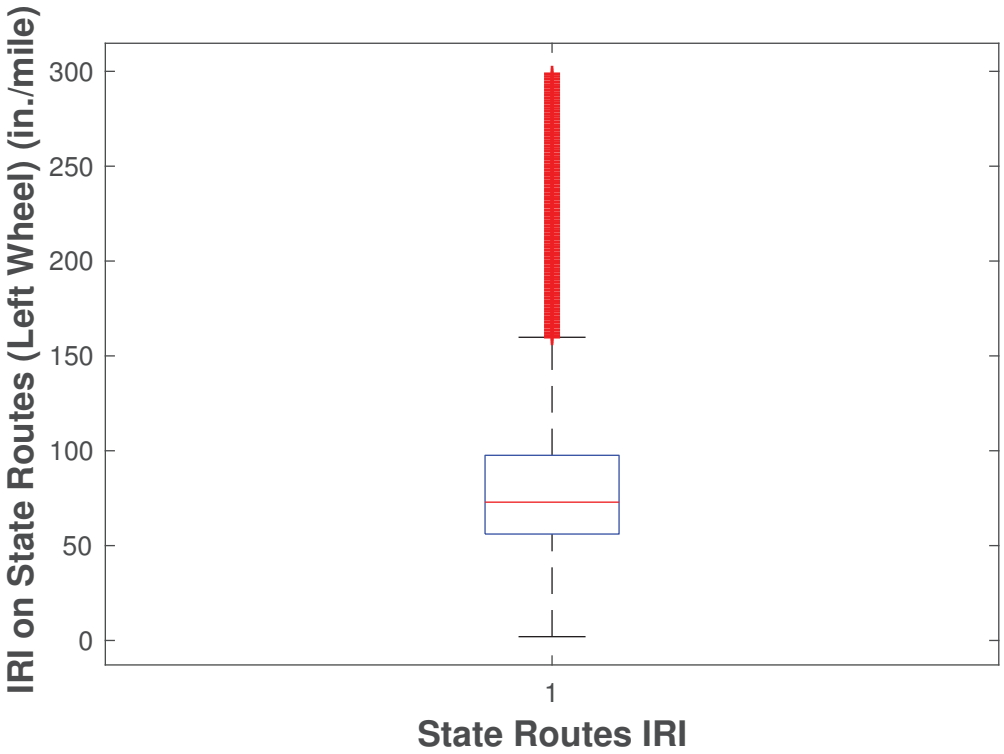

Figure 9.6 Box-plot of IRI on State Routes (Left wheel)

Figure 9.6 shows a box plot of the left wheel IRI on State Routes. The maximum of this dataset goes as high as 299.9 in./mile, but most of the data are lower than 170 in./mile. As also can be observed from Figure 6, the noises of the IRI data from State Routes are larger than those from Interstates, as more observations lay over the upper whisker. The median of this dataset is 72.9 in./mile.

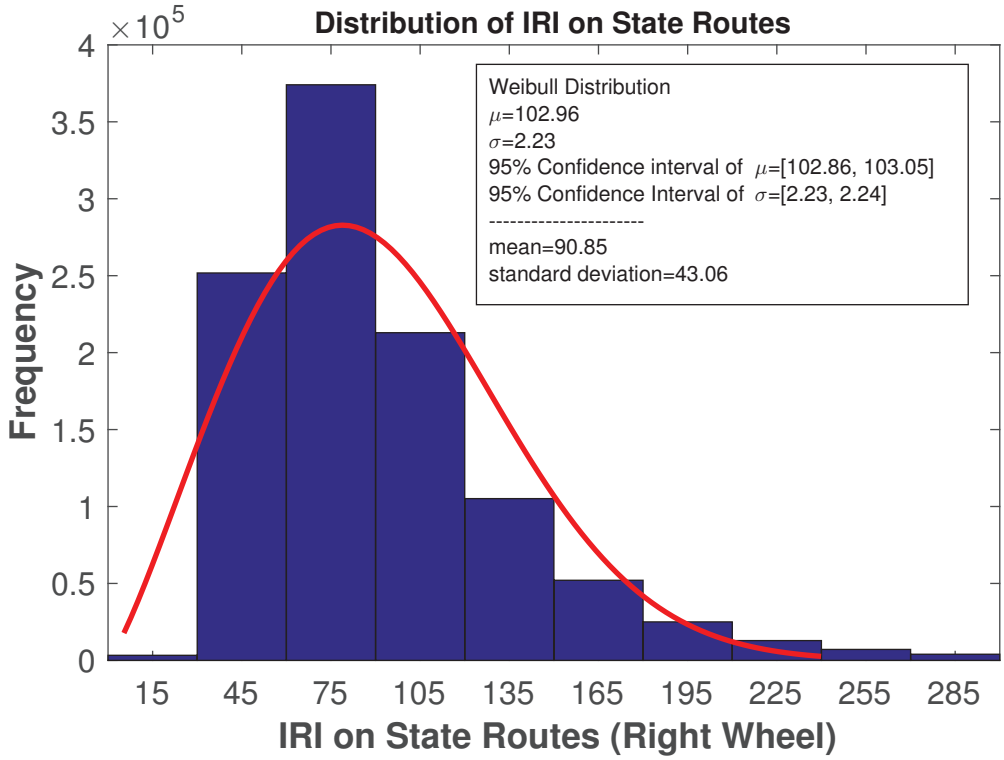

Figure 9.7 Distribution of IRI on State Routes (right wheel)

As shown in Figure 9.7, still, Weibull distribution fits the data set best, when compared to the normal, gamma, and beta distribution. The fitted location and shape parameters are, μ=102.96, σ=2.23. The 95% confidence intervals for the two parameters are, μ= [102.86, 103.05], σ= [2.23, 2.24], respectively. The widths of both confidence intervals are quite small, which indicates the Weibull distribution fits the data well. The mean of right wheel IRI on State Routes is 90.85 in./mile, and the corresponding standard deviation is 43.06. It was observed in Figure 7 that 90% of the observations are lower than 146 in./mile, 85% of them are lower than 135.5 in./mile, 50% are lower than 90.9 in./mile, 25% are lower than 61.8 in./mile, 10% are lower than 35.7 in./mile.

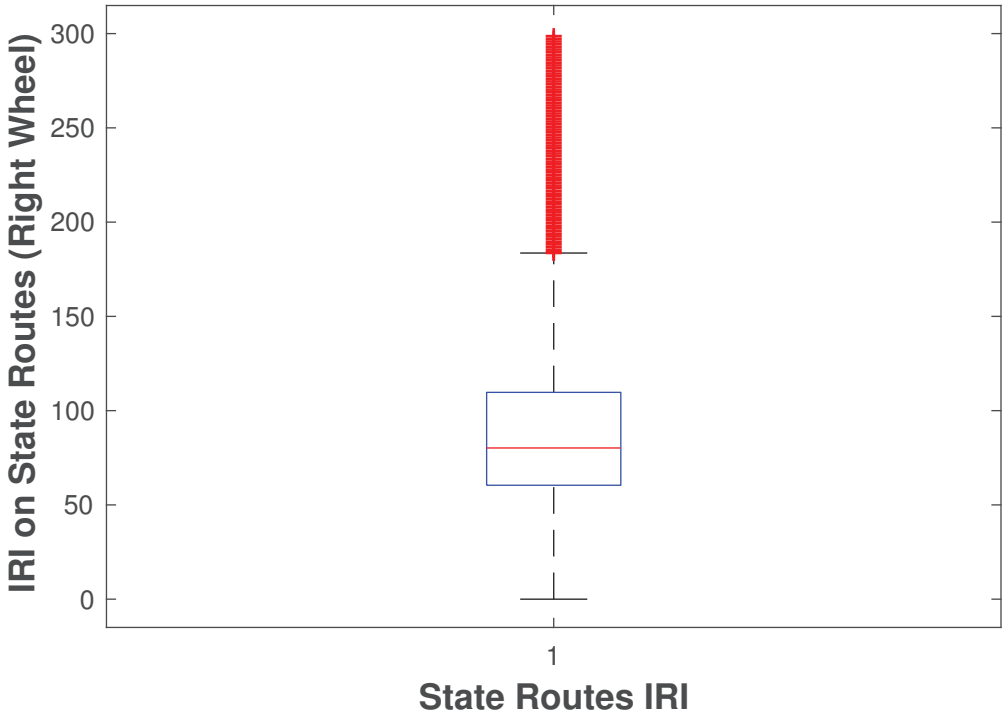

Figure 9.8 Box-plot of IRI on State Routes (right wheel)

Figure 9.8 shows a box plot of the right wheel IRI on the State Routes. The maximum this dataset goes as high as 300 in./mile. However, most of the observations are lower than 150 in./mile. The median of this dataset is 80.2 in./mile. Similar to the left wheel IRI on the State Routes, more noises were spotted in the state routes than the Interstates.

To summarize, the State Routes have a higher level of IRI than the Interstates, the median of the State Routes is about 80 in./mile, while this value is 50 in./mile for the Interstates. However, most of the IRI on the State Routes are much smaller than the value recommended for this class of highway in the MOP (200 in./mile). If the recommended value was used for pavement design, this would yield an over design. Therefore, a decrease of this criteria in HMA overlay design may result in a big saving of the construction cost.

9.2 DISTRESSES

9.2.1 INTERSTATES

9.2.1.1 Alligator Cracking

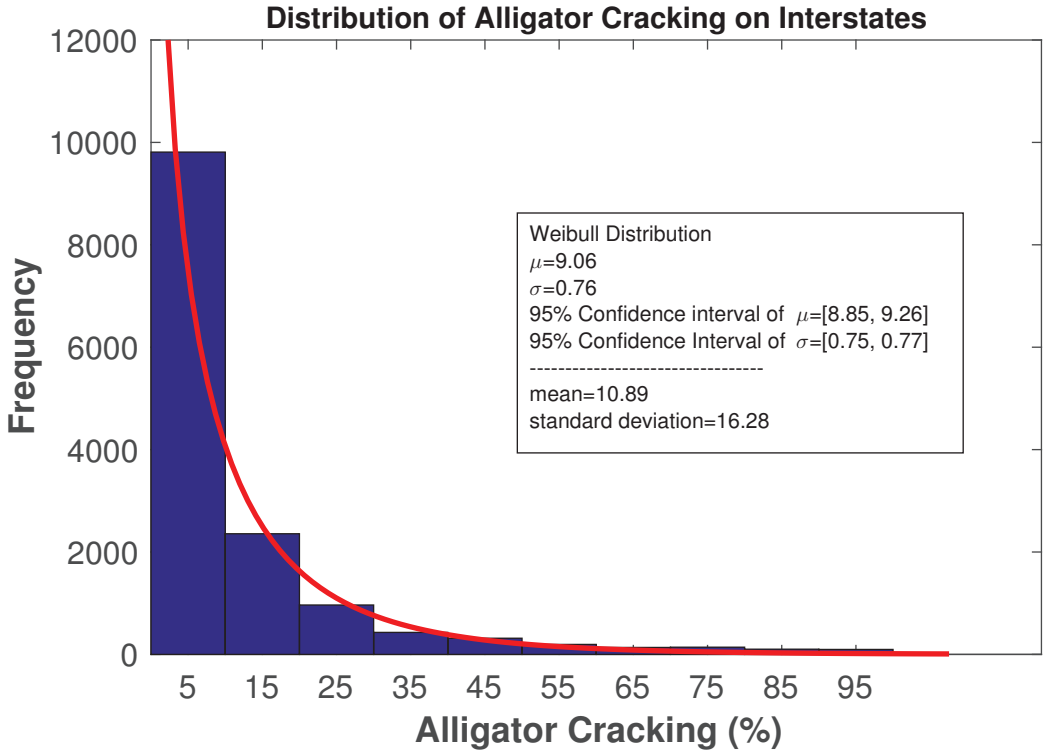

Figure 9.9 Distribution of Alligator Cracking on Interstates

Figure 9.9 shows a distribution of alligator cracking (bottom-up cracking) on the Interstates. Compared to normal, gamma, and distribution, Weibull distribution again fits the data better. As shown in Figure 9.9, the fitted location and shape parameter is, μ=9.06, σ=0.76, respectively. The 95% confidence intervals for these two parameters are, μ = [8.85, 9.26], and σ = [0.75, 0.77]. Both confidence intervals are narrow, which implies the Weibull distribution fits the data very well. The mean of alligator cracking on the Interstates is 10.9%; the corresponding standard deviation is 16.28. As can be observed from Figure 9, 90% of the observations are lower than 31.8 percent of the lane area, 85% of them are lower than 27 percent, and 50% are lower than 10.9 percent.

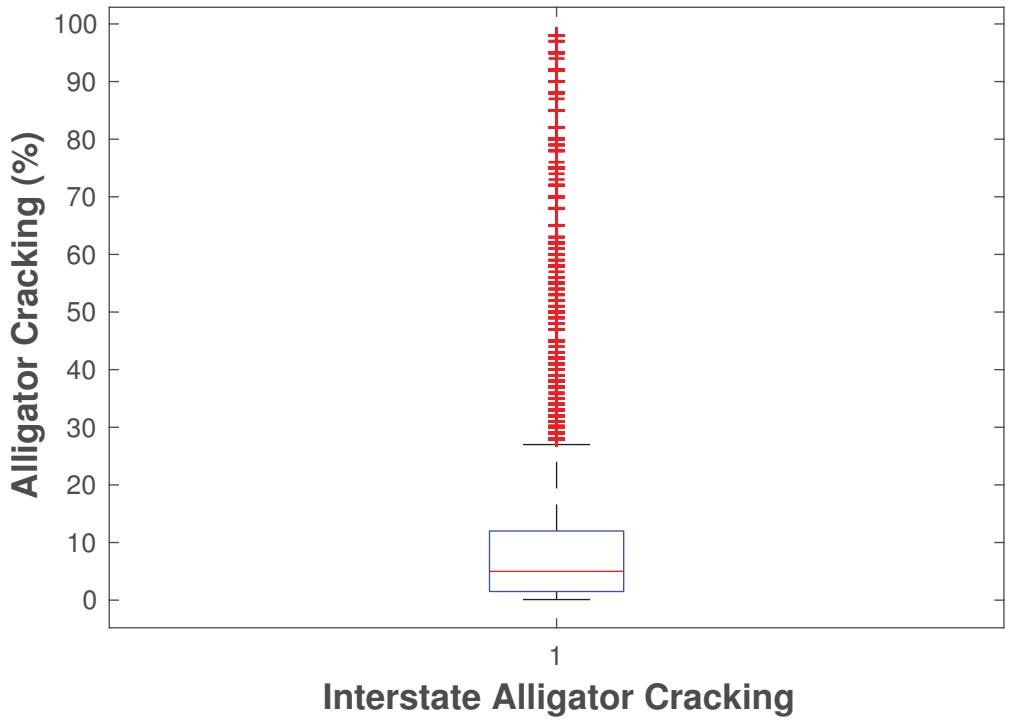

Figure 9.10 Box-plot of Alligator Cracking on Interstates

Figure 9.10 shows a box plot of alligator cracking on the Interstates. As indicated in Figure 9.10, a large amount of the observations lay over the upper whisker. Concretely, 952 observations among 177,726 observations exceed 30 percent, which is only about 0.1% of the total dataset. The median of the dataset is 5%.

As shown in Figure 9.9 and Figure 9.10, for alligator cracking, only 50% of the observations are lower than 10.9 percent, which implies alligator cracking is possibly a more severe problem than IRI in Tennessee. When designing an asphalt pavement, in weighing different performance criteria, more consideration may be given to control alligator cracking. In other words, the trigger value for alligator cracking on the Interstates may increase slightly.

9.2.1.2 Longitudinal Cracking

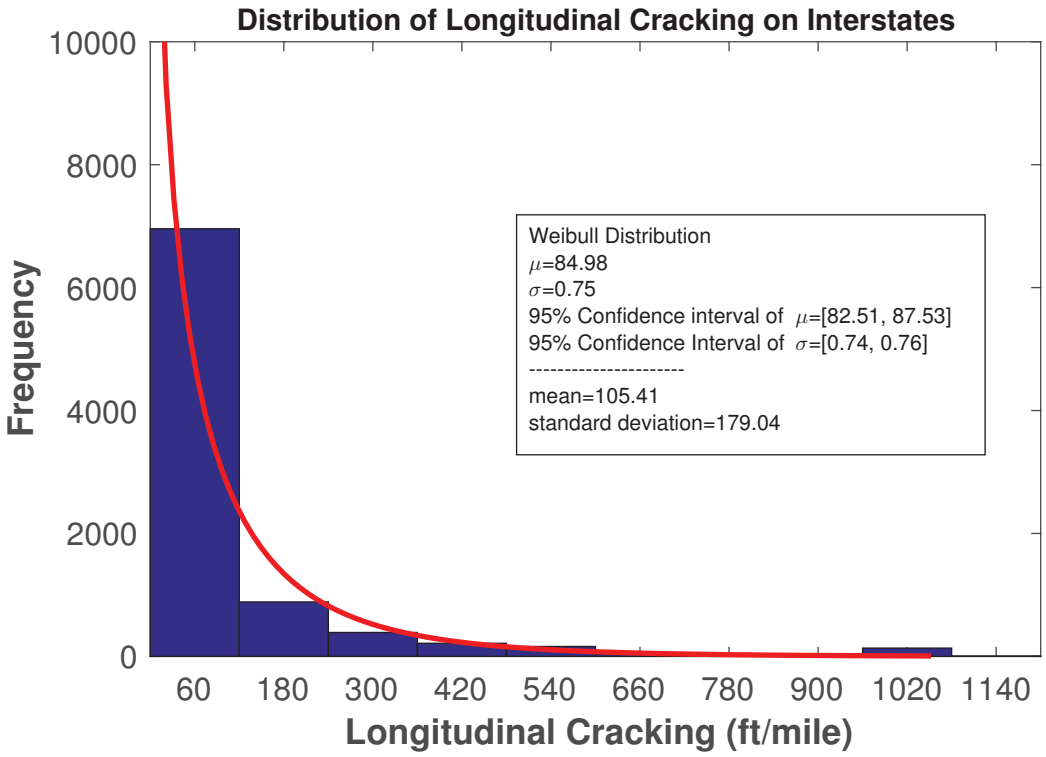

Figure 9.11 Distribution of Longitudinal Cracking on Interstates

Figure 9.11 shows a distribution of wheel-path longitudinal cracking on the Interstates. Among all the distribution functions considered in the research project, the Weibull distribution works the best. As shown in Figure 9.11, the fitted location and shape parameters for the Weibull distribution are μ=84.98, σ=0.75, respectively. The confidence intervals for both parameters are quite narrow, which implies that the data were fitted well by the Weibull distribution. The mean of longitudinal cracking on the Interstates is 105.4 ft./mile, and the corresponding standard deviation is 179.04. As can be observed from Figure 9.11, 90% of the observations are lower than 334.8 ft./mile, 85% of them are lower than 291ft./mile, and 50% are lower than 105.4 ft./mile.

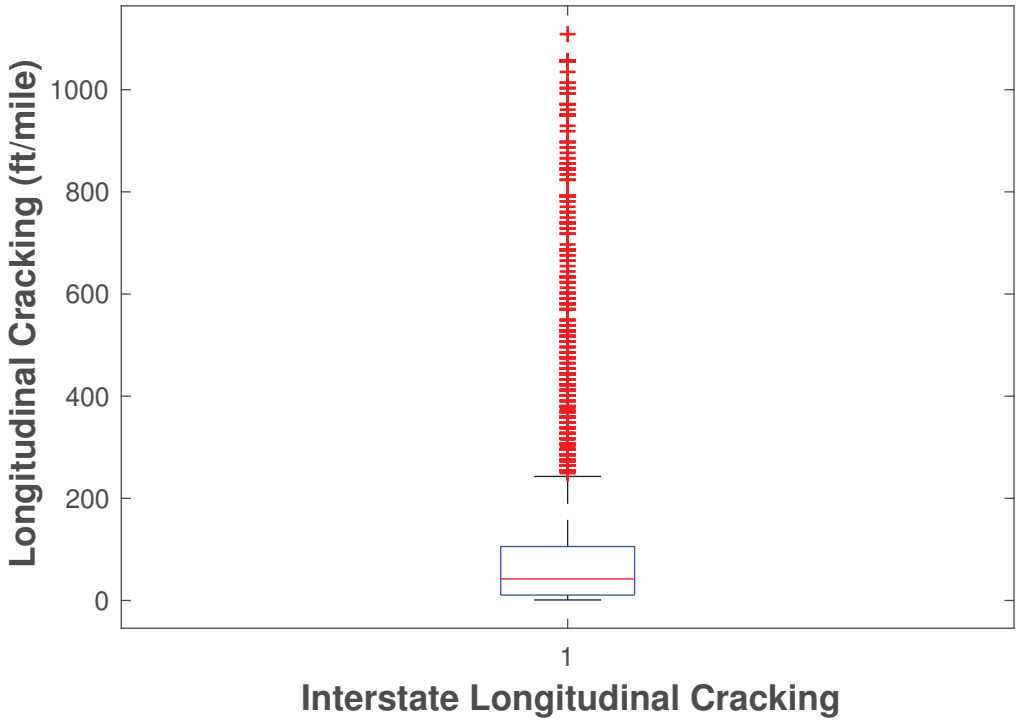

Figure 9.12 Box-plot Longitudinal Cracking on Interstates

Figure 9.12 used a box plot to characterize the longitudinal cracking on the Interstates. The maximum longitudinal cracking on the Interstates reaches 1108 ft./mile. The median of the dataset is 42.4 ft./mile. There are 177,726 observations in the dataset, within which 8866 observations are nonzero. Among the total number of nonzero, only 1119 observations are greater than 200 ft./mile, which is only 12.6% of the nonzero subset.

Compared to the recommended value in the MOP for the Interstates, the amount of longitudinal cracking on the Interstates of Tennessee is much smaller. When the critical value in the MOP was used, MEPDG could yield an over design, which may cause unnecessary construction cost increase.

9.2.1.3 Transverse Cracking

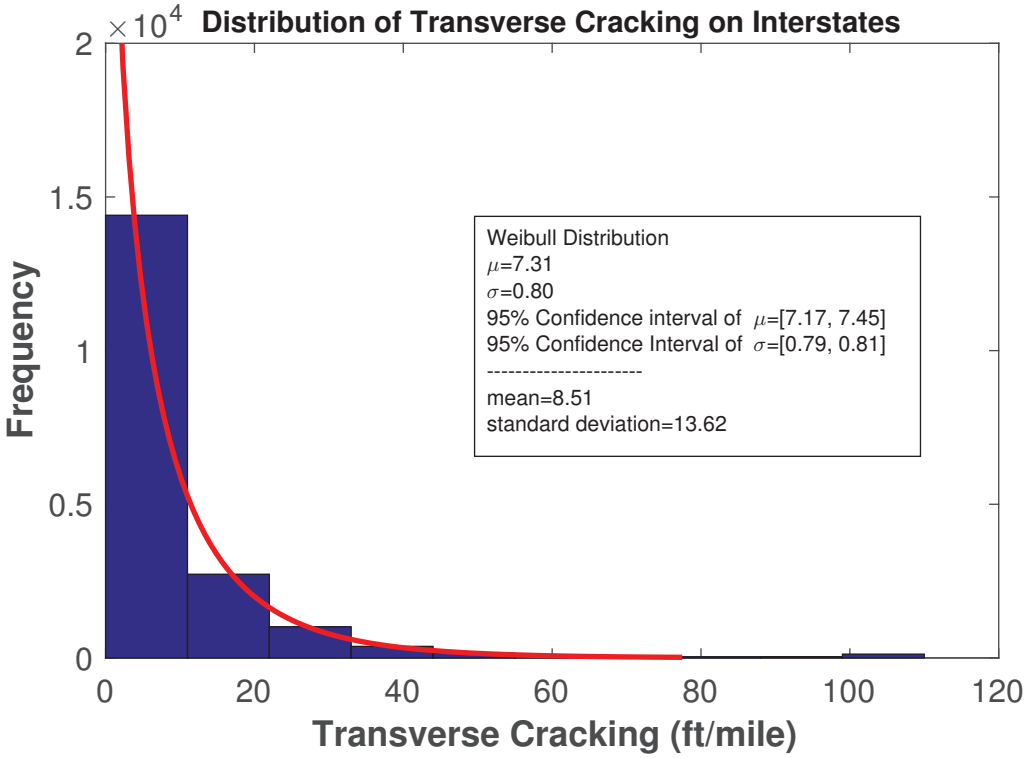

Figure 9.13 Distribution of Transverse Cracking on Interstates

Figure 9.13 shows a distribution of transverse cracking on the Interstates. Among all the other distribution functions considered in the research project (gamma, normal, and beta), the Weibull distribution fits best. The fitted location and shape parameters for the Weibull distribution are, μ=7.31, σ=0.8, respectively. The confidence intervals for the two parameters are, μ = [7.17, 7.45], and σ = [0.79, 0.81], respectively. The mean of this dataset is 8.51 ft./mile; the corresponding standard deviation is 13.62. As can be observed from Figure 13, 90% of the observations are lower than 26 ft./mile, 85% of them are lower than 22.6ft/mile, and 50% are lower than 8.5 ft./mile.

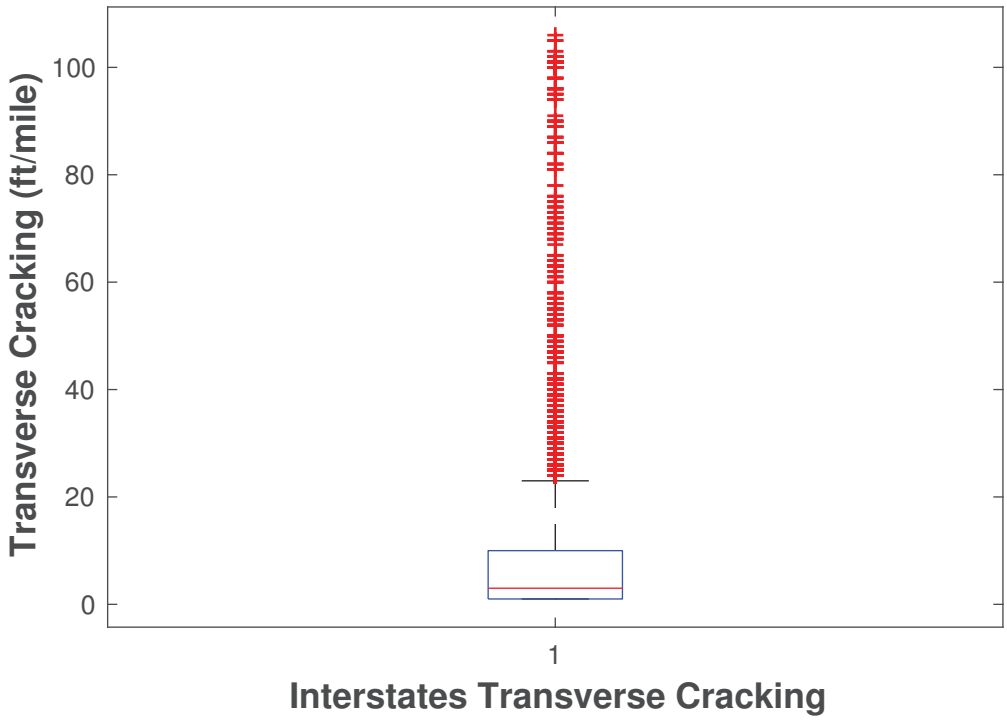

Figure 9.14 Box-plot of transverse cracking on State Routes

Figure 9.14 shows a box plot of the transverse cracking on the Interstates. The median of the dataset is 3 ft./mile. It is seen that the maximum transverse cracking reaches only 106 ft./mile. Among 19,006 nonzero observations in the dataset, only 2011 observations exceed 20 ft./mile, which is 10.6% of the nonzero subset.

Compared to the recommended transverse cracking in the MOP (500 ft./mile for Interstates), the level of transverse cracking on Interstates of Tennessee is much lower. Compared to the northern states of the United States, low temperature damage is not a severe problem for the pavements in Tennessee. Therefore, the threshold value in the MOP may be too high for Tennessee.

9.2.2 STATE ROUTES

9.2.2.1 Alligator Cracking

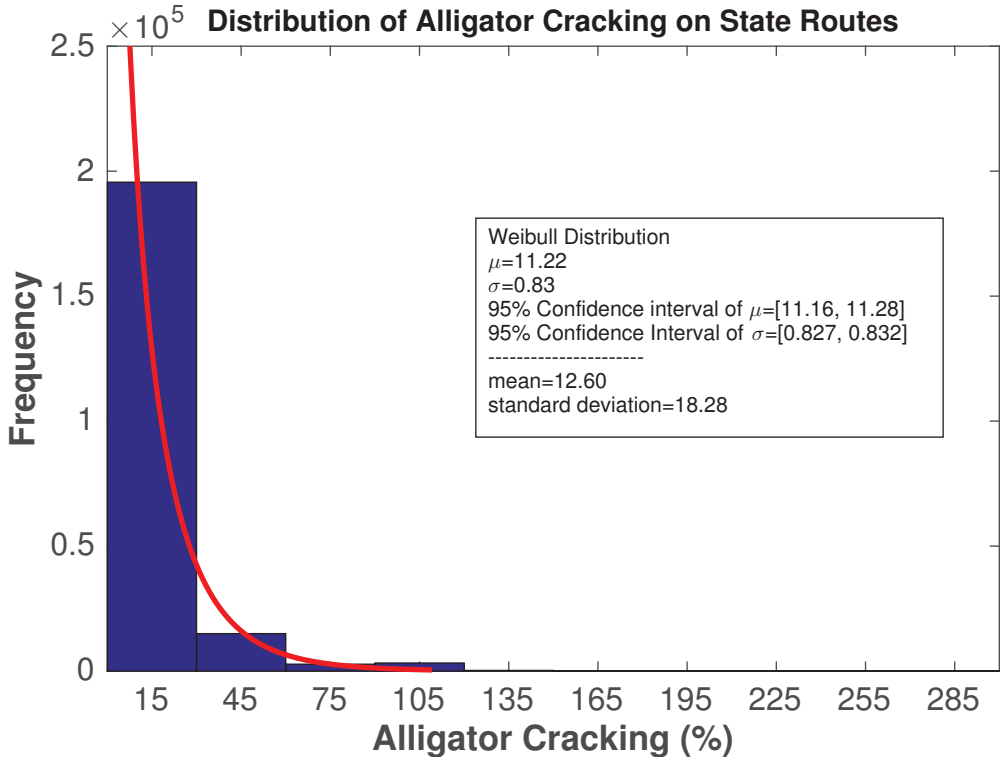

Figure 9.15 distribution of Alligator Cracking on State Routes

Figure 9.15 shows a distribution of alligator cracking on the State Routes. A Weibull distribution is used to fit the data, as used in the previous sections. The fitted location and shape parameters of the Weibull distribution are, μ=11.22, σ=0.83, respectively. The 95% confidence intervals for the two parameters are, μ = [11.16, 11.28], σ = [0.827, 0.832], respectively. The mean of this dataset is 12.6%, and the corresponding standard deviation is 18.28. As shown in Figure 15, 90% of the observations are lower than 36%, 85% of them are lower than 31.5%, 50% are lower than 12.6%, and only 25% are lower than 0.3%. Similar to the case in Interstates, alligator cracking should be paid more attention to when designing an asphalt pavement.

9.2.2.2 Longitudinal Cracking

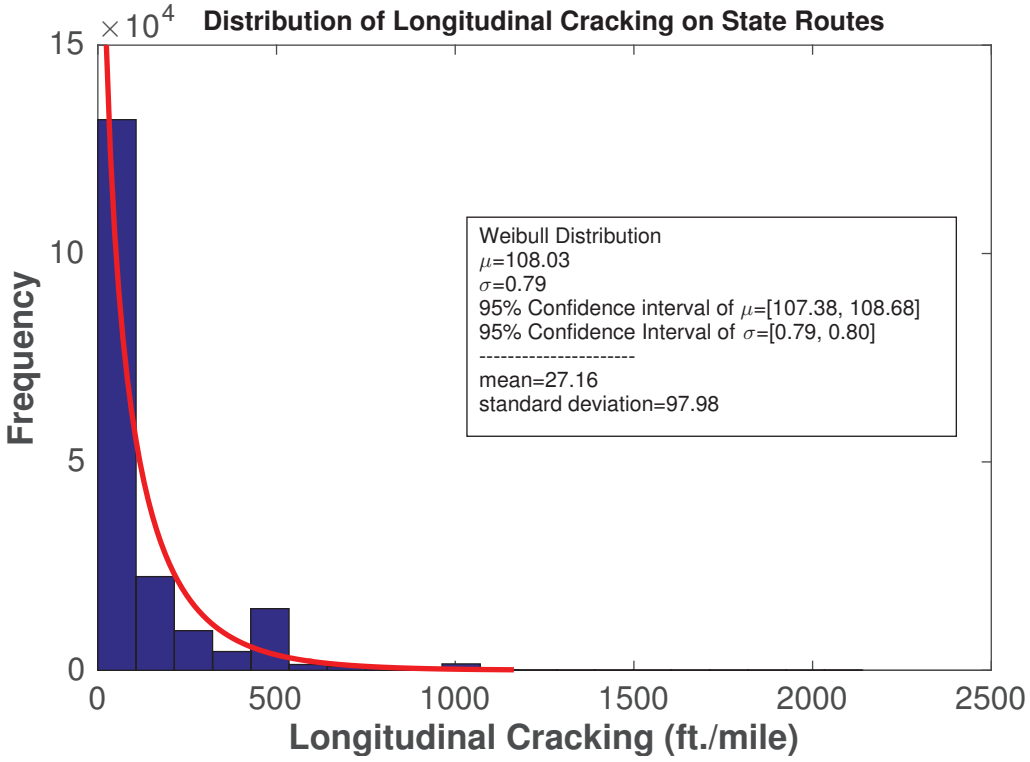

Figure 9.16 Distribution of Longitudinal Cracking on State Routes

Figure 9.16 is a distribution plot of longitudinal cracking on the State Routes. After a comparison, the Weibull distribution works better than the normal, gamma, and beta distribution. The fitted location and shape parameters for the longitudinal cracking on State Routes are, μ=108.03, σ=0.79. The 95% confidence interval for these two parameters are, μ= [107.38, 108.68], σ= [0.79, 0.80], respectively. The mean of these data is 27.2 ft./mile, and the corresponding standard deviation is 97.98. As Figure 16 shows, 90% of the observations are lower than 152.7ft./mile, 85% of them are lower than 128.7ft/mile, and 50% are lower than 27.2 ft./mile. Compared to the recommended trigger value for longitudinal cracking in the MOP (2000 ft./mile), the average longitudinal cracking on the State Routes of Tennessee is much smaller. If the trigger value in the MOP was used, clearly, an over design would produce, thus making the pavements in Tennessee too strong to allow developing any longitudinal cracking. In all, for asphalt pavement design, the longitudinal cracking on the pavements of Tennessee is not a problem as severe as alligator cracking, a drop in this criteria may give rise to a more cost-saving scenario.

9.2.2.3 Transverse Cracking

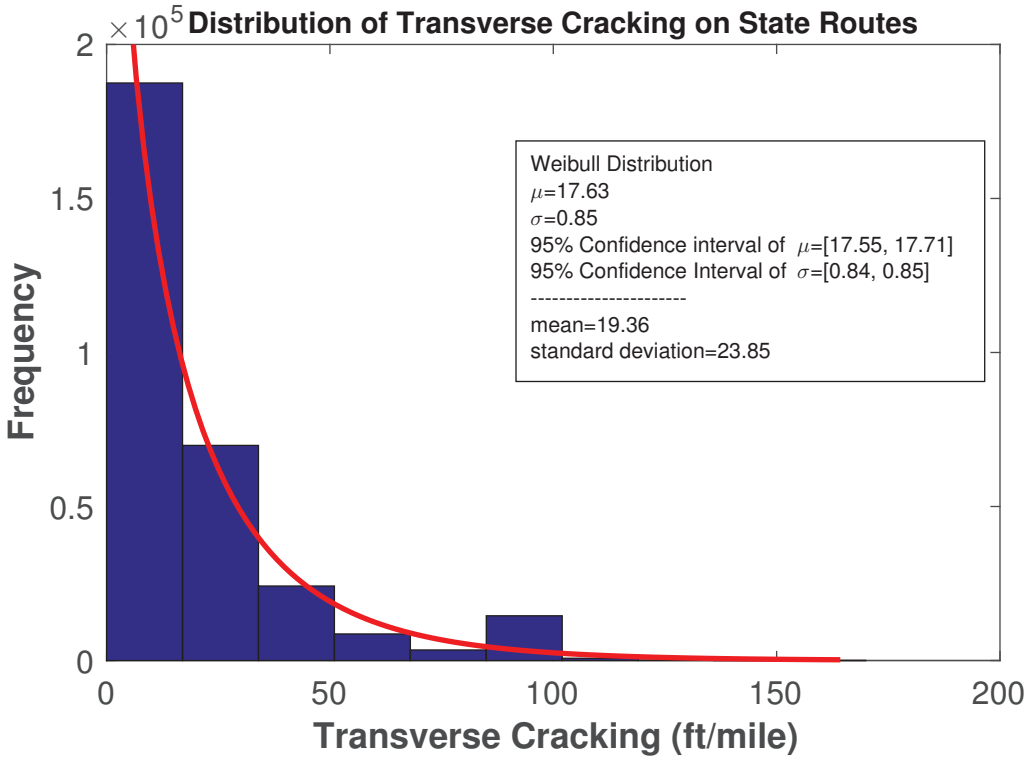

Figure 9.17 Distribution of transverse cracking on State Routes

Figure 9.17 used a Weibull distribution to characterize the transverse cracking on the State Routes, as employed in the previous sections. The fitted location and shape parameter are, μ=17.63, σ=0.85. The ranges of the 95% confidence intervals of both parameters are quite small, which indicated the Weibull distribution works well in fitting the data. The mean of the data is 19.36 ft./mile, and the corresponding standard deviation is 23.85. It can also be seen in Figure 17, 90% of the observations are lower than 50 ft./mile, 85% of them are lower than 44 ft./mile, and 50% are lower than 19.4 ft./mile. The maximum of this dataset is 167 ft./mile, and its median is 11 ft./mile. In comparison to the critical value in the MOP (700 ft./mile), the level of transverse cracking on the State Routes is much lower. When a higher threshold value was used in asphalt pavement design, an over design might still happen, even though cold temperature damage is not a serious problem in Tennessee.

9.2.3 RUTTING

9.2.3.1 Interstates

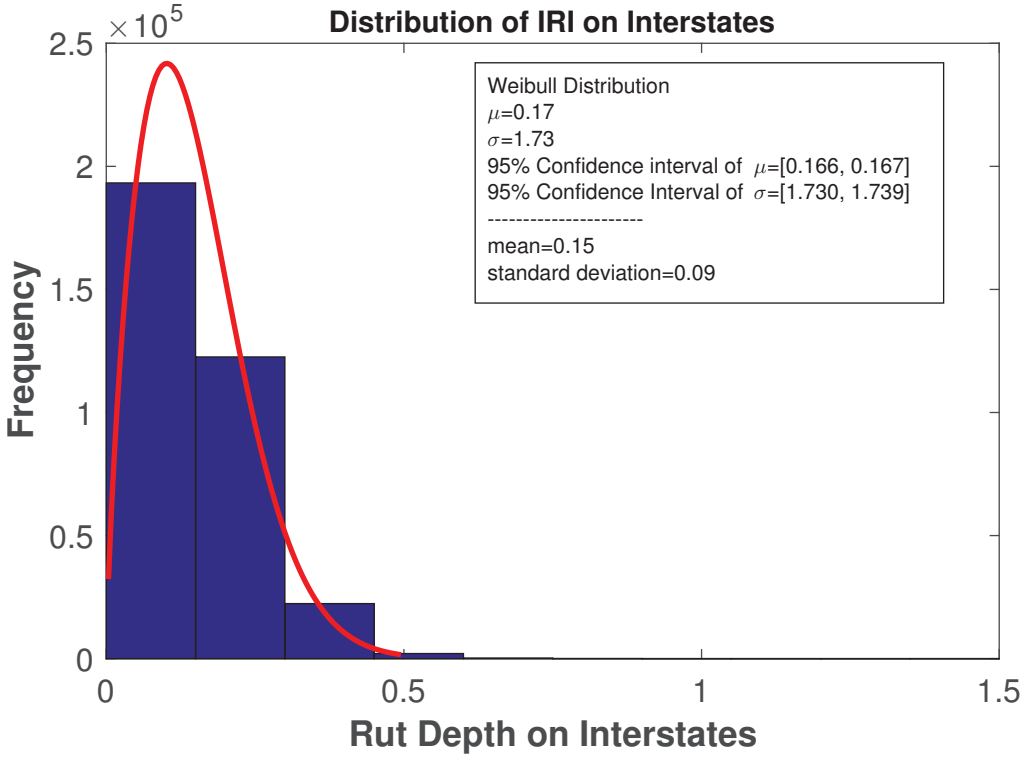

Figure 9.18 Distribution of Rutting on Interstates

Figure 9.18 indicated the distribution of rutting on Interstates. Likewise, a Weibull distribution was used to fit the data. The fitted the location and shape parameters as shown in Figure 18 are, μ=0.17, σ=1.77, respectively. The mean of rutting on the Interstates is 0.15 inches, and the corresponding standard deviation is 0.09. The median of this dataset is 0.13 inches, and its maximum is 1.48 inch. As also implied in Figure 18, 90% of the observations are lower than 0.27 inches, 85% of them are lower than 0.24 inches, 50% are lower than 0.15 inch, and about 25% are lower than 0.09 inches. Still, compared to the suggested value in the MOP (0.4 inch), the amount of rutting in the Interstates of Tennessee was much smaller. Among 340,551 nonzero observations, only 4295 observations exceed 0.4 inches, which is only about 1.3% of total dataset. Obviously, when the suggested value in the MOP was to use, an over design would happen.

9.2.3.2 State Routes

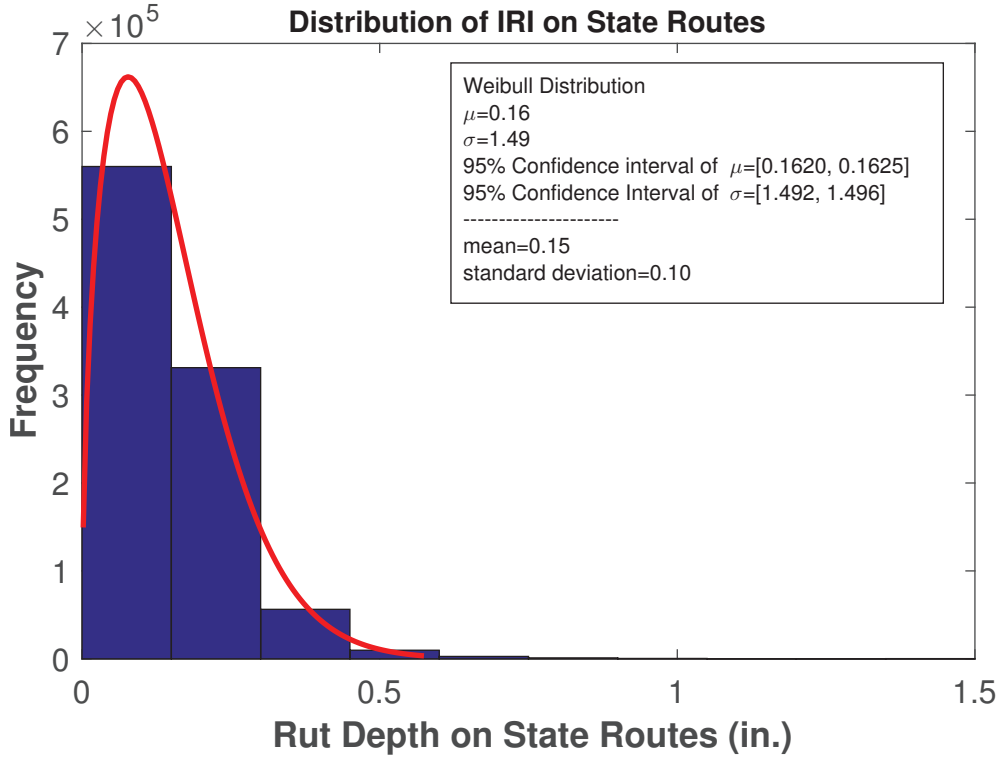

Figure 9.19 Distribution of Rutting on State Routes

Figure 9.19 employed a Weibull distribution to characterize rutting on the State Routes. The fitted location and shape parameter is, μ=0.16, σ=1.49, respectively. The 95% confidence intervals for these two parameters are very narrow, which implies the Weibull distribution fits the data well. The mean and standard deviation of this dataset are, 0.15 inch, and 0.10 inches, respectively. The median and maximum of these data are, 0.13 inches, and 1.5 inches, respectively. As can be found in Figure 19, 90% of the observations are lower than 0.28 inch, 85% of them are lower than 0.25 inch, 50% are lower than 0.15 inches, and about 25% are lower than 0.1 inches. Again, the amount of rutting in the State Routes of Tennessee is much lower than the one recommend by the MOP (0.5 inches). Among 962,042 nonzero observations in this dataset, only 8841 observations are greater than 0.5 inches. At the current stage, when the recommended trigger value for rut depth was used, obviously, an overall design would take place.

CHAPTER 10 CONCLUSIONS AND RECOMMENDATIONS

10.1 OBSERVATIONS FROM THE CALIBRATION

In the process of calibrating the distresses and roughness models for Tennessee, several observations are summarized as follows:

- In calibrating the alligator-cracking model, it was found that for a thick pavement, especially for a pavement with thick asphalt layers, the predicted alligator cracking was very small and sometimes even negligible. The main cause of this problem could be that the asphalt treated base (ATB) course was treated in the same manner as the asphalt surface course. As such, a more reasonable modeling of the ATB course could help to address this issue.

- For the flexible pavement rehabilitation analyses in the AASHTOware, reflective cracking is the major proportion of the predicted total cracking, regardless of the thickness of pavement structure or the AADTT. This could also be an explanation to the alligator cracking level being extremely low for most sections included in the study.

- For the asphalt pavement rehabilitation analyses, when a pavement received more than two HMA overlays, the original pavements would then become very thick. Under this circumstance, the amount of alligator cracking predicted by the MEPDG was extremely small. However, a large amount of alligator cracking was frequently observed on these pavements. In this case, a procedure in the MEPDG to consider a loss in thickness according to the age and structural condition of the pavements could help to improve the accuracy in prediction of alligator cracking.

10.2 SUMMARY

10.2.1 SUMMARIZATION OF THE SURVEY

In the survey, 35 out of 53 surveys sent out to United States and Canada transportation administration agencies responded. Based on the survey results, the following conclusions were drawn:

- Most of the States in the United States or provinces in Canada still use AASHTO 1993 for flexible and rigid pavement design.
- A majority of States in the US or provinces in Canada have plan to make a transition from AASHTO 1993 to the Pavement Mechanistic-Empirical Design Guide.
- About half of the responses indicated that LTPP database and data from the pavement management system were employed as the main source of data for local calibration.
- More than 50% of the responses showed that the input database of asphalt materials was developed.

- Among the 27 responses on setting up weigh-in-motion station to collect traffic data, a total of 15 states have plans to implement this plan.
- Generally, 10-30 sections were used in the local calibration of flexible pavement.
- Most of the States reported that the bottom-up cracking (alligator) was the most difficult model to calibration, followed by the longitudinal-cracking and thermal cracking (transverse cracking).
- Most of the States showed they are not quite satisfied with the current version of AASHTOWare Pavement ME Design software, because there are too many parameters to input and too many information to interpret.

10.2.2 CALIBRATION OF THE RUTTING MODELS

More than 70 sections across the whole state were collected, 29 sections in Region I, 11 sections in region II, 13 sections in Region III and 23 section in region IV. The traffic volume in each region was compared. It was found that the traffic volume in all four Regions is very close. The necessity of calibrating rutting model for each region was investigated. It was found, calibrating rutting model for each region could significantly increase the quality of calibration, and thus increase the prediction accuracy of model. The rutting model for each region was calibrated separately. Local calibration coefficients for each region were provided.

10.2.3 CALIBRATION OF THE DISTRESSES MODELS

The alligator cracking, longitudinal cracking, and the roughness (IRI) models were calibrated and validated in this study and the following conclusions have been drawn. The local calibration coefficients are summarized in Table 10.1.

- Specifically, the alligator cracking and longitudinal cracking models were calibrated using the curve fitting procedure in MATLAB and then validated using the Jackknife method. Results showed that after the calibration, the biases were removed, and the prediction accuracy was significantly improved. In addition, the dispersion of the prediction was also decreased; i.e. the precision of the prediction increased significantly.

- The transverse cracking model in Tennessee was verified using data collected from the HPMA. Due to the limited data availability in HMPA and its low occurrence, the research team recommends use the national defaults for the transverse cracking for Tennessee at the current stage.

- The roughness model was calibrated on the basis of all the calibrated models, such as the rutting, alligator cracking, and longitudinal cracking. Results indicated that the Jackknife method was not only able to validate the calibrated models without bias, but also worked well in detecting outliers. It was recommended that the Jackknife method to be used for analyzing pavements for future calibrations.

Table 10.1 Summarization of the local calibration coefficients

Model	C_1	C_2	C_3
Alligator Cracking	1.023	0.045	6000
Longitudinal Cracking	6.44	0.27	204.54
Rutting (plain area)	β_{r1}=0.111	β_{BS}=0.196	β_{SG}=0.722
Rutting (Mountain area)	β_{r1}=0.177	β_{BS}=1.034	β_{SG}=0.159
IRI (national defaults)	*SF*=0.015; Total Cracking=0.400; *TC*=0.0080; *RD*=40.0		

10.2.4 DESIGN CRITERIA

The distributions of several performance criteria in the MEPDG were analyzed. These performance criteria include IRI, rut depth, alligator, longitudinal, and transverse cracking. The data stored in the pavement management system (PMS) of Tennessee were used to determine the best distribution. The collected data were divided into two classes, the Interstates and State Routes. Based on the analyses, the following conclusions were reached:

- After a comparison with the normal, gamma, and beta distribution, the Weibull distribution fits all the data the best; thus, the Weibull distribution was used to predict the amount of IRI or distresses under a certain probability.

- The amount of IRI on both Interstates and State Routes is much lower than the recommended values in the MOP. When using the recommended values in the MOP to design asphalt pavement for Tennessee, an over design could happen.

- The level of alligator cracking on both Interstates and States Routes is about the same scale as those in the MOP. Therefore, more weights may be given to control the alligator cracking. The extent of longitudinal cracking on both Interstates and State Routes is much smaller than the recommended ones in the MOP.

- The use of the values from the MOP to control the longitudinal cracking could result in an unnecessarily thicker pavement for Tennessee.

- Similar to the longitudinal cracking, transverse cracking is not a severe problem in Tennessee, a drop in the threshold value for the transverse cracking may result in a more cost-saving design.

10.3 RECOMMENDATIONS

During the calibration of the distress models, several issues were identified and could be addressed in the future to improve the accuracy of the calibration:

1. To improve the predictability of the transfer functions in this project, it is recommended to include more data with longer maintenance history and higher quality to conduct the local calibration. In Tennessee, the cracking data, including alligator and longitudinal cracking, were collected since1998. The collection frequency for the State Routes is once every

other year and that for Interstates is once a year). Therefore, there are only 8 data points for State Routes, and 16 data points for Interstates, when considering removing data with high measuring error, relatively few data of quality are available for the local calibration.

2. The calibration of the standard error for each transfer function is not included for this study, but it is vital part for using MEPDG for pavement design, because the standard error directly related the design reliability. However, it is found that the model in the MEPDG manual of practice (MOP) is questionable. Because, for both alligator and longitudinal cracking, the standard error increases as the amount of alligator or longitudinal cracking increases. This indicates that the larger the amount of cracking the larger the standard error, and the less reliable of the estimation. A reasonable standard error should stay constant, in statistics parlance, homoscedasticity. To reach a constant standard error for each model, more data of high quality are needed. Therefore, it is recommended to include more data of high quality to determine the standard error for each of the model.

CHAPTER 11 REFERENCES

AASHTO. (2008). "Mechanistic-Empirical Pavement Design-A Manual of Practice." *Interim Edition*,

Aguiar-Moya, J.P. et al. (2009). "Sensitivity analysis of the MEPDG using measured probability distributions of pavement layer thickness."

ARA. (2004). *Mechanistic-Empirical Pavement Design Guide (NCHRP 1-37A),*

Bari, J., and Witczak, M.W. *Development of a new revised version of the Witczak E* predictive model for hot mix asphalt mixtures (with discussion)*. Times cited: 138. 2006.

Darter, M. (2006). "NCHRP project 1-40D (02), technical assistance to NCHRP and NCHRP project 1-40A: Versions 0.9 and 1.0 of the ME pavement design software." *Transportation Research Board*,

Darter, M.I. et al. (2009). "Implementation of the Mechanistic-Empirical Pavement Design Guide in Utah: validation, calibration, and development of the UDOT MEPDG User's Guide."

El-Basyouny, M., and Witczak, M. *Part 2: Flexible Pavements: Calibration of Alligator Fatigue Cracking Model for 2002 Design Guide*. Times cited: 40. 2005.

Glover, L.T., and Mallela, J. (2009). "Guidelines for Implementing NCHRP 1-37A ME Design Procedures in Ohio: Volume 4-MEPDG Models Validation & Recalibration." *Ohio Department of Transportation*,

Hall, K. et al. *Calibration of the mechanistic-empirical pavement design guide for flexible pavement design in Arkansas*. Times cited: 17. 2011.

Jannat, G. et al. *Local Calibration of MEPDG Distress Models for Flexible Pavements Using Ontario's Long-Term PMS Data*. 2013.

Kang, M., and Adams, T. *Local calibration for fatigue cracking models used in the Mechanistic-empirical pavement design guide*. Times cited: 13. 2007.

Kim, Y.R., and Muthadi, N.R. (2007). "Implementation Plan for the New Mechanistic-empirical Pavement Design Guide: Final Report." *NC Department of Transportation ...*,

Li, J. et al. *Sensitivity of axle load spectra in the mechanistic-empirical pavement design guide for Washington state*. Times cited: 30. 2009a.

Li, J. et al. *Calibration of flexible pavement in mechanistic-empirical pavement design guide for Washington state*. Times cited: 37. 2009b.

Schram, S., and Abdelrahman, M. *Improving prediction accuracy in mechanistic-empirical pavement design guide*. Times cited: 15. 2006.

Souliman, M.I. et al. (2010). "Calibration of the AASHTO MEPDG for flexible pavement for Arizona conditions."

Tarefder, R., and Rodriguez-Ruiz, J.I. *Local Calibration of MEPDG for Flexible Pavements in New Mexico*. Times cited: 3. 2013.

Velasquez, R. et al. (2009). "Implementation of the MEPDG for new and rehabilitated pavement structures for design of concrete and asphalt pavements in Minnesota."

Zhou, C. et al. *Validating MEPDG with Tennessee pavement performance data*. Times cited: 5. 2013.

AASHTO (1993). *Aashto Guide for Design of Pavement Structures, 1993*, AASHTO.

AASHTO (2008). *Mechanistic-Empirical Pavement Design Guide-a Manual of Practice*, American Association of State Highway and Transportation Officials.

ARA, I., ERES Division (2004). "Guide for Mechanistic-Empirical Design of New and Rehabilitated Pavement Structures." National Cooperative Highway Research Program.

Bari, J., and Witczak, M. W. (2006). "Development of a New Revised Version of the Witczak E* Predictive Model for Hot Mix Asphalt Mixtures (with Discussion)." *Journal of the Association of Asphalt Paving Technologists*, 75.

Darter, M. I., Mallela, J., Titus-Glover, L., Rao, C., Larson, G., Gotlif, A., Von Quintus, H. L., Khazanovich, L., Witczak, M., and El-Basyouny, M. M. (2006). "Changes to the" Mechanistic-Empirical Pavement Design Guide" Software through Version 0.900, July 2006." *NCHRP Research Results Digest*(308).

Darter, M. I., Titus-Glover, L., and Von Quintus, H. L. (2009). "Implementation of the Mechanistic-Empirical Pavement Design Guide in Utah: Validation, Calibration, and Development of the Udot Mepdg User's Guide."

Gulfam-E-Jannat, Yuan, X.-X., and Shehata, M. (2014). "Development of Regression Equations for Local Calibration of Rutting and Iri as Predicted by the Mepdg Models for Flexible Pavements Using Ontario's Long-Term Pms Data." *International Journal of Pavement Engineering*(ahead-of-print), 1-10.

Guo, X., and Timm, D. H. (2014). "Local Calibration of the Mepdg Using Ncat Test Track Data." *Proc., 94th Annual Meeting of the Transportation Research Board*.

Huang, Y. H. (1993). *Pavement Analysis and Design*.

Kang, M., and Adams, T. "Local Calibration for Fatigue Cracking Models Used in the Mechanistic-Empirical Pavement Design Guide." *Proc., CD-ROM Proceedings of the 2007 Annual Meeting of the Transportation Research Board, Paper*, 08-1102.

Li, J., Pierce, L., Hallenbeck, M., and Uhlmeyer, J. (2009a). "Sensitivity of Axle Load Spectra in the Mechanistic-Empirical Pavement Design Guide for Washington State." *Transportation Research Record: Journal of the Transportation Research Board*(2093), 50-56.

Li, J., Pierce, L. M., and Uhlmeyer, J. (2009b). "Calibration of Flexible Pavement in Mechanistic-Empirical Pavement Design Guide for Washington State." *Transportation Research Record: Journal of the Transportation Research Board*, 2095(1), 73-83.

Muthadi, N. R. (2007). "Local Calibration of the Mepdg for Flexible Pavement Design."Master, North Carolina State University.

Pierce, L. M., and McGovern, G. (2014). *Implementation of the Aashto Mechanistic-Empirical Pavement Design Guide and Software*.

Schram, S., and Abdelrahman, M. (2006). "Improving Prediction Accuracy in Mechanistic-Empirical Pavement Design Guide." *Transportation Research Record: Journal of the Transportation Research Board*, 1947(1), 59-68.

Snee, R. D. (1977). "Validation of Regression Models: Methods and Examples." *Technometrics*, 19(4), 415-428.

Souliman, M. I., Mamlouk, M. S., El-Basyouny, M. M., and Zapata, C. E. "Calibration of the Aashto Mepdg for Flexible Pavement for Arizona Conditions." *Proc., Transportation Research Board 89th Annual Meeting*.

Ullidtz, P., Harvey, J., Tsai, B.-W., and Monismith, C. (2008). "Calibration of Mechanistic-Empirical Models for Flexible Pavements Using California Heavy Vehicle Simulators." *Transportation Research Record: Journal of the Transportation Research Board*(2087), 20-28.

Velasquez, R., Hoegh, K., Yut, I., Funk, N., Cochran, G., Marasteanu, M., and Khazanovich, L. (2009). "Implementation of the Mepdg for New and Rehabilitated Pavement Structures for Design of Concrete and Asphalt Pavements in Minnesota."

Zhou, C., Huang, B., Shu, X., and Dong, Q. (2013a). "Validating Mepdg with Tennessee Pavement Performance Data." *Journal of Transportation Engineering*.